Dynamics of strongly interacting parton-hadron matter

Elena Bratkovskaya
(GSI, Darmstadt)

for the PHSD group

EMMI - NQM seminar
20April 2016

The ‚holy grail‘ of heavy-ion physics:

- Search for the critical point

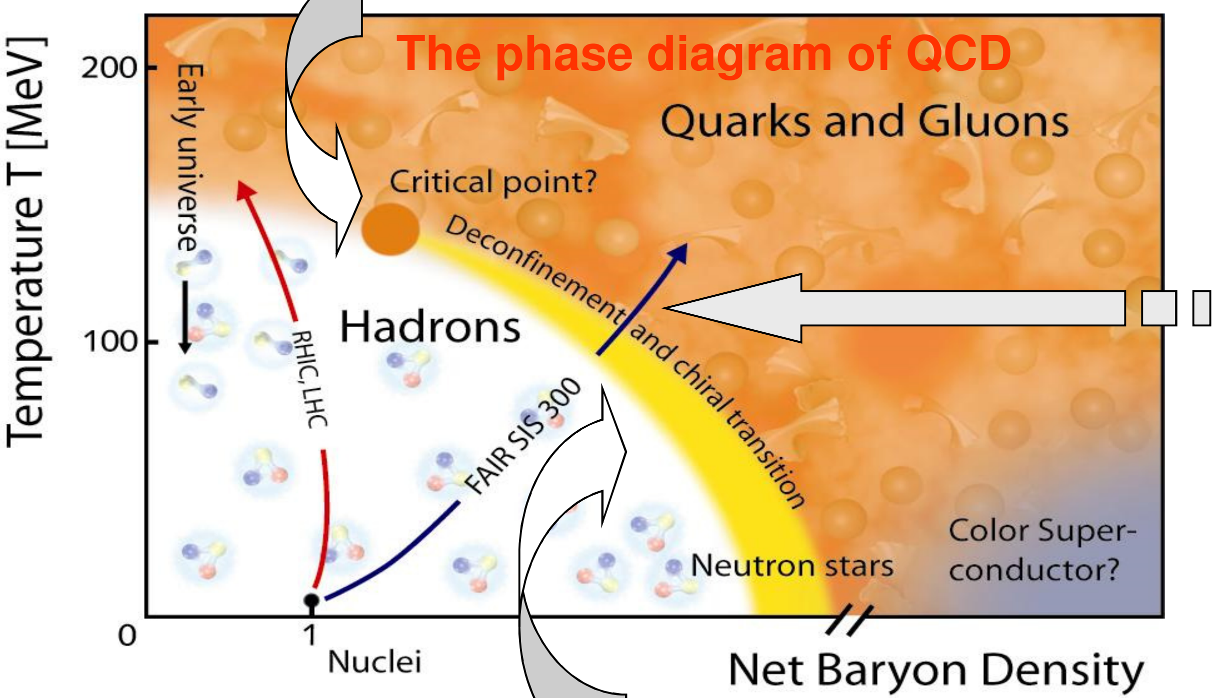

- Study of the phase transition from hadronic to partonic matter – Quark-Gluon-Plasma

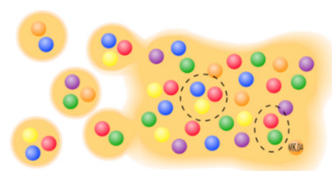

- Study of the in-medium properties of hadrons at high baryon density and temperature
- Search for the signals of chiral symmetry restoration

From SIS to LHC: from hadrons to partons

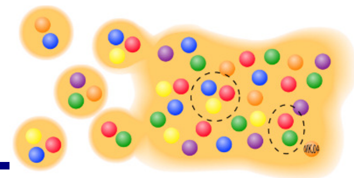

The goal: to study of the phase transition from hadronic to partonic matter and properties of the Quark-Gluon-Plasma on a microscopic level

➔ need a consistent non-equilibrium transport model

- ❑ with explicit parton-parton interactions (i.e. between quarks and gluons)
- ❑ explicit phase transition from hadronic to partonic degrees of freedom
- ❑ lQCD EoS for partonic phase (‚cross over' at μ_q=0)

❑ Transport theory for strongly interacting systems: off-shell Kadanoff-Baym equations for the Green-functions $S^<_h(x,p)$ in phase-space representation for the partonic and hadronic phase

PHSD

⇨ **Parton-Hadron-String-Dynamics (PHSD)**

QGP phase is described by

DQPM

Dynamical QuasiParticle Model (DQPM)

W. Cassing, E. Bratkovskaya, PRC 78 (2008) 034919;
NPA831 (2009) 215;
W. Cassing, EPJ ST 168 (2009) 3

A. Peshier, W. Cassing, PRL 94 (2005) 172301;
Cassing, NPA 791 (2007) 365: NPA 793 (2007)

Interacting quasiparticles

- **Entropy density of interacting bosons and fermions in quasiparticle limit (G. Baym 1998):**

$$s^{dqp} = -d_g \int \frac{d\omega}{2\pi} \frac{d^3p}{(2\pi)^3} \frac{\partial n_B}{\partial T} \left(\mathrm{Im}\ln(-\Delta^{-1}) + \mathrm{Im}\,\Pi\,\mathrm{Re}\,\Delta\right)$$ **gluons**

$$- d_q \int \frac{d\omega}{2\pi} \frac{d^3p}{(2\pi)^3} \frac{\partial n_F((\omega-\mu_q)/T)}{\partial T} \left(\mathrm{Im}\ln(-S_q^{-1}) + \mathrm{Im}\,\Sigma_q\,\mathrm{Re}\,S_q\right)$$ **quarks**

$$- d_{\bar q} \int \frac{d\omega}{2\pi} \frac{d^3p}{(2\pi)^3} \frac{\partial n_F((\omega+\mu_q)/T)}{\partial T} \left(\mathrm{Im}\ln(-S_{\bar q}^{-1}) + \mathrm{Im}\,\Sigma_{\bar q}\,\mathrm{Re}\,S_{\bar q}\right)$$ **antiquarks**

QGP

with d_g = 16 for 8 transverse gluons and d_q = 18 for quarks with 3 colors, 3 flavors and 2 spin projections

Bose distribution function: $n_B(\omega/T) = \left(\exp(\omega/T) - 1\right)^{-1}$

Fermi distribution function: $n_F((\omega-\mu_q)/T) = \left(\exp((\omega-\mu_q)/T) + 1\right)^{-1}$

- **Gluon propagator: $\Delta^{-1} = P^2 - \Pi$ & Quark propagator $S_q^{-1} = P^2 - \Sigma_q$** $\quad (P^2 = \omega^2 - \vec{p}^{\,2})$

➔ **Properties of a system in many-body theory are defined by the complex self-energies, i.e. for QGP - quark self-energy Σ_q and gluon self-energy Π**

How to model Σ_q and Π ?!

e.g.: nonperturbative Dyson-Schwinger Bethe-Salpeter approaches

Simple approximation → DQPM

Dynamical QuasiParticle Model (DQPM) - Basic ideas:

DQPM describes QCD properties in terms of ‚resummed‘ single-particle Green‘s functions (propagators) – in the sense of a two-particle irreducible (2PI) approach:

gluon propagator: $\Delta^{-1} = P^2 - \Pi$ & quark propagator $S_q^{-1} = P^2 - \Sigma_q$

gluon self-energy: $\Pi = M_g^2 - i2\Gamma_g\omega$ & quark self-energy: $\Sigma_q = M_q^2 - i2\Gamma_q\omega$

(scalar approximation)

- the resummed properties are specified by complex (retarded) self-energies which depend on temperature:
  - the real part of self-energies (Σ_q, Π) describes a dynamically generated mass (M_q,M_g);
  - the imaginary part describes the interaction width of partons (Γ_q, Γ_g)

- space-like part of energy-momentum tensor $T_{\mu\nu}$ defines the potential energy density and the mean-field potential (1PI) for quarks and gluons (U_q, U_g)

- 2PI framework guaranties a consistent description of the system in- and out-off equilibrium on the basis of Kadanoff-Baym equations with proper states in equilibrium

A. Peshier, W. Cassing, PRL 94 (2005) 172301;
Cassing, NPA 791 (2007) 365: NPA 793 (2007)

The Dynamical QuasiParticle Model (DQPM) – v.1 (as in PHSD)

Properties of interacting quasi-particles: massive quarks and gluons (g, q, q_{bar}) with Lorentzian spectral functions:

$$\boxed{A_i(\omega,T) = \frac{4\omega\Gamma_i(T)}{\left(\omega^2 - \vec{p}^2 - M_i^2(T)\right)^2 + 4\omega^2\Gamma_i^2(T)}}$$

$$(i = q, \bar{q}, g)$$

- **Modeling of the quark/gluon masses and widths → HTL limit at high T**

  - **quarks:**

    mass: $$M^2_{q(\bar{q})}(T) = \frac{N_c^2 - 1}{8N_c} g^2 \left(T^2 + \frac{\mu_q^2}{\pi^2}\right)$$

    width: $$\Gamma_{q(\bar{q})}(T) = \frac{1}{3}\frac{N_c^2 - 1}{2N_c}\frac{g^2 T}{8\pi} \ln\left(\frac{2c}{g^2} + 1\right)$$

  - **gluons:**

    $$M_g^2(T) = \frac{g^2}{6}\left(\left(N_c + \frac{N_f}{2}\right)T^2 + \frac{N_c}{2}\sum_q \frac{\mu_q^2}{\pi^2}\right)$$

    $$\Gamma_g(T) = \frac{1}{3}N_c\frac{g^2 T}{8\pi}\ln\left(\frac{2c}{g^2} + 1\right)$$

    $N_c = 3$, $N_f = 3$

  - **running coupling: T-dependent $\alpha_S(T)$**

$$\alpha_s(T) = \frac{g^2(T)}{4\pi} = \frac{12\pi}{(11N_c - 2N_f)\ln[\lambda^2(T/T_c - T_s/T_c)^2]}$$

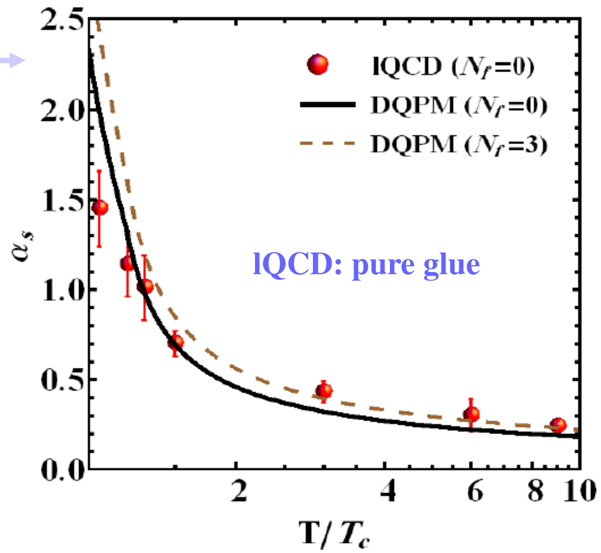

- **fit to lattice (lQCD) results (e.g. entropy density)**

  with 3 parameters: T_s/T_c=0.46; c=28.8; λ=2.42
  (for pure glue N_f=0)

DQPM: Peshier, Cassing, PRL 94 (2005) 172301; Cassing, NPA 791 (2007) 365: NPA 793 (2007)

DQPM thermodynamics (N_f=3) and lQCD

entropy $$s = \frac{\partial P}{dT}$$ → pressure P

energy density: $$\epsilon = Ts - P$$

lQCD: Wuppertal-Budapest group
Y. Aoki et al., JHEP 0906 (2009) 088.

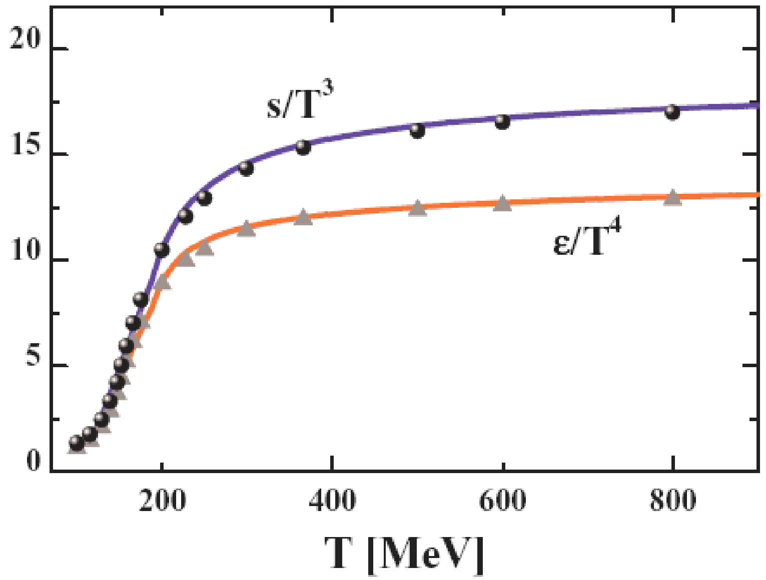

interaction measure:

$$W(T) := \epsilon(T) - 3P(T) = Ts - 4P$$

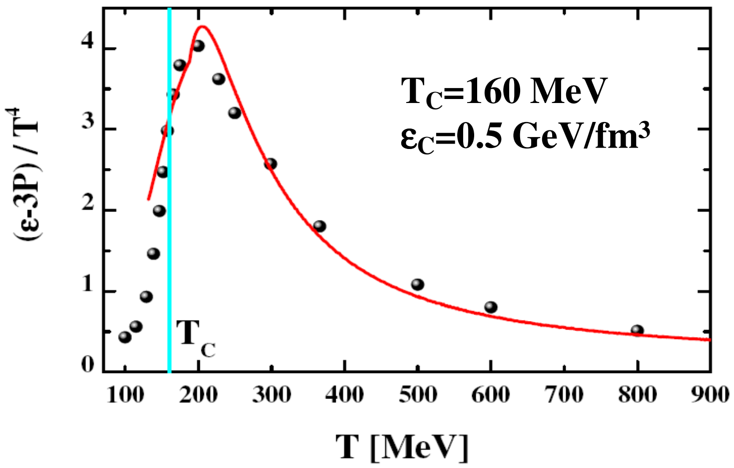

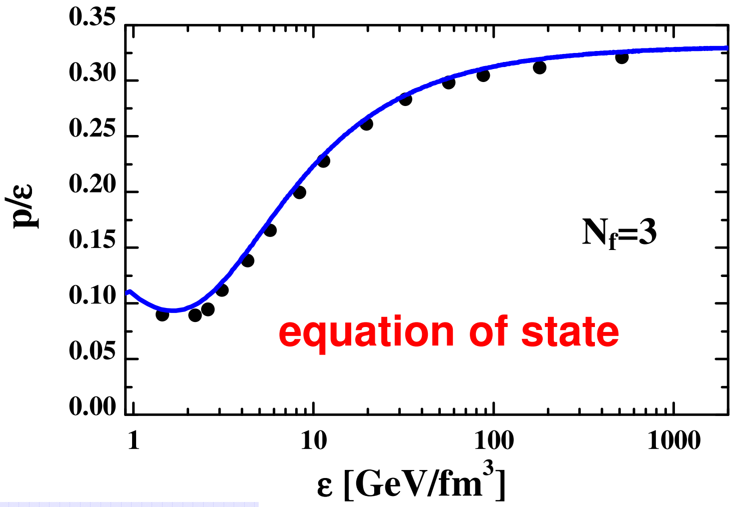

DQPM gives a good description of lQCD results !

Time-like and space-like quantities

Separate time-like and space-like single-particle quantities by $\Theta(+P^2)$, $\Theta(-P^2)$:

$$\tilde{\mathrm{Tr}}_{\mathrm{g}}^{\pm} \cdots = \mathrm{d_g} \int \frac{\mathrm{d}\omega}{2\pi} \frac{\mathrm{d^3p}}{(2\pi)^3}\, 2\omega\, \rho_{\mathrm{g}}(\omega)\, \Theta(\omega)\, \mathrm{n_B}(\omega/\mathrm{T})\ \underline{\Theta(\pm \mathrm{P}^2)} \cdots$$

gluons

$$\tilde{\mathrm{Tr}}_{q}^{\pm} \cdots = d_q \int \frac{d\omega}{2\pi} \frac{d^3p}{(2\pi)^3}\, 2\omega\, \rho_q(\omega)\, \Theta(\omega)\, n_F((\omega - \mu_q)/T)\ \underline{\Theta(\pm P^2)} \cdots$$

quarks

$$\tilde{\mathrm{Tr}}_{\bar{q}}^{\pm} \cdots = d_{\bar{q}} \int \frac{d\omega}{2\pi} \frac{d^3p}{(2\pi)^3}\, 2\omega\, \rho_{\bar{q}}(\omega)\, \Theta(\omega)\, n_F((\omega + \mu_q)/T)\ \underline{\Theta(\pm P^2)} \cdots$$

antiquarks

Time-like: $\Theta(+P^2)$: particles may decay to real particles or interact

Space-like: $\Theta(-P^2)$: particles are virtuell and appear as exchange quanta in interaction processes of real particles

Examples:

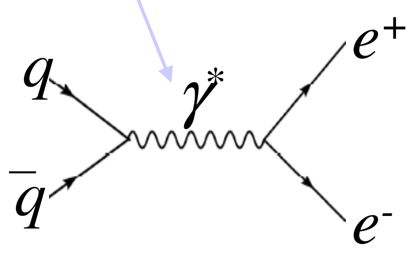

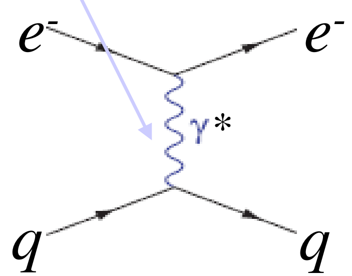

Cassing, NPA 791 (2007) 365: NPA 793 (2007)

Time-like and ‚space-like' energy densities

Time/space-like part of energy-momentum tensor $T_{\mu\nu}$ for quarks and gluons:

$$T^{\pm}_{00,x}(T) = \tilde{T}r^{\pm}_{x}\ \omega$$

x: gluons, quarks, antiquarks

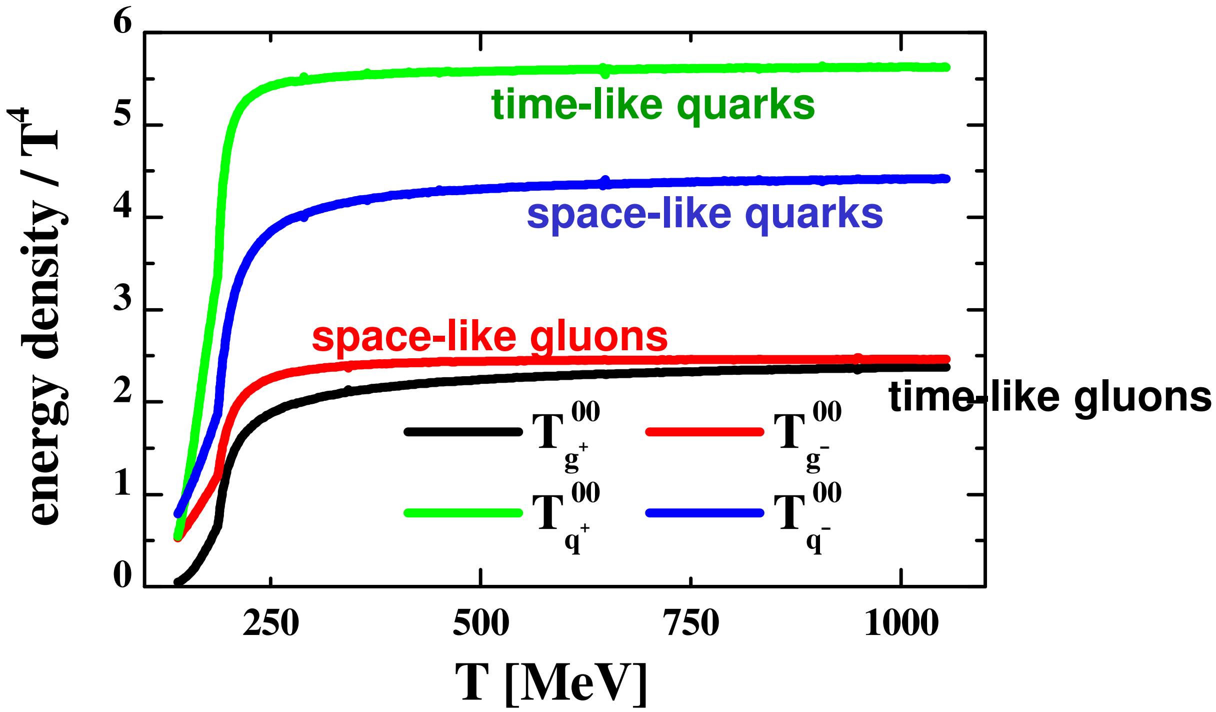

- space-like energy density of quarks and gluons = ~1/3 of total energy density
- space-like energy density dominates for gluons
- space-like parts are identified with potential energy densities

Cassing, NPA 791 (2007) 365: NPA 793 (2007)

Mean-field potential for quasiparticles

- Space-like part of energy-momentum tensor $T_{\mu\nu}$ defines the potential energy density:

$$V_p(T,\mu_q) = T^{00}_{g-}(T,\mu_q) + T^{00}_{q-}(T,\mu_q) + T^{00}_{\bar{q}-}(T,\mu_q)$$

space-like gluons space-like quarks+antiquarks

➔ mean-field scalar potential (1PI) for quarks and gluons (U_q, U_g) vs scalar density ρ_S:

$$U_s(\rho_s) = \frac{dV_p(\rho_s)}{d\rho_s}$$

$U_q = U_S$, $U_g \sim 2U_S$

Quasiparticle potentials (U_q, U_g) are repulsive !

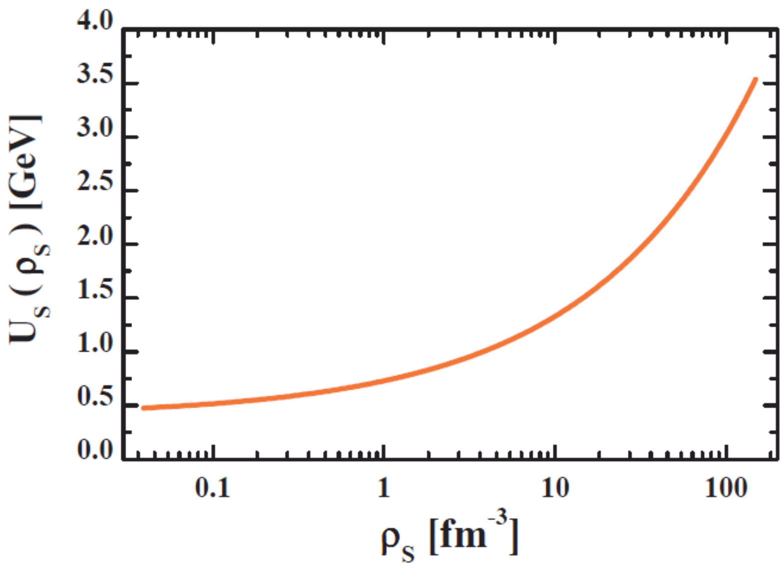

➔ the force acting on a quasiparticle j:

$$F \sim M_j/E_j \nabla U_s(x) = M_j/E_j \; dU_s/d\rho_s \; \nabla\rho_s(x)$$

$$j = g, q, \bar{q}$$

➔ accelerates particles

Cassing, NPA 791 (2007) 365: NPA 793 (2007)

The Dynamical QuasiParticle Model (DQPM)

- fit to lattice (lQCD) results (e.g. entropy density)
  - * BMW lQCD data S. Borsanyi et al., JHEP 1009 (2010) 073

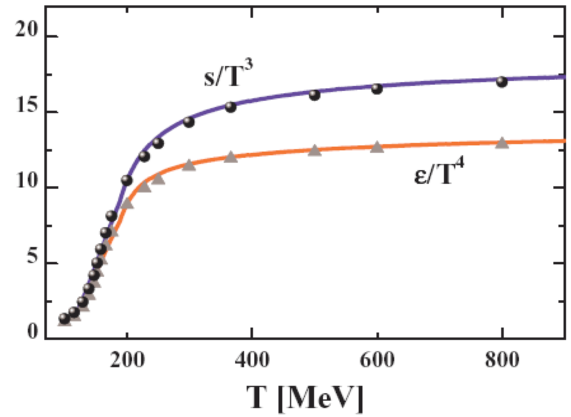

→ Quasiparticle properties:

- large width and mass for gluons and quarks

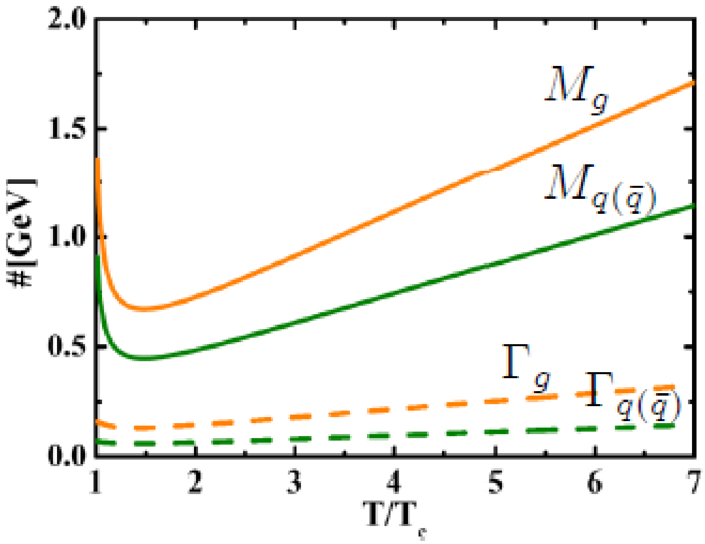

T_C=158 MeV
ε_C=0.5 GeV/fm^3

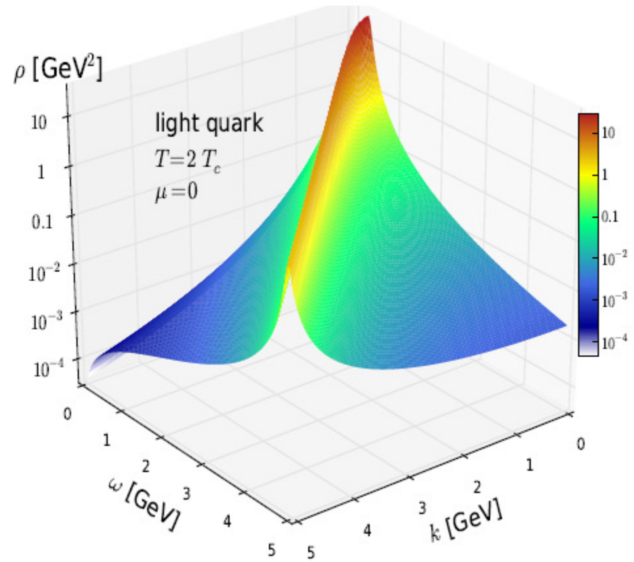

- DQPM matches well lattice QCD
- DQPM provides mean-fields (1PI) for gluons and quarks as well as effective 2-body interactions (2PI)
- DQPM gives transition rates for the formation of hadrons → PHSD

Peshier, Cassing, PRL 94 (2005) 172301; Cassing, NPA 791 (2007) 365: NPA 793 (2007)

I. PHSD - basic concept

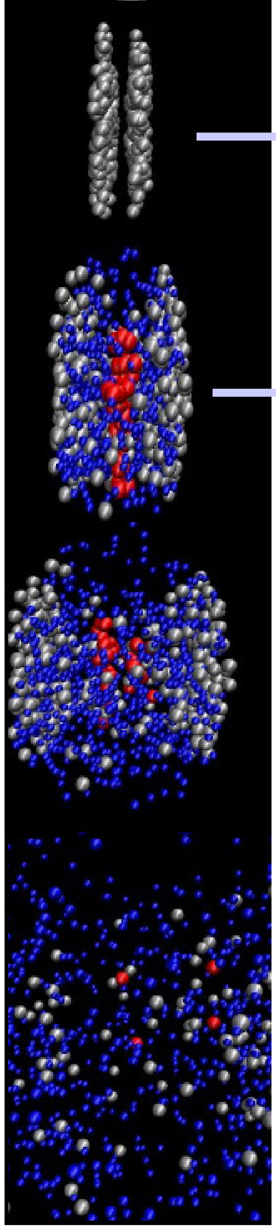

I. From hadrons to QGP:

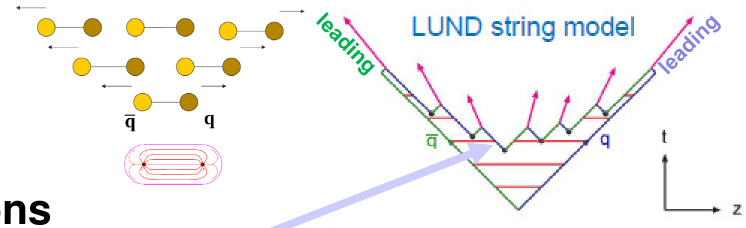

- **Initial A+A collisions – as in HSD:**
  - string formation in primary NN collisions
  - string decay to pre-hadrons (= new produced secondary hadrons: *B* - baryons, *m* - mesons) ➔ ‚flavor chemistry' from strings

- **Formation of initial QGP stage - if local energy density $\varepsilon > \varepsilon_c$ =0.5 GeV/fm^3:**

I. Dynamical Quasi-Particle Model (DQPM) defines:

1) properties of quasiparticles in equilibrium, i.e. masses $M_q(T)$ and widths $\Gamma_q(T)$ (T→ε by lQCD EoS)

2) ‚chemistry' of ‚initial state' of QGP: number of q, qbar, g

3) ‚energy balance' , i.e. the fraction of mean-field quark and gluon potentials U_q, U_g from the energy density ε

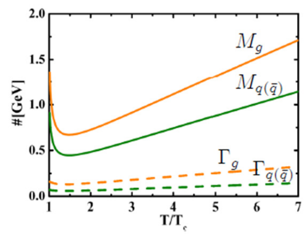

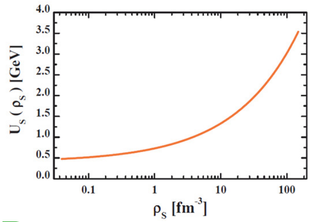

II. Realization of the initial QGP stage from DQPM in the PHSD: by dissolution of pre-hadrons (keep ‚leading' hadrons!) into massive colored quarks (and gluons) + mean-field energy

$$B \to qqq, \quad \tilde{m} \to q\bar{q}, \quad (q\bar{q}) \Rightarrow g \quad \forall \quad U_q, U_g$$

➔ allows to keep initial non-equilibrium momentum anisotropy !

W. Cassing, E. Bratkovskaya, PRC 78 (2008) 034919; NPA831 (2009) 215; W. Cassing, EPJ ST 168 (2009) 3

II. PHSD - basic concept

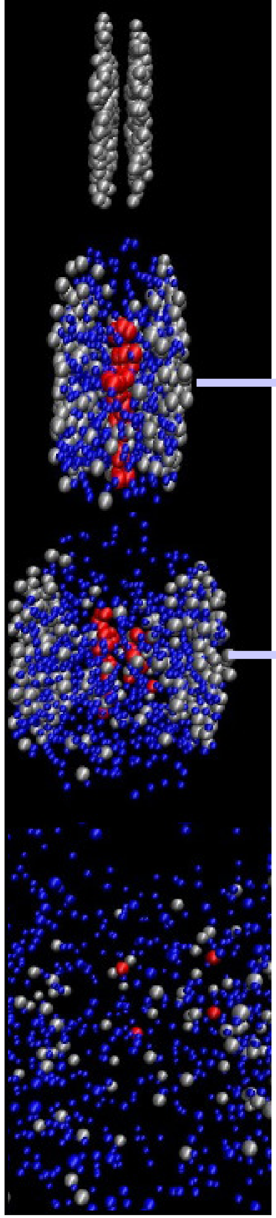

II. Partonic phase - QGP:

- Propagation of quarks and gluons (= ‚dynamical quasiparticles‘) with off-shell spectral functions (width, mass) defined by the DQPM in self-generated mean-field potential for quarks and gluons U_q, U_g

- EoS of partonic phase: ‚crossover‘ from lattice QCD (fitted by DQPM)

- (quasi-) elastic and inelastic parton-parton interactions: using the effective cross sections from the DQPM

▪ (quasi-) elastic collisions:

$$q+q \rightarrow q+q \qquad g+q \rightarrow g+q$$
$$q+\bar{q} \rightarrow q+\bar{q} \qquad g+\bar{q} \rightarrow g+\bar{q}$$
$$\bar{q}+\bar{q} \rightarrow \bar{q}+\bar{q} \qquad g+g \rightarrow g+g$$

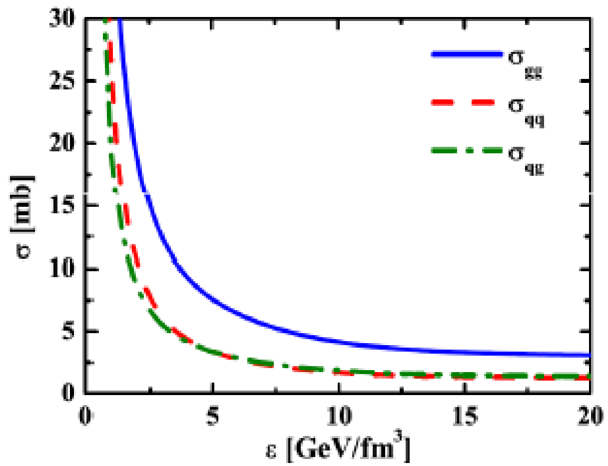

▪ inelastic collisions:
(Breight-Wigner cross sections)

$$\left\{ \begin{array}{l} q+\bar{q} \rightarrow g \\ g \rightarrow q+\bar{q} \end{array} \right.$$

$$\left. \begin{array}{l} q+\bar{q} \rightarrow g+g \\ g \rightarrow g+g \end{array} \right\}$$

suppressed (<1%) due to the large mass of gluons

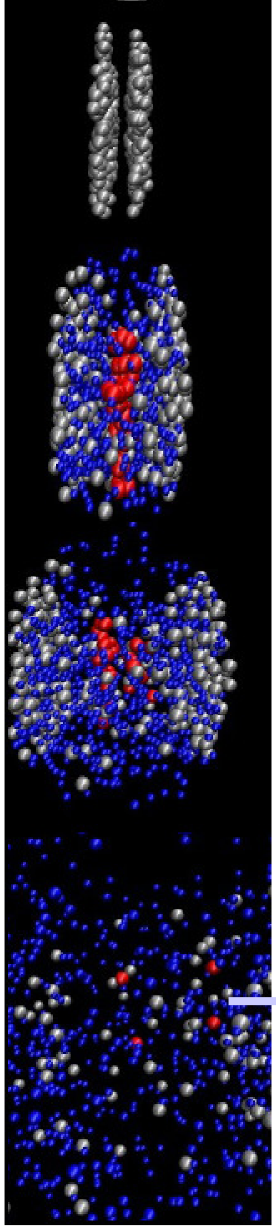

III. PHSD - basic concept

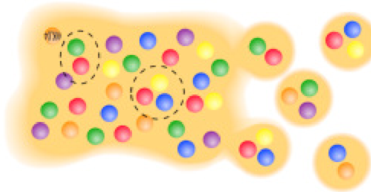

III. Hadronization (based on DQPM):

- massive, off-shell (anti-)quarks with broad spectral functions hadronize to off-shell mesons and baryons or color neutral excited states - ‚strings' (strings act as ‚doorway states' for hadrons)

$$\boxed{\begin{aligned} g \to q+\bar{q}, \qquad q+\bar{q} &\leftrightarrow meson \;\; ('\,string\,') \\ q+q+q &\leftrightarrow baryon \;\; ('\,string\,') \end{aligned}}$$

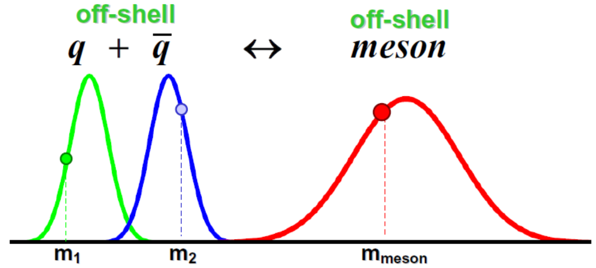

- Local covariant off-shell transition rate for q+qbar fusion
  ➔ meson formation:

$$Tr_j = \sum_j \int d^4x_j d^4p_j /(2\pi)^4$$

$$\frac{dN^{q+\bar{q}\to m}}{d^4x\, d^4p} = Tr_q Tr_{\bar{q}}\; \delta^4(p-p_q-p_{\bar{q}})\; \delta^4\left(\frac{x_q+x_{\bar{q}}}{2}-x\right)\; \delta(\,flavor,color\,)$$

$$\cdot N_q(x_q,p_q)\; N_{\bar{q}}(x_{\bar{q}},p_{\bar{q}})\cdot \omega_q\; \rho_q(p_q)\cdot \omega_{\bar{q}}\; \rho_{\bar{q}}(p_{\bar{q}})\cdot |M_{q\bar{q}}|^2\; W_m\left(x_q-x_{\bar{q}},p_q-p_{\bar{q}}\right)$$

- $N_j(x,p)$ is the phase-space density of parton j at space-time position x and 4-momentum p
- W_m is the phase-space distribution of the formed ‚pre-hadrons' (Gaussian in phase space)
- $|M_{qq}|^2$ is the effective quark-antiquark interaction from the DQPM

➔ Strict 4-momentum and quantum number (flavour, color) conservation

IV. Hadronic phase: hadron-string interactions – off-shell HSD

Time evolution of a central Au+Au collision at 200 GeV

Number of partons and hadrons as a function of time:

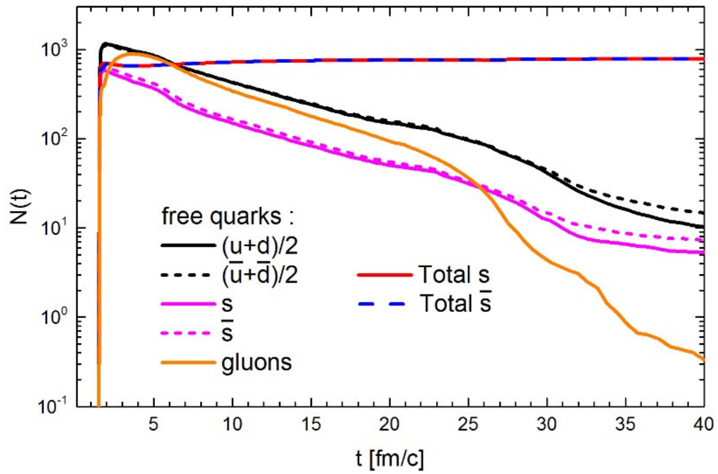

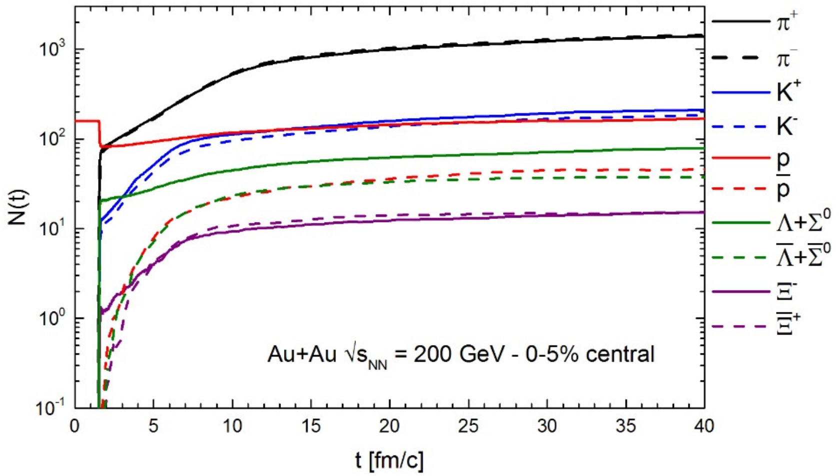

Energy distribution vs. time:

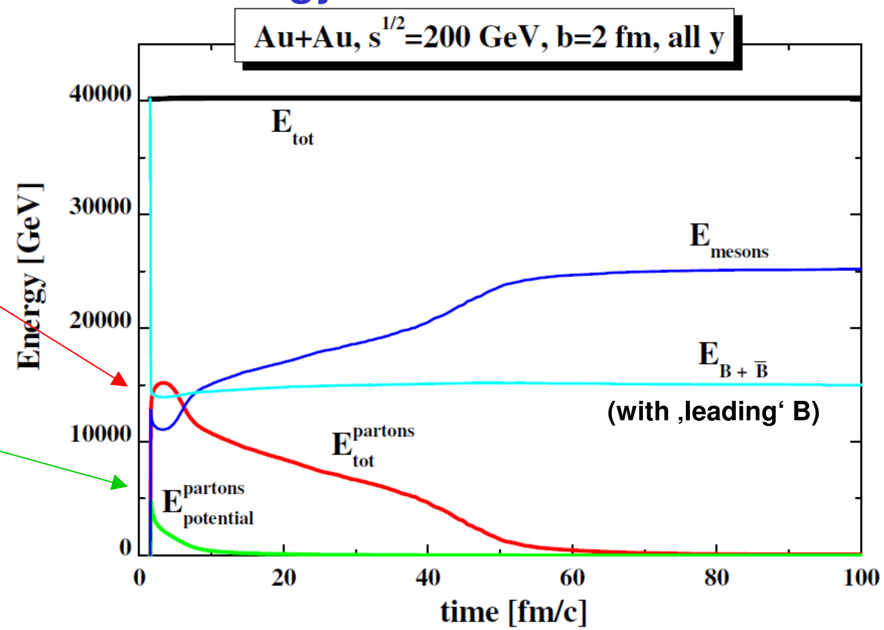

Energy balance in the PHSD:

- ~1/3 of the total energy in central Au+Au at 200 GeV goes to the QGP
- ~1/3 of the total QGP energy is potential energy

Au+Au at 200 A GeV, b=2.2 fm

Au+Au at 200 A GeV, b=2.2 fm

t = 1.63549 fm/c

Au + Au $\sqrt{s_{NN}}$ = 200 GeV

b = 2.2 fm – Section view

Baryons (394)

Antibaryons (0)

Mesons (1598)

Quarks (4383)

Gluons (344)

P.Moreau

Au+Au at 200 A GeV, b=2.2 fm

t = 2.06543 fm/c

Au + Au $\sqrt{s_{NN}}$ = 200 GeV

b = 2.2 fm – Section view

Baryons (396)

Antibaryons (2)

Mesons (1136)

Quarks (5066)

Gluons (516)

P.Moreau

Au+Au at 200 A GeV, b=2.2 fm

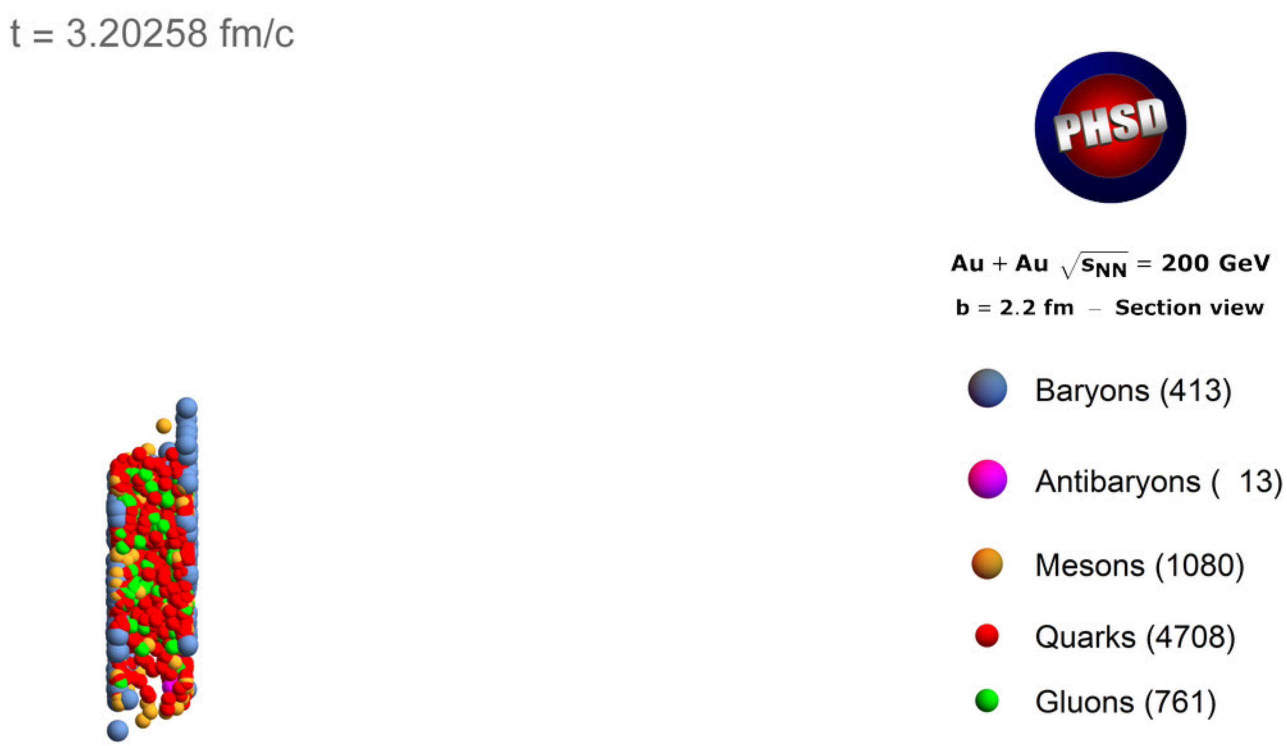

P.Moreau

Au+Au at 200 A GeV, b=2.2 fm

t = 5.56921 fm/c

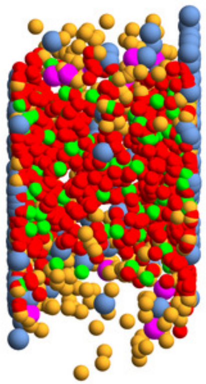

Au + Au $\sqrt{s_{NN}}$ = 200 GeV

b = 2.2 fm – Section view

Baryons (472)

Antibaryons (70)

Mesons (1724)

Quarks (3843)

Gluons (652)

P.Moreau

Au+Au at 200 A GeV, b=2.2 fm

t = 8.06922 fm/c

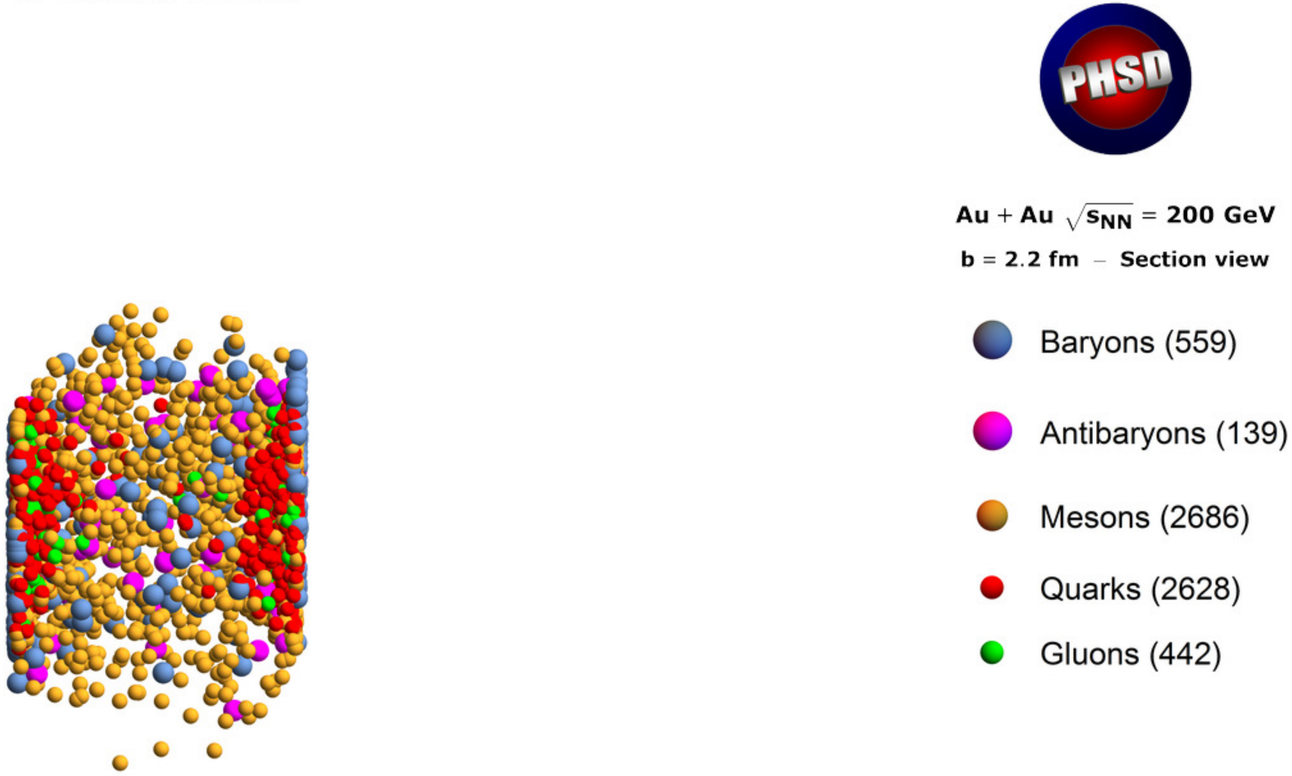

P.Moreau

Au+Au at 200 A GeV, b=2.2 fm

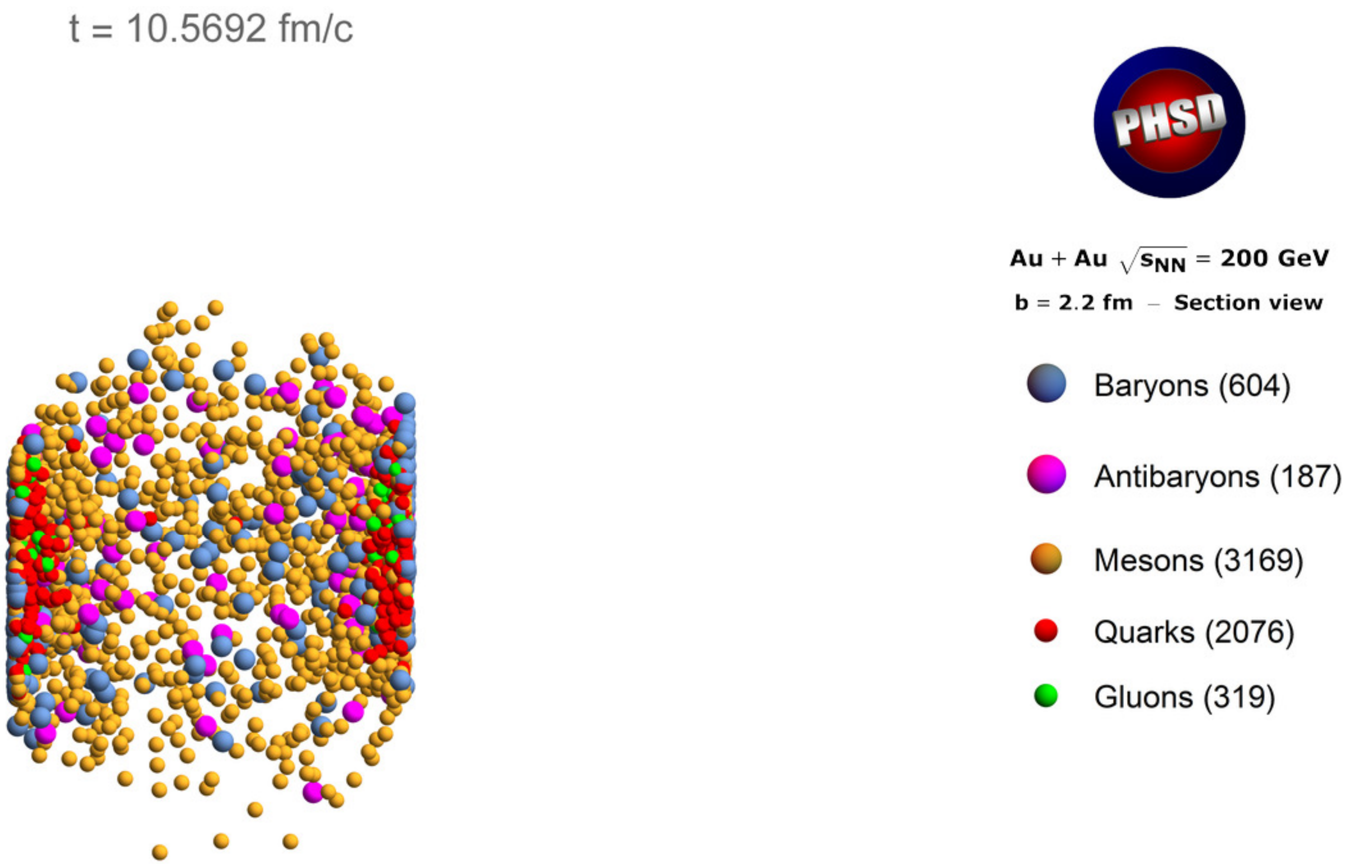

P.Moreau

Au+Au at 200 A GeV, b=2.2 fm

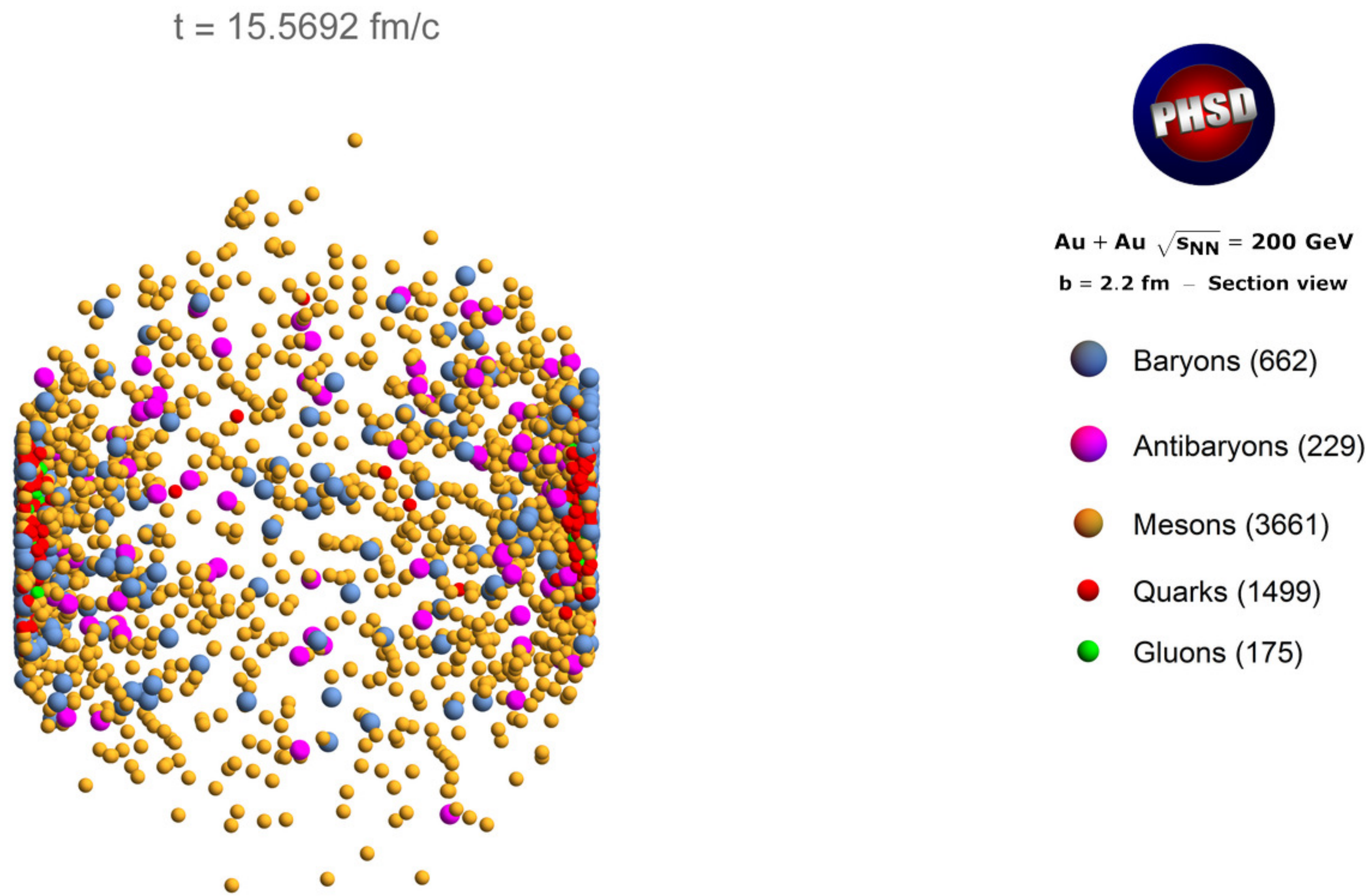

P.Moreau

Au+Au at 200 A GeV, b=2.2 fm

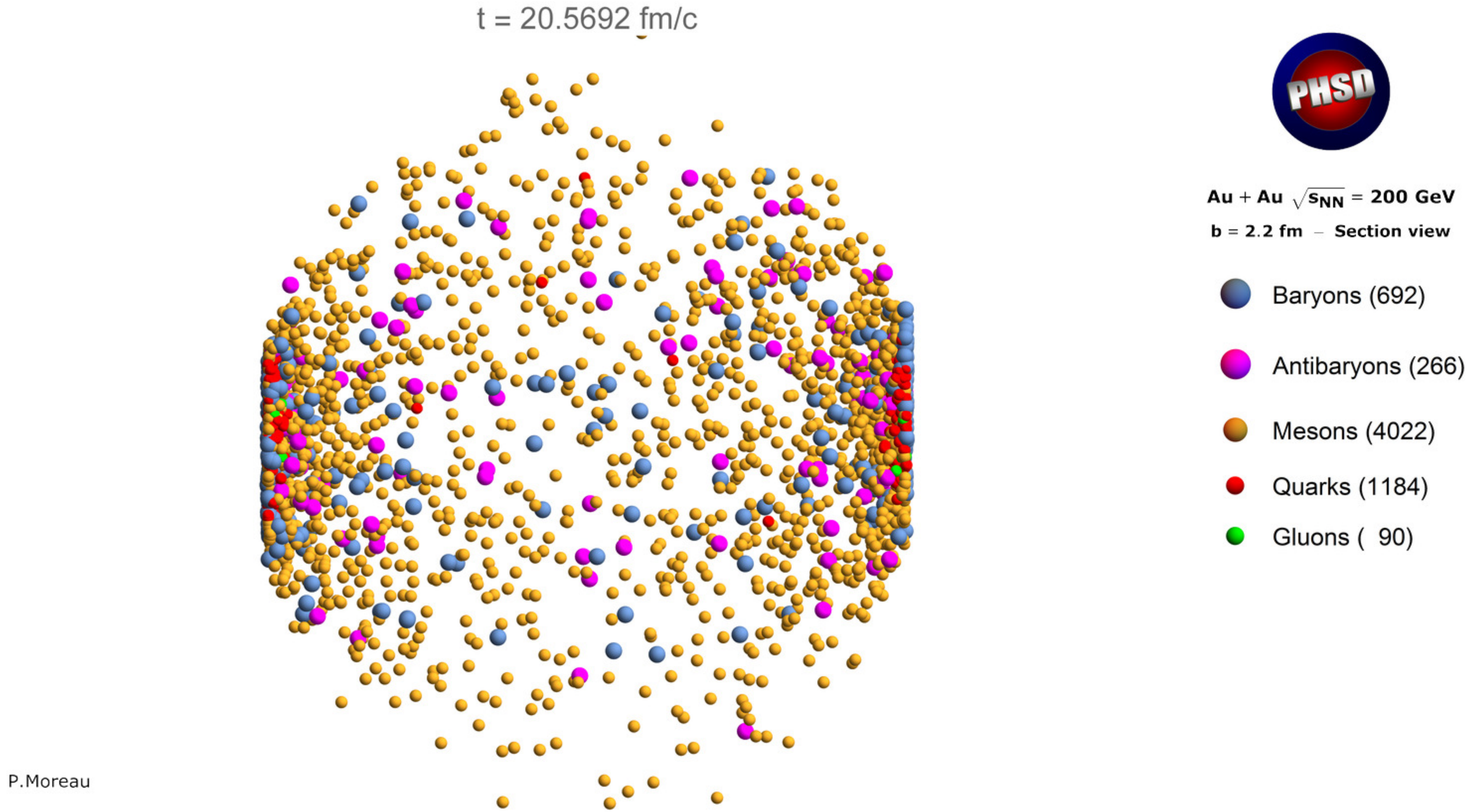

‚Bulk‘ properties in Au+Au

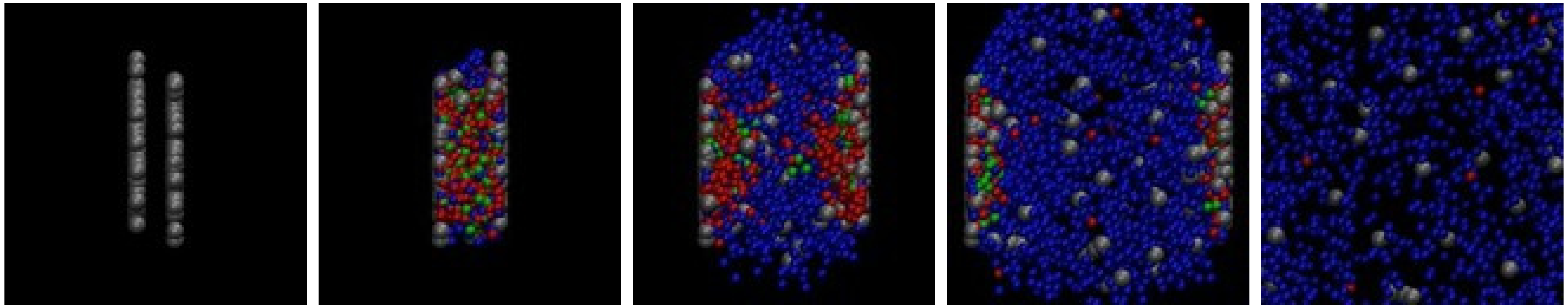

Time evolution of energy density

PHSD: 1 event Au+Au, 200 GeV, b = 2 fm

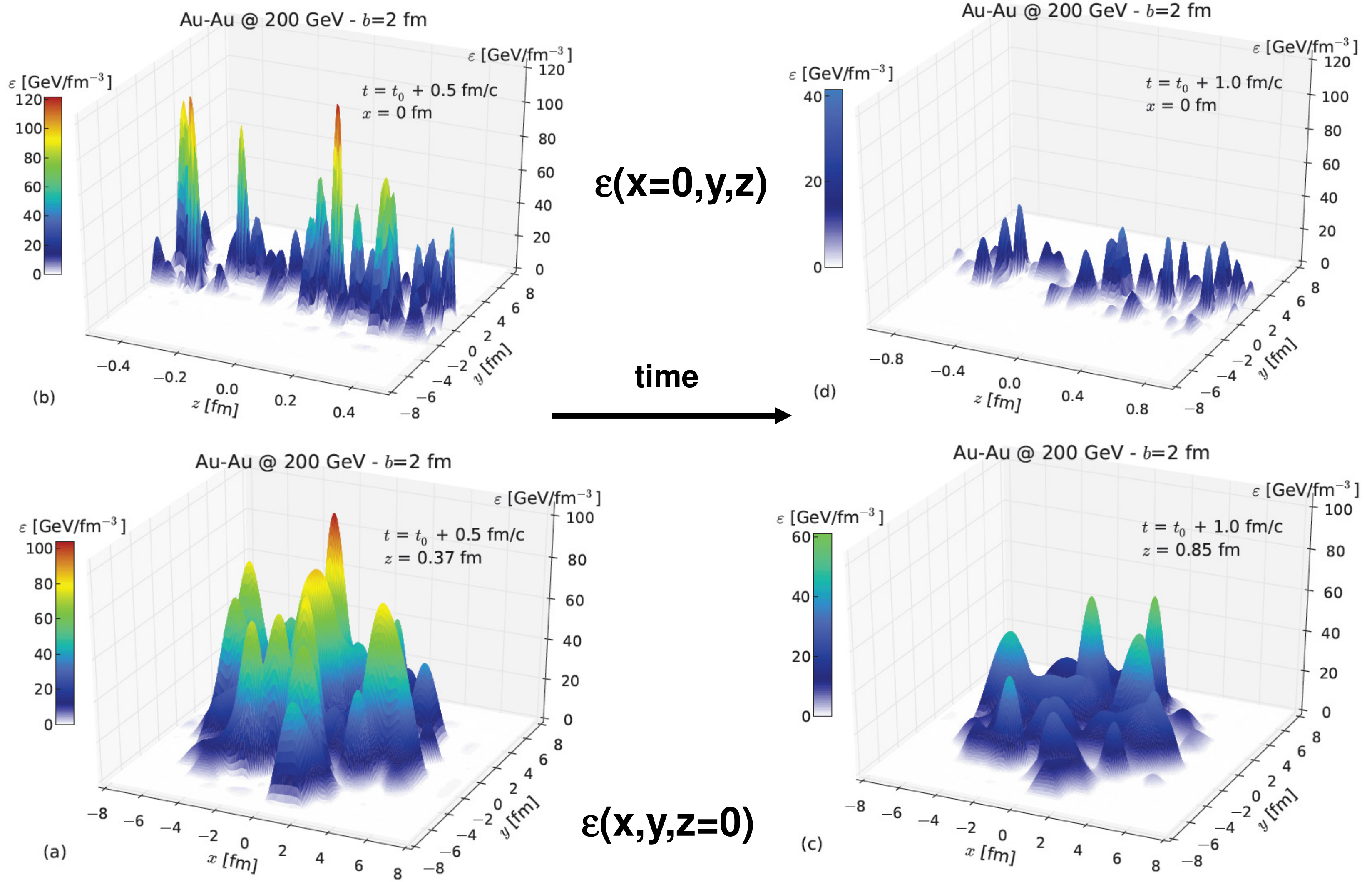

ΔV: Δx=Δy=1fm, Δz=1/γ fm

R. Marty et al, PRC92 (2015) 015201

Partonic energy fraction in central A+A

Time evolution of the partonic energy fraction vs energy

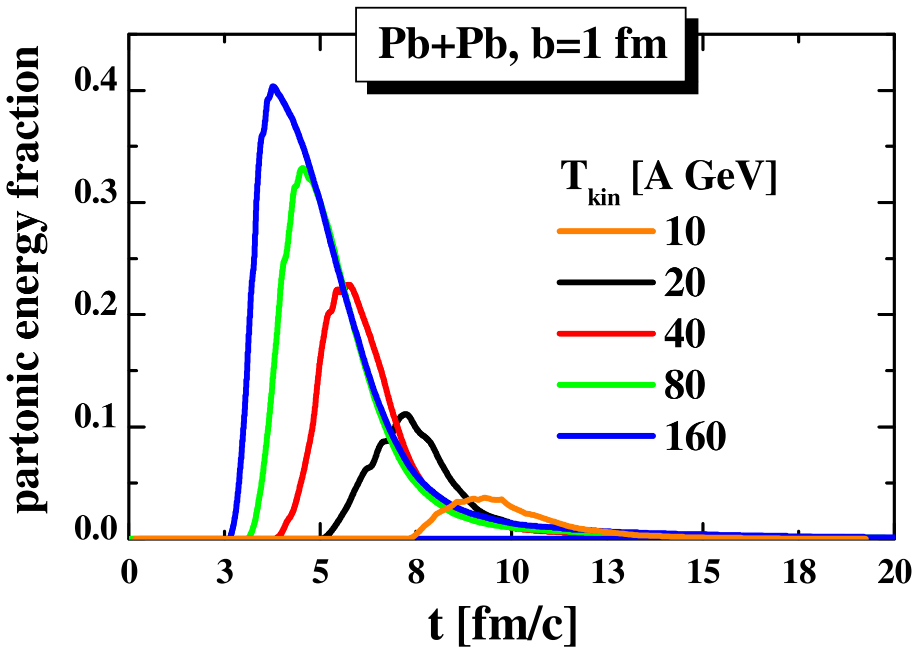

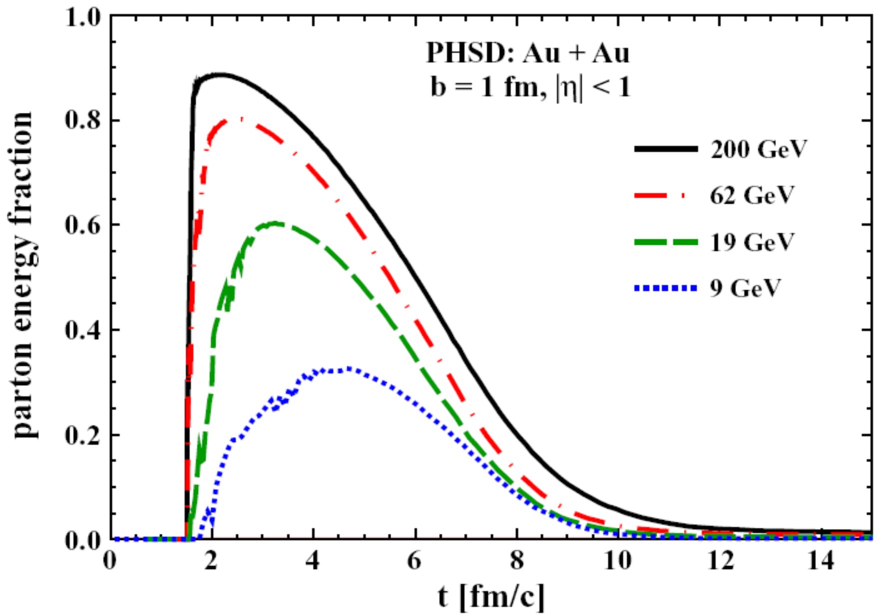

- Strong increase of partonic phase with energy from AGS to RHIC

- SPS: Pb+Pb, 160 A GeV: only about 40% of the converted energy goes to partons; the rest is contained in the large hadronic corona and leading particles
- RHIC: Au+Au, 21.3 A TeV: up to 90% - QGP

W. Cassing & E. Bratkovskaya, NPA 831 (2009) 215
V. Konchakovski et al., Phys. Rev. C 85 (2012) 011902

Non-equilibrium dynamics: description of A+A with PHSD

❑ PHSD: highlights

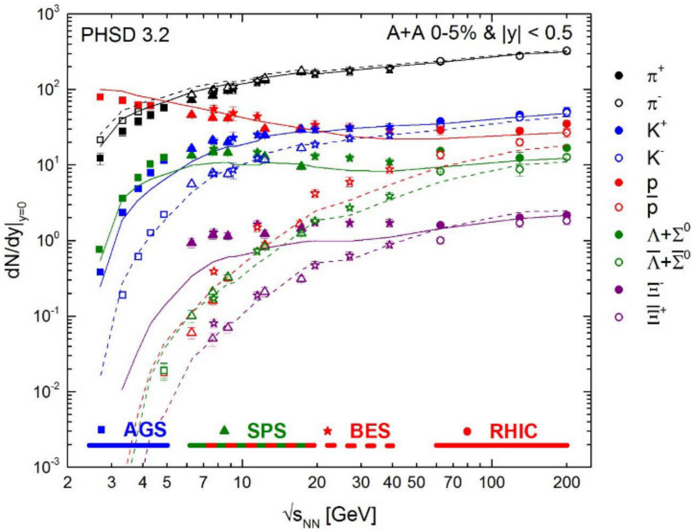

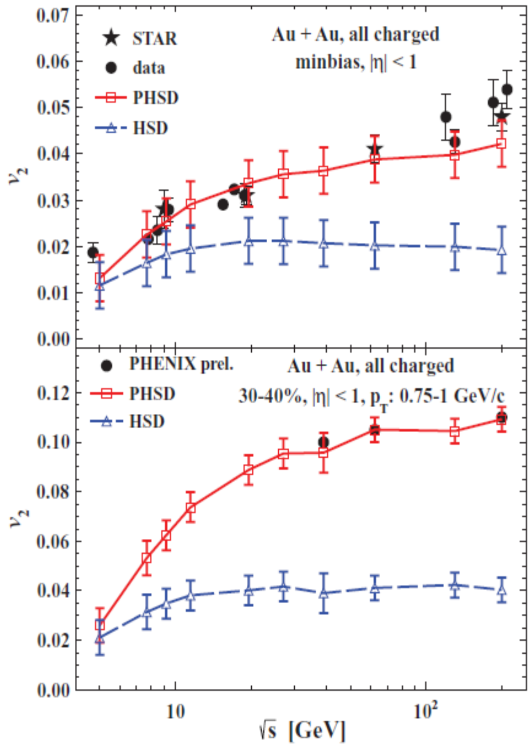

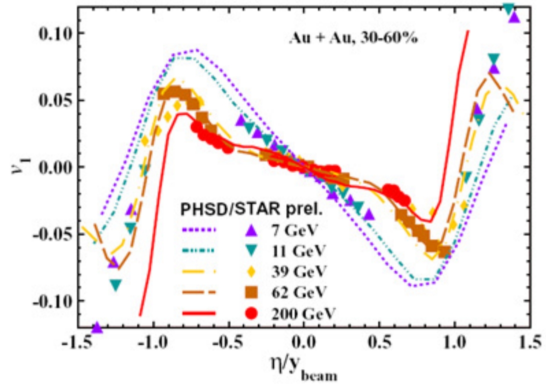

PHSD: P. Moreau

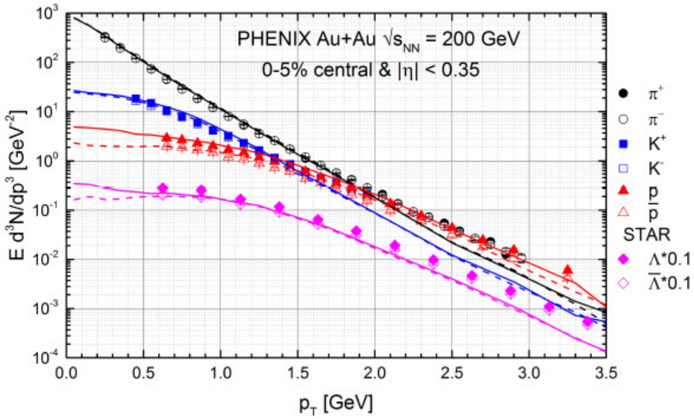

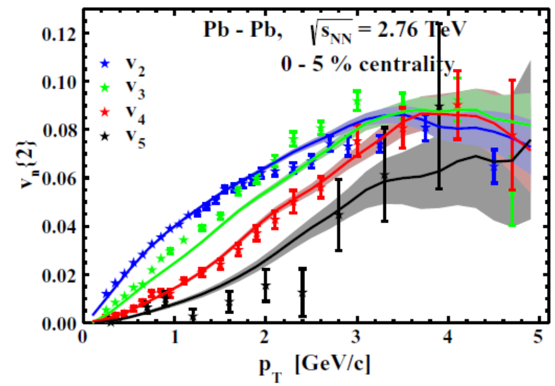

V. Konchakovski et al.,
PRC 85 (2012) 011902; JPG42 (2015) 055106

❑ **PHSD** provides a **good description of ‚bulk' observables** (y-, p_T-distributions, flow coeficients v_n, ...) from SPS to LHC

Strangeness in A+A

HSD, UrQMD, PRC 69 (2004) 032302

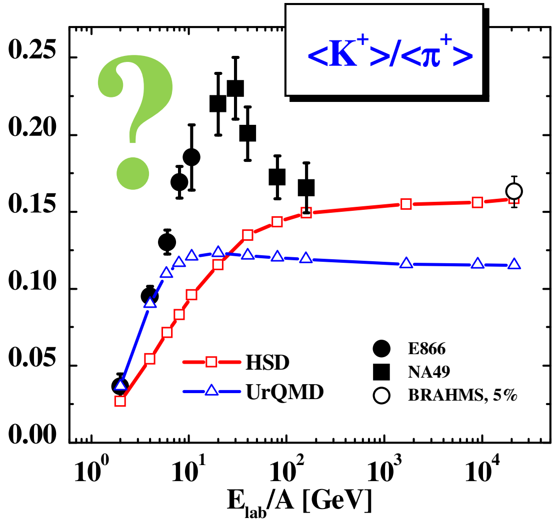

Thermal model: A. Andronic et al., NPA 834 (2010)

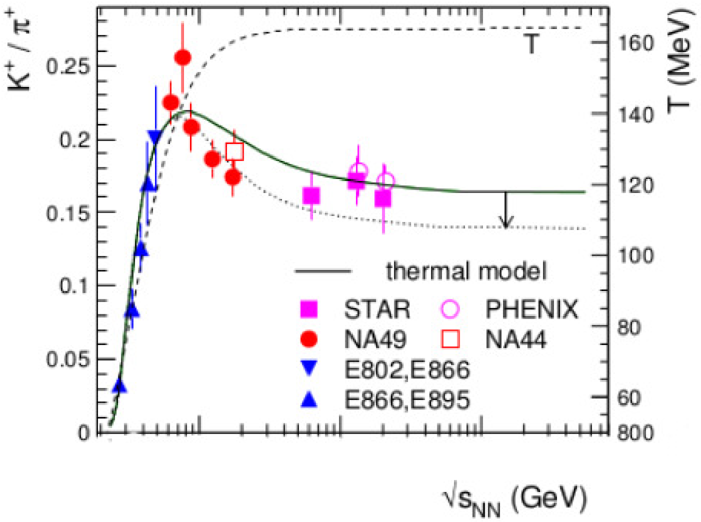

Thanks to Alessia Palmese, Pierre Moreau

K^+/π^+ 'horn'

PHSD: even when considering the creation of a QGP phase, the strangeness enhancement seen experimentally by NA49 and STAR at a bombarding energy ~20 A GeV (FAIR/NICA energies!) remains unexplained

➔ 'Horn' is not traced back to deconfinement ?!

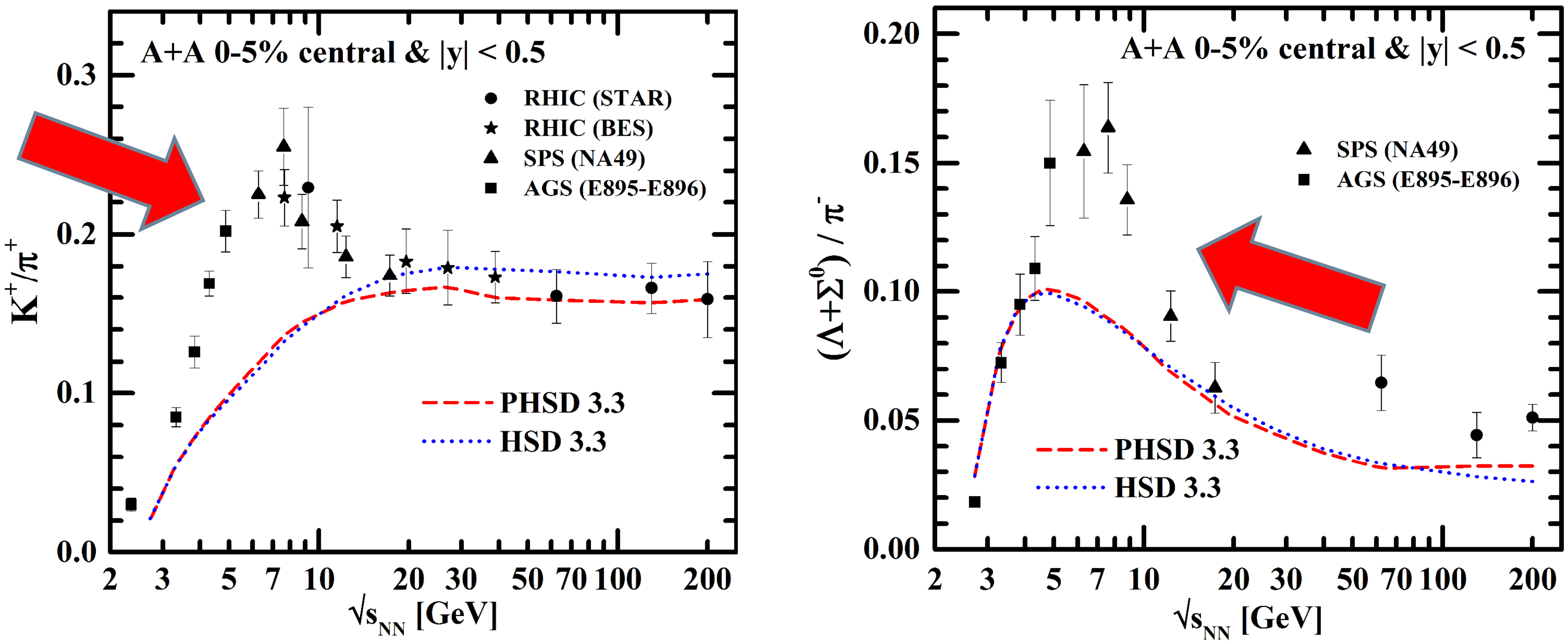

W. Cassing, A. Palmese, P. Moreau, E.L. Bratkovskaya, PRC 93, 014902 (2016), arXiv:1510.04120

‚Quark flavor chemistry‘ in the LUND string model

- **In PHSD:**
  the ‚flavor chemistry‘ of the final hadrons is mainly defined by the LUND string model

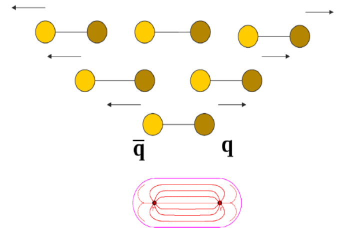

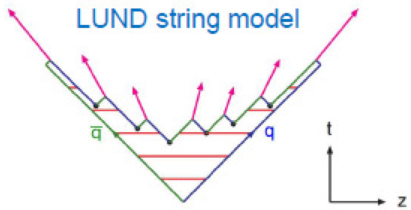

- **LUND model:**

1) ‘quark flavor chemistry’ is determined by the Schwinger-formula

According to the Schwinger-formula, the probability to form a massive $s\bar{s}$ in a string-decay is suppressed in comparison to light flavor $(u\bar{u}, d\bar{d})$:

$$\frac{P(s\bar{s})}{P(u\bar{u})} = \frac{P(s\bar{s})}{P(d\bar{d})} = \gamma_s = \exp\left(-\pi \frac{m_s^2 - m_q^2}{2\kappa}\right)$$

with κ- string tension;
in vacuum: κ~0.9 GeV/fm=0.176GeV^2

The relative production factors in PHSD/HSD are:

$$u : d : s : uu = \begin{cases} 1 : 1 : 0.3 : 0.07 & \text{at SPS to RHIC;} \\ 1 : 1 : 0.4 : 0.07 & \text{at AGS energies.} \end{cases}$$

m_s, m_q (q=u,d) – constituent (‘dressed’) quark masses

2) ‘Kinematics’ is determined by the fragmentation function f (x,m_T)

$$f(x, m_T) \approx \frac{1}{x}(1 - x^a)exp(-bm_T^2/x)$$

W. Cassing, A. Palmese, P. Moreau, E.L. Bratkovskaya, PRC 93, 014902 (2016), arXiv:1510.04120

Schwinger mechanism in vacuum

I. In vacuum (e.g. p+p collisions) :

- 'dressing' of bare quark masses is due to the coupling to the vacuum scalar quark condensate (cf. Dyson-Schwinger Bethe-Salpeter approaches)

$$m_q^V = m_q^0 - g_s < q\bar{q} >_V$$

bare quark masses:
$m_u^0 = m_d^0 \approx 7\,MeV,\ m_s^0 \approx 100MeV$

- vacuum scalar quark condensate is fixed by Gell-Mann-Oakes-Renner relation:

$$f_\pi^2 m_\pi^2 = -\frac{1}{2}(m_u^0 + m_d^0) < \bar{q}q >_V \Rightarrow < \bar{q}q >_V \approx -3.2\, fm^{-3}$$

f_π and m_π are the pion decay constant and pion mass

→ Constituent quark masses in vacuum : $m_q \equiv m_q^V$

$$\boxed{m_u^V = m_d^V \approx 0.35GeV, \quad m_s^V \approx 0.5GeV}$$

W. Cassing, A. Palmese, P. Moreau, E.L. Bratkovskaya, PRC 93, 014902 (2016), arXiv:1510.04120

Schwinger mechanism in medium

II. In medium (e.g. A+A collisions) :

- **In the presence of a hot and dense hadronic medium, the degrees of freedom modify their properties, e.g. the in-medium constituent masses:**

$$m_s^* = m_s^0 + (m_s^v - m_s^0)\frac{\langle q\bar{q}\rangle}{\langle q\bar{q}\rangle_V} \qquad m_q^* = m_q^0 + (m_q^v - m_q^0)\frac{\langle q\bar{q}\rangle}{\langle q\bar{q}\rangle_V}$$

- **The scalar quark condensate $\langle q\bar{q}\rangle$ is viewed as an order parameter for the restoration of chiral symmetry:**

$$<\bar{q}q> = \begin{cases} \neq 0 & \text{chiral non-symmetric phase;} \\ = 0 & \text{chiral symmetric phase.} \end{cases}$$

- **The behavior of the scalar quark condensate $\langle q\bar{q}\rangle$ in the hadronic medium (baryons + mesons) can be obtained e.g. from the non-linear $\sigma - \omega$ model**

See B. Friman et al., Eur. Phys. J. A 3, 165, 1998

$$\frac{\langle q\bar{q}\rangle}{\langle q\bar{q}\rangle_V} = 1 - \underbrace{\frac{\Sigma_\pi}{f_\pi^2 m_\pi^2}\rho_S}_{\text{baryonic medium}} - \underbrace{\sum_h \frac{\sigma_h \rho_S^h}{f_\pi^2 m_\pi^2}}_{\text{mesonic medium}}$$

where ρ_s is the scalar nucleon density (depends on EoS)
$\Sigma_\pi \approx 45$ MeV is the pion-nucleon Σ-term
$\sigma_h = m_\pi/2$ for light mesons; $= m_\pi/4$ - strange mesons

- **pion-nucleon Σ-term : 45 MeV**

Yi-Bo Yang et al., arXiv 1511.09089

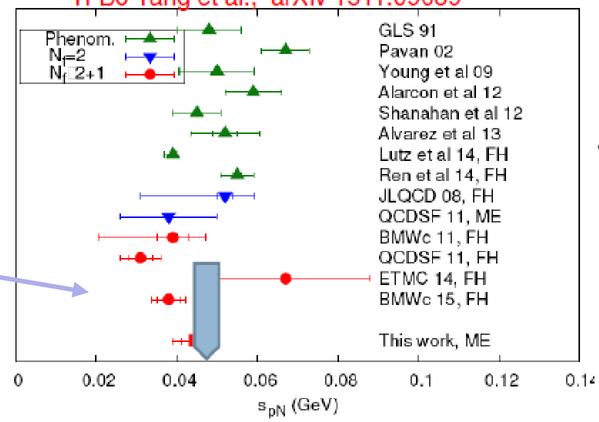

W. Cassing, A. Palmese, P. Moreau, E.L. Bratkovskaya, PRC 93, 014902 (2016), arXiv:1510.04120

Scalar density in PHSD

1) ρ_s is the **scalar density of baryonic matter:**

d = 4 in case of isospin symmetric nuclear matter

$$\rho_s = d \int \frac{d^3p}{(2\pi)^3} \frac{m_N^*(x)}{\sqrt{p^2 + m_N^{*2}}} f_N(x, \mathbf{p})$$

where in-medium nucleon mass is

$$m_N^*(x) = m_N^V - g_s \sigma(x)$$

with m^V_N denoting the nucleon mass in vacuum
Scalar field $\sigma(x)$ mediates the scalar interaction with the surrounding medium with g_s coupling.
$\sigma(x)$ is defined determined locally by the nonlinear gap equation:

$$m_\sigma^2 \sigma(x) + B\sigma^2(x) + C\sigma^3(x) = g_s \rho_S = g_s d \int \frac{d^3p}{(2\pi)^3} \frac{m_N^*(x)}{\sqrt{p^2 + m_N^{*2}}} f_N(x, \mathbf{p})$$

Within the non-linear $\sigma - \omega$ model for nuclear matter, the parameters g_s, m_σ, B, C can be fixed in order to reproduce the main nuclear matter quantities at saturation, i.e. saturation density, binding energy per nucleon, compression modulus and the effective nucleon mass.

2) ρ_s^h **is the scalar density of mesons of type h (from PHSD):**

$$\rho_S^h(x) = \frac{(2s+1)(2t+1)}{(2\pi)^3} \int d^3\mathbf{p} \frac{m_h}{\sqrt{\mathbf{p}^2 + m_h^2}} f_h(x, \mathbf{p})$$

W. Cassing, A. Palmese, P. Moreau, E.L. Bratkovskaya, PRC 93, 014902 (2016), arXiv:1510.04120

Modeling of the chiral symmetry restoration in PHSD

- In the Schwinger formula the in-medium constituent masses $m^*_{q;s} \rightarrow m_{q;s}$ have to be considered:

$$\frac{P(s\bar{s})}{P(u\bar{u})} = \frac{P(s\bar{s})}{P(d\bar{d})} = \gamma_s = \exp\left(-\pi\frac{m_s^2 - m_q^2}{2\kappa}\right)$$

scalar quark condensate $\langle q\bar{q}\rangle$ for NL3

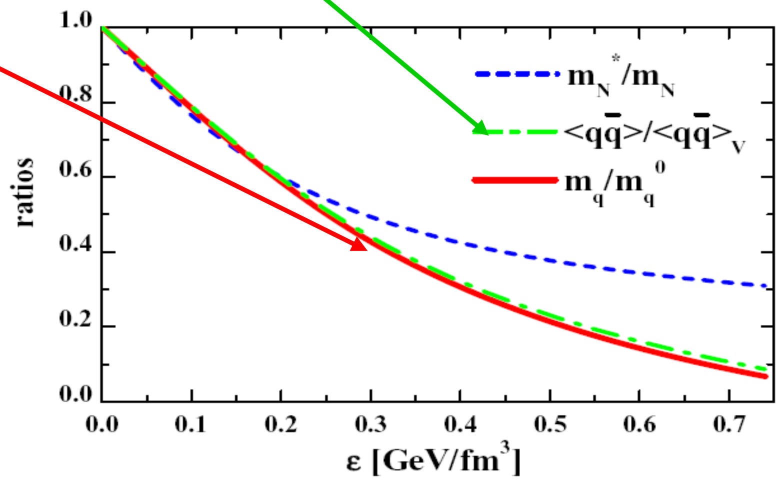

- As a consequence of the chiral symmetry restoration (CSR), the strangeness production probability increases with the energy density ε.

1) Scenario 'HSD' – assume NO QGP:

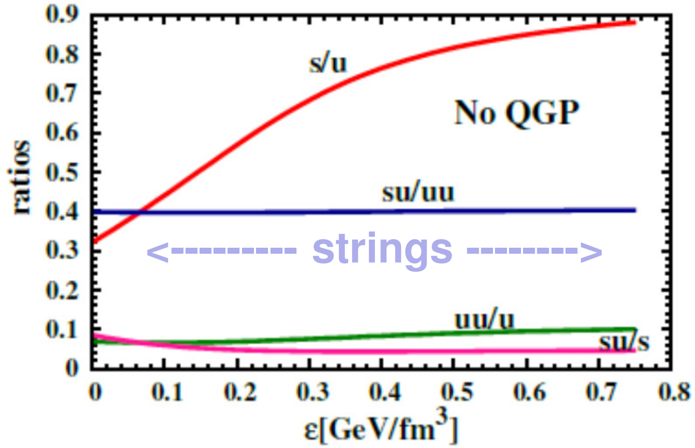

2) Scenario 'PHSD' – CSR+QGP:

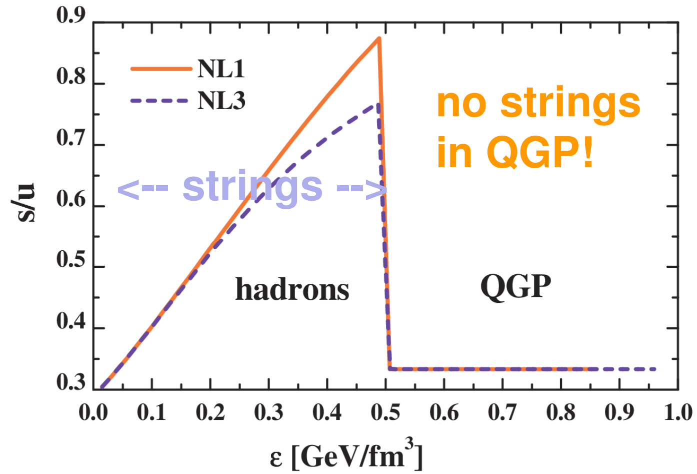

W. Cassing, A. Palmese, P. Moreau, E.L. Bratkovskaya, PRC 93, 014902 (2016), arXiv:1510.04120

Pb+Pb @ 30 AGeV – 0-5% central

Ratio of the quark scalar condensate compared to vacuum as a function of time:

$$\frac{< q\,\bar{q} >}{< q\,\bar{q} >_V}$$

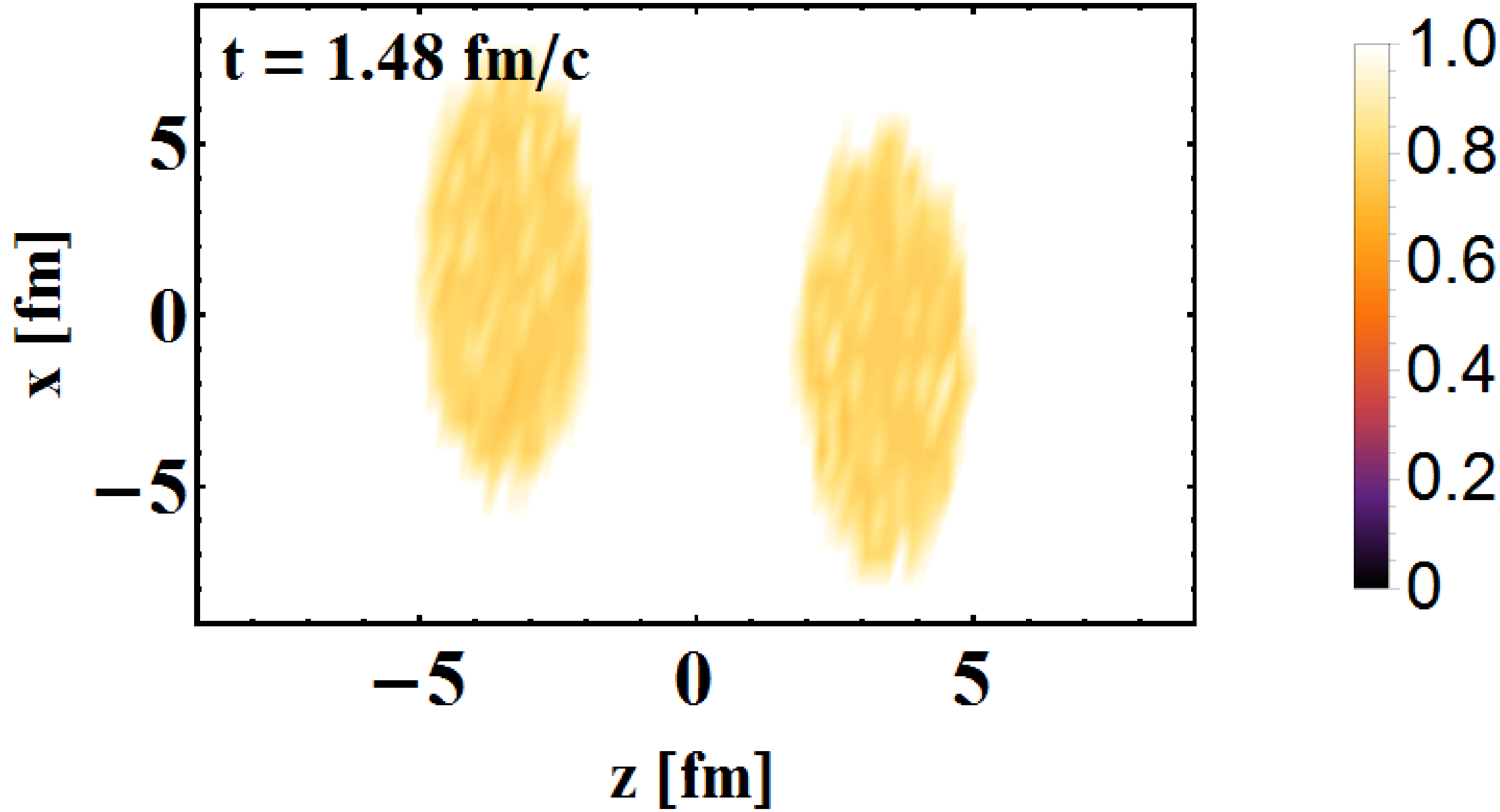

Pb+Pb @ 30 AGeV – 0-5% central

Ratio of the quark scalar condensate compared to vacuum as a function of time:

$$\frac{<q\bar{q}>}{<q\bar{q}>_V}$$

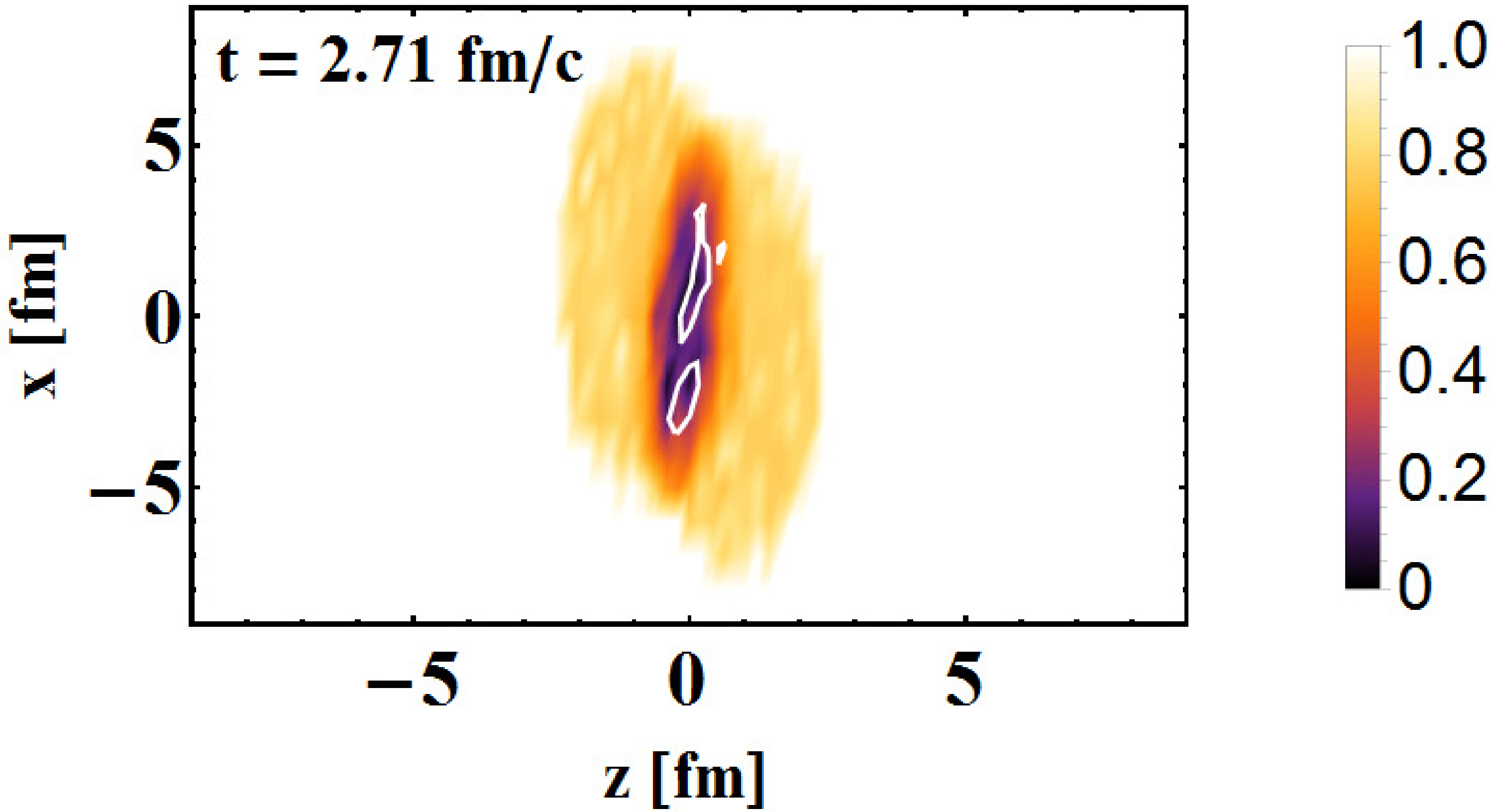

Pb+Pb @ 30 AGeV – 0-5% central

Ratio of the quark scalar condensate compared to vacuum as a function of time:

$$\frac{<q\,\bar{q}>}{<q\,\bar{q}>_V}$$

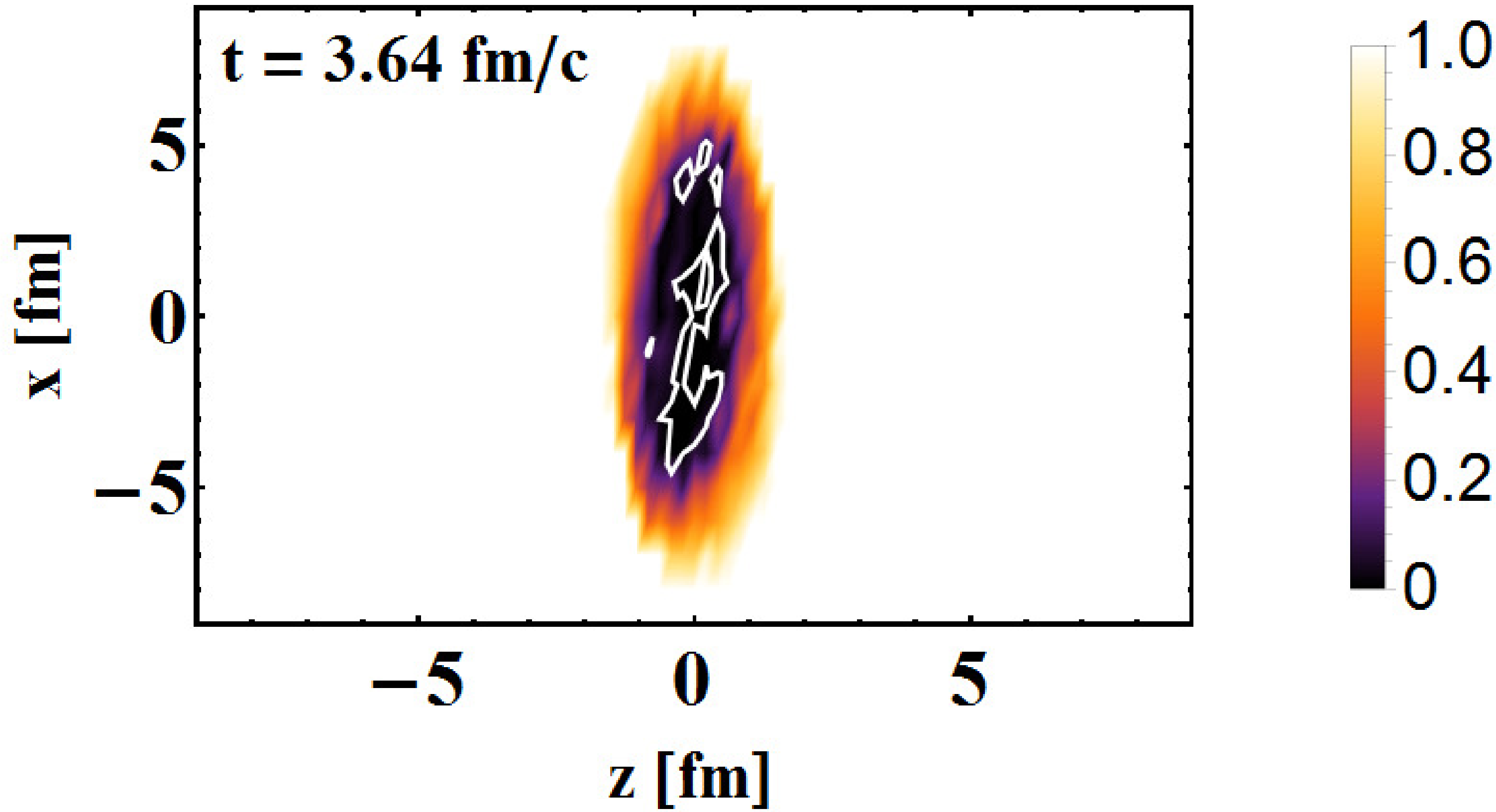

Pb+Pb @ 30 AGeV – 0-5% central

Ratio of the quark scalar condensate compared to vacuum as a function of time:

$$\frac{< q\,\bar{q} >}{< q\,\bar{q} >_V}$$

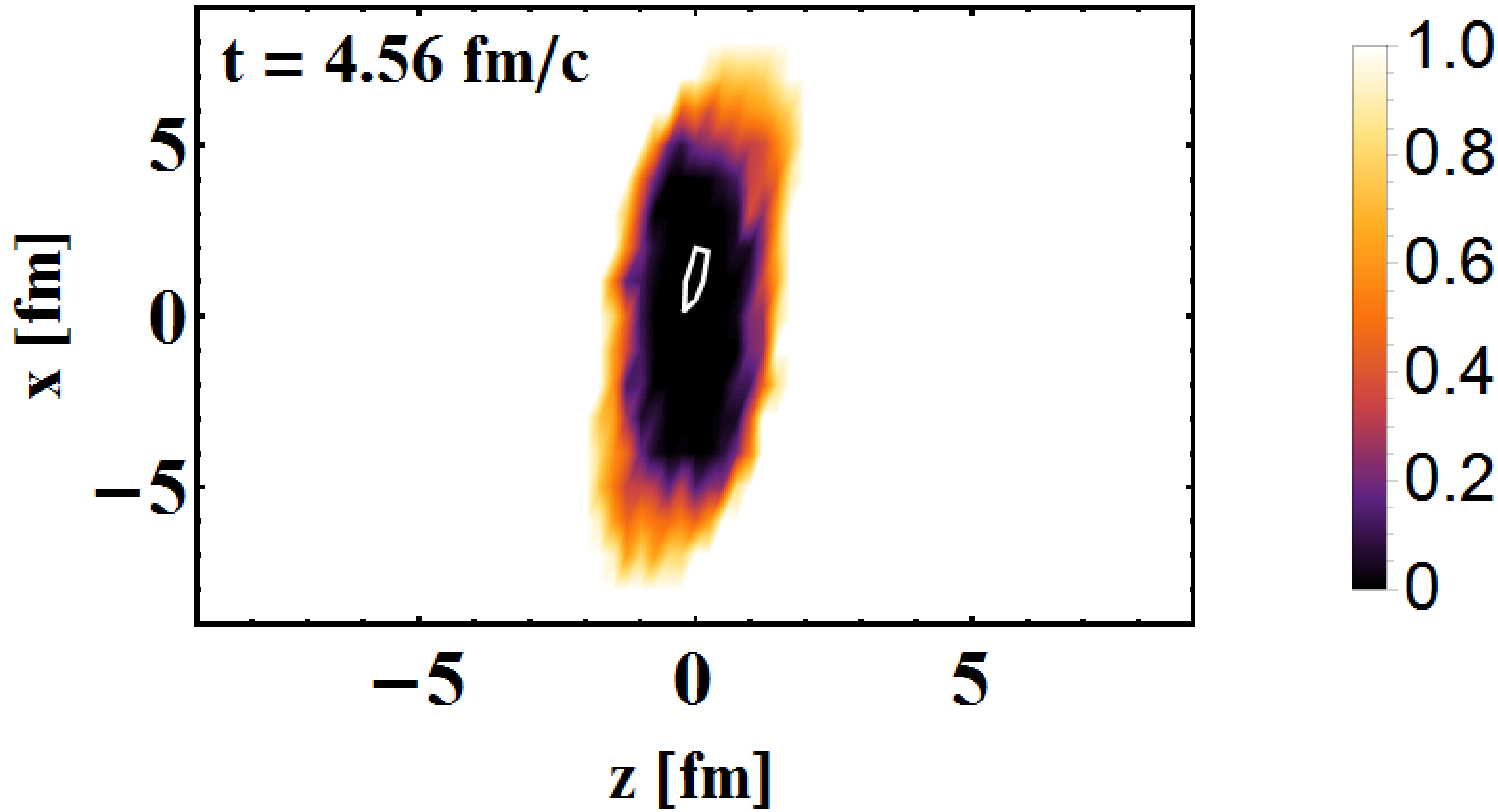

Pb+Pb @ 30 AGeV – 0-5% central

Ratio of the quark scalar condensate compared to vacuum as a function of time:

$$\frac{< q\,\bar{q} >}{< q\,\bar{q} >_V}$$

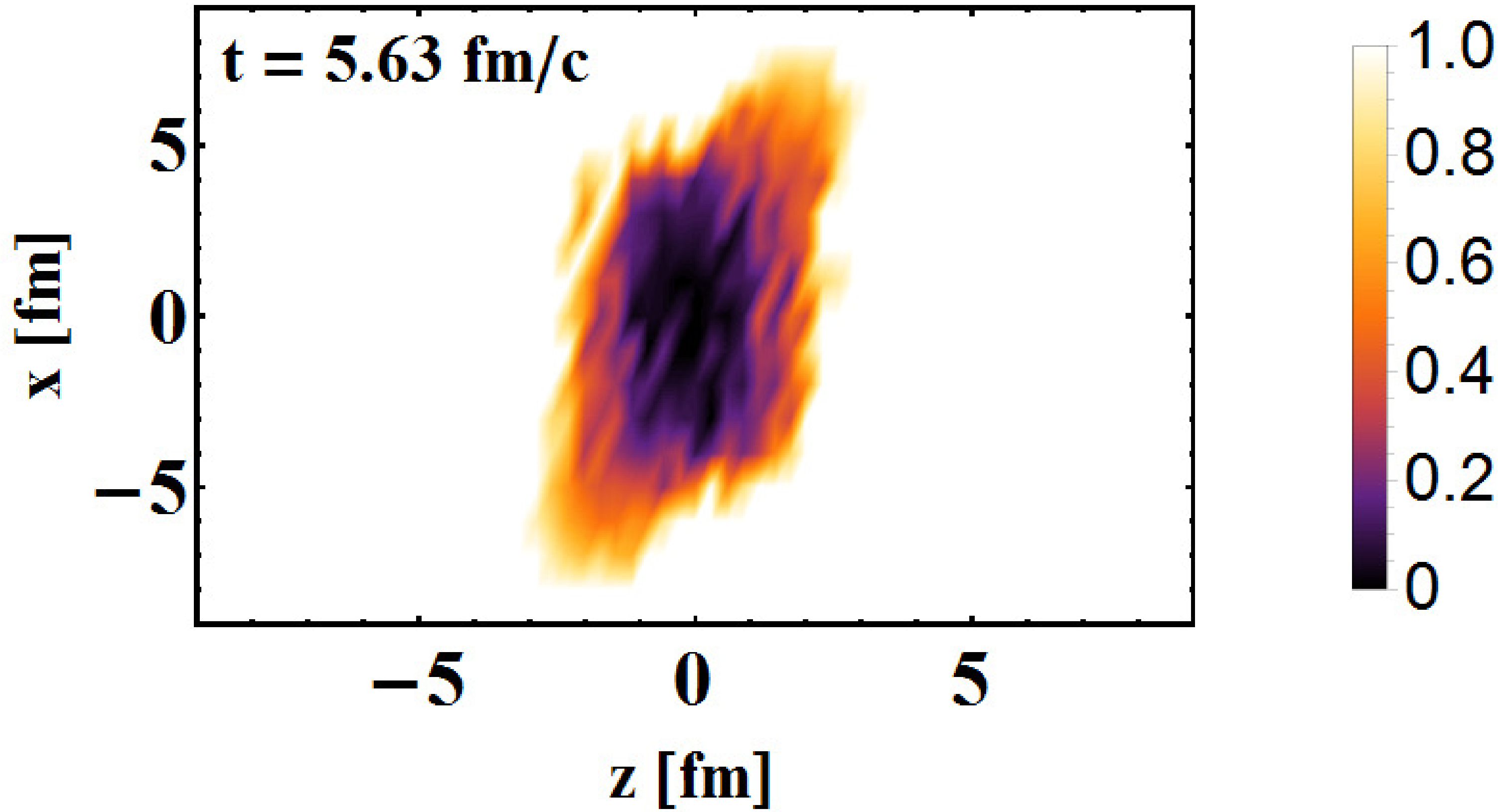

Pb+Pb @ 30 AGeV – 0-5% central

Ratio of the quark scalar condensate compared to vacuum as a function of time:

$$\frac{< q\,\bar{q} >}{< q\,\bar{q} >_V}$$

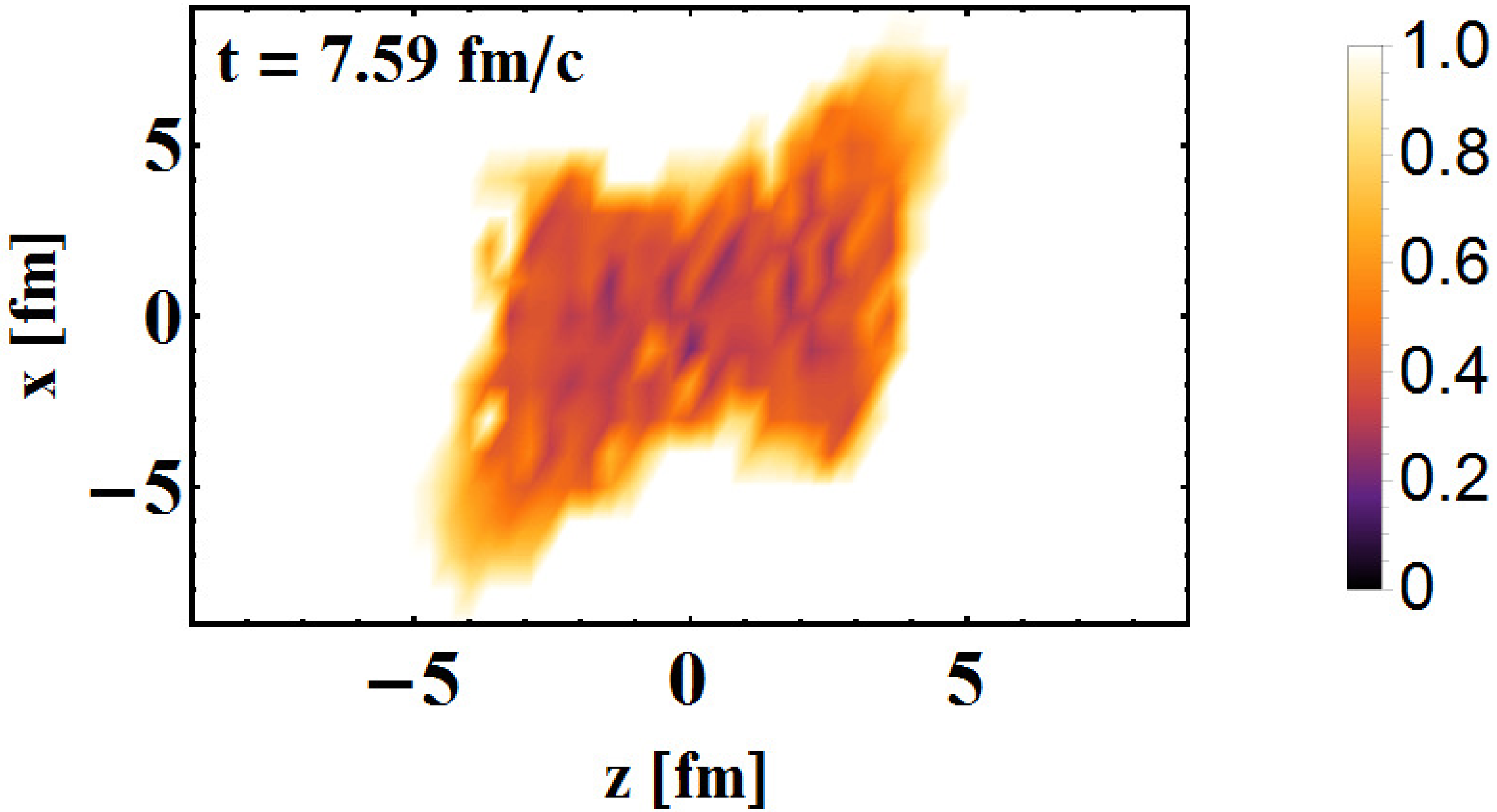

Pb+Pb @ 30 AGeV – 0-5% central

Ratio of the quark scalar condensate compared to vacuum as a function of time:

$$\frac{< q\,\bar{q} >}{< q\,\bar{q} >_V}$$

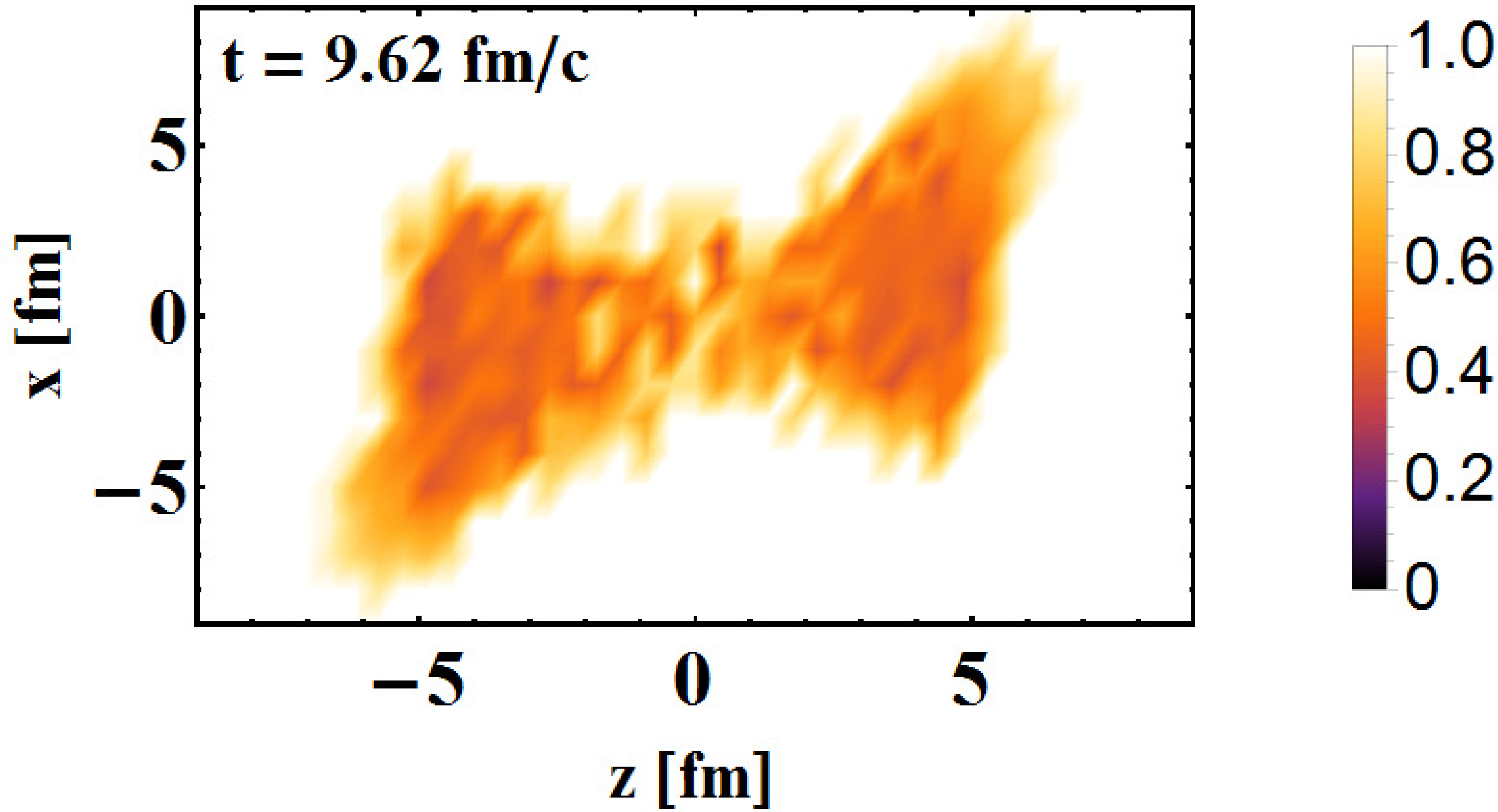

Pb+Pb @ 30 AGeV – 0-5% central

Ratio of the quark scalar condensate compared to vacuum as a function of time:

$$\frac{< q\,\bar{q} >}{< q\,\bar{q} >_V}$$

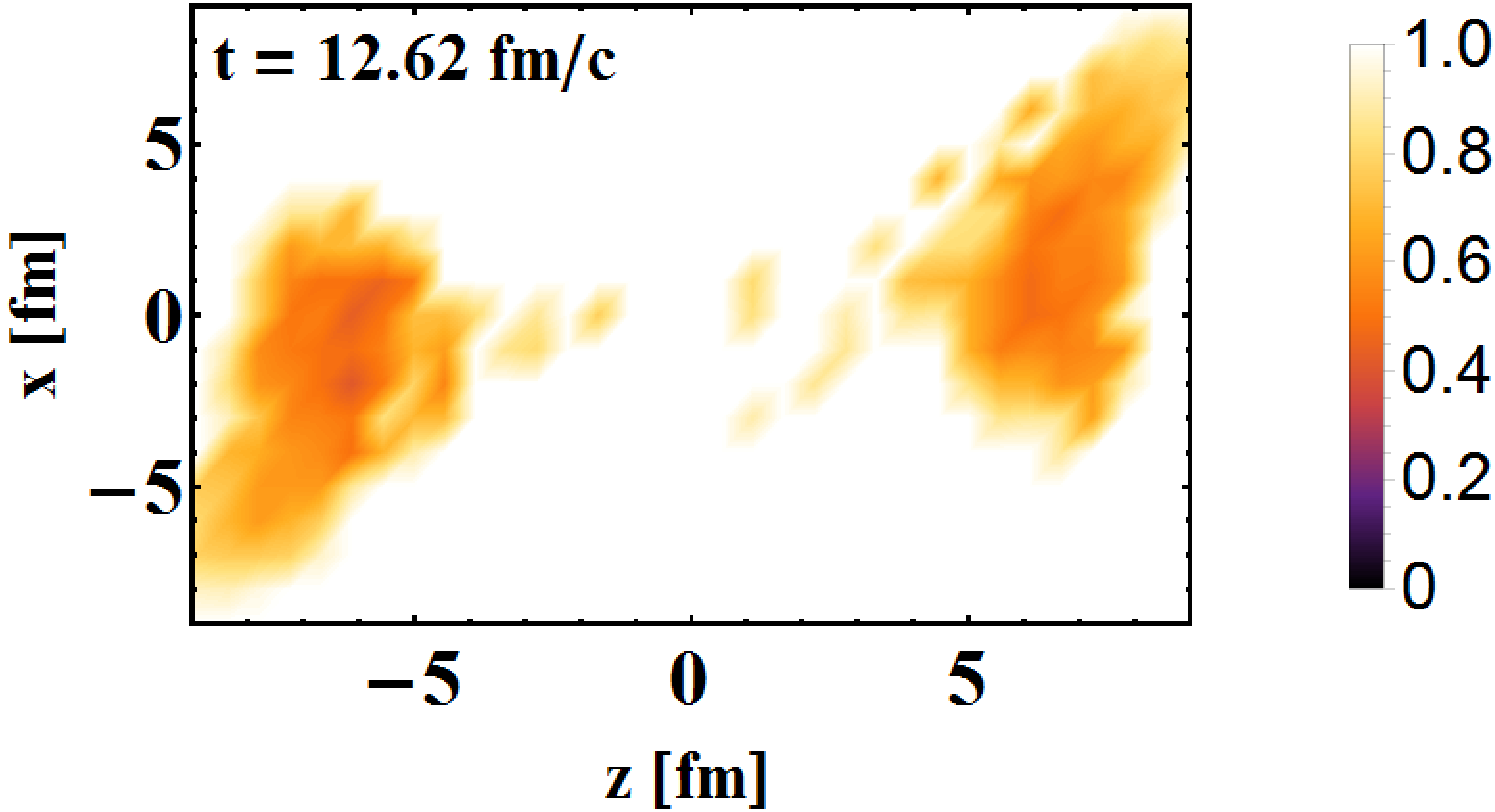

PHSD results with chiral symmetry restoration

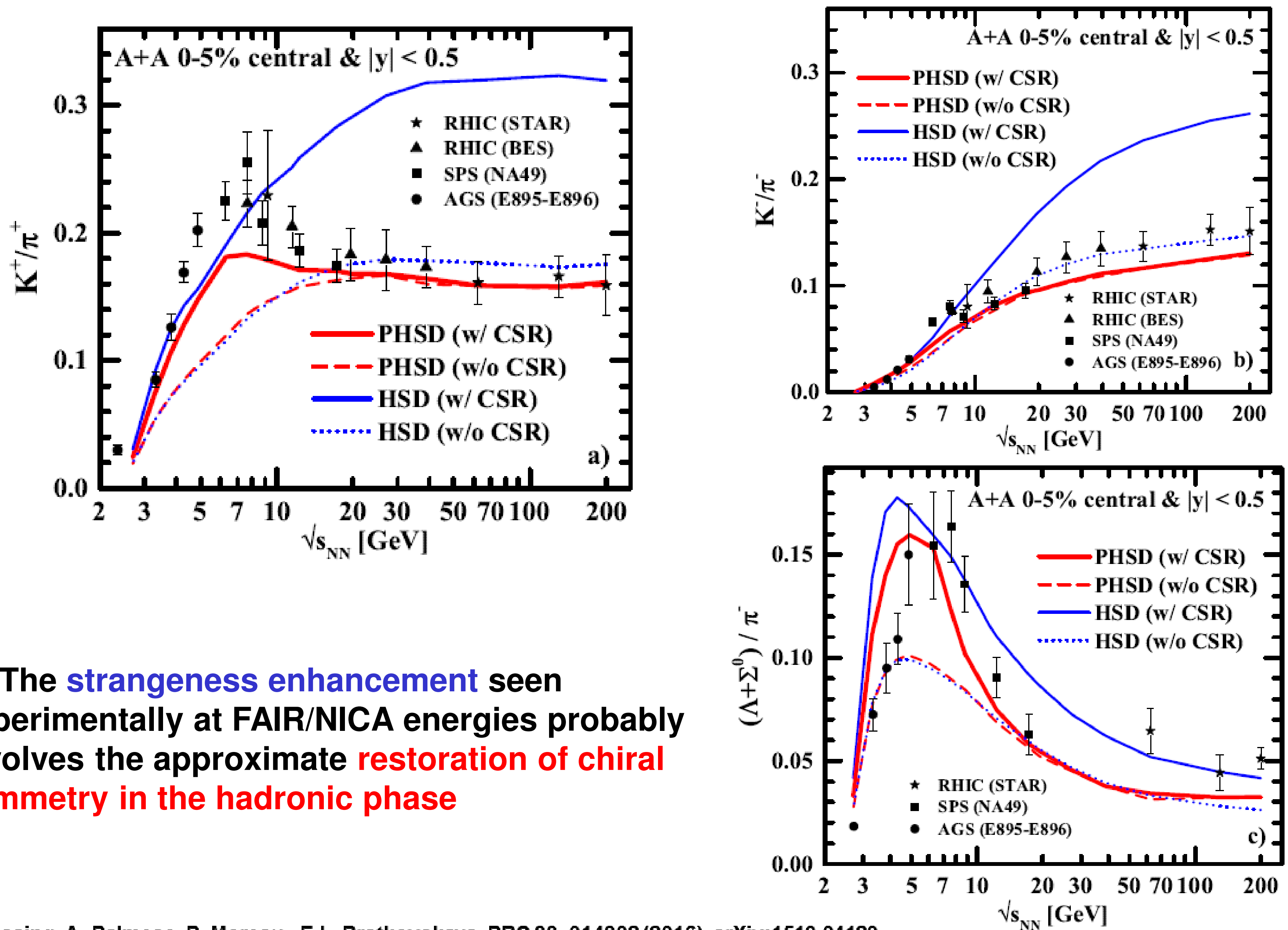

➔ The strangeness enhancement seen experimentally at FAIR/NICA energies probably involves the approximate restoration of chiral symmetry in the hadronic phase

W. Cassing, A. Palmese, P. Moreau, E.L. Bratkovskaya, PRC 93, 014902 (2016), arXiv:1510.04120

Excitation function of hadron ratios

Alessia Palmese, Pierre Moreau:

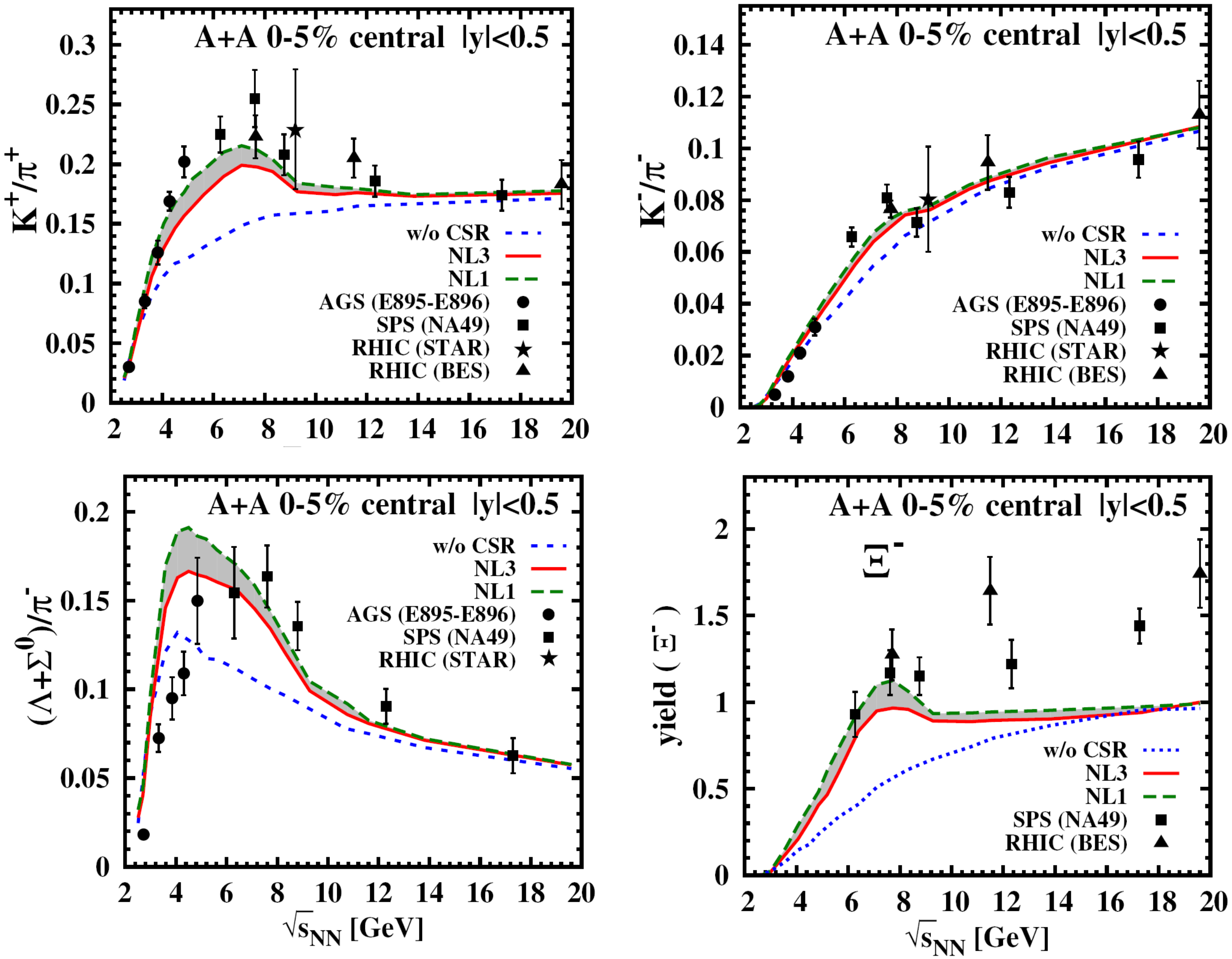

→ **low sensitivity to the nuclear EoS**

Summary I

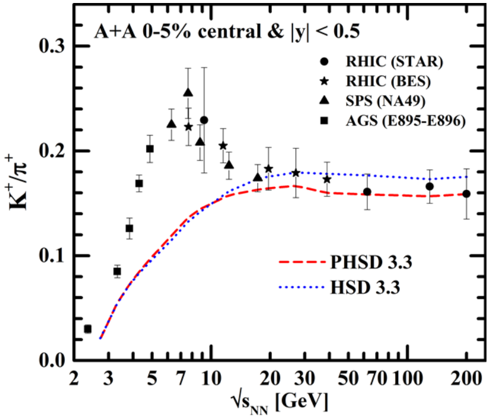

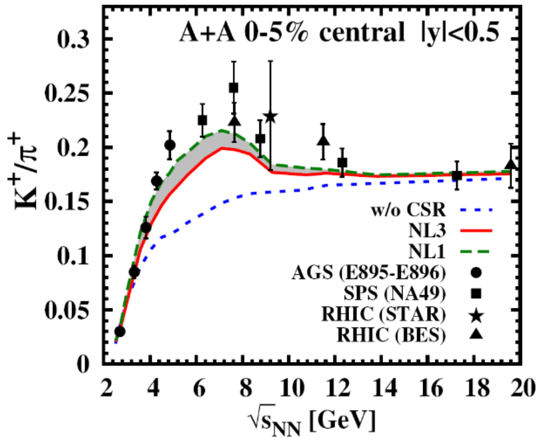

- The strangeness enhancement seen experimentally by NA49 and STAR at a bombarding energy ~20 A GeV (FAIR/NICA energies!) cannot be attributed to deconfinement

- Including essential aspects of chiral symmetry restoration in the hadronic phase, we observe a rise in the K^+/π^+ ratio at low $\sqrt{s_{NN}}$ and then a drop due to the appearance of a deconfined partonic medium → a 'horn' emerges

Charm
in A+A

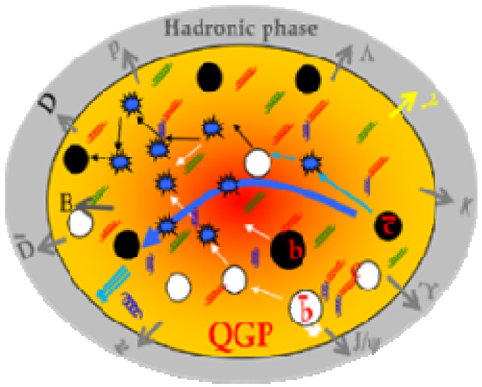

Thanks to Taesoo Song, Hamza Berrehrah

Tomography of QGP by heavy quarks

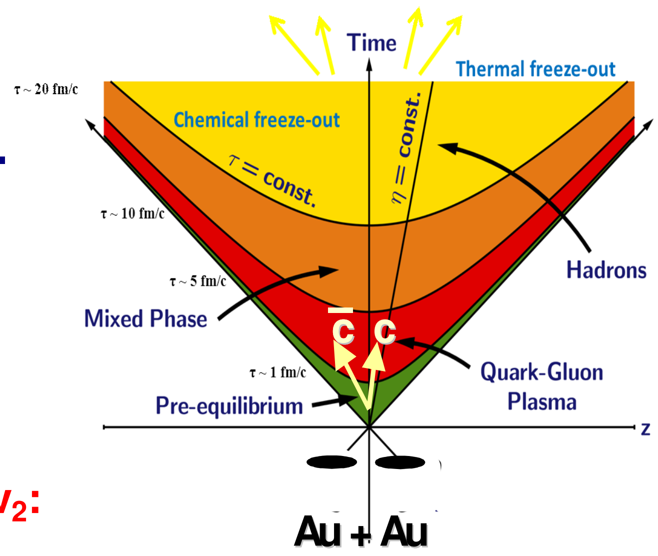

- Hope to use **'heavy quark probes'** for a **tomography of the early stage of the QGP**

- **Experimental signals:**

  1. Nuclear modification factor:

$$R_{AA}(p_T) \equiv \frac{dN_D^{Au+Au}/dp_T}{N_{\rm binary}^{Au+Au} \times dN_D^{p+p}/dp_T}$$

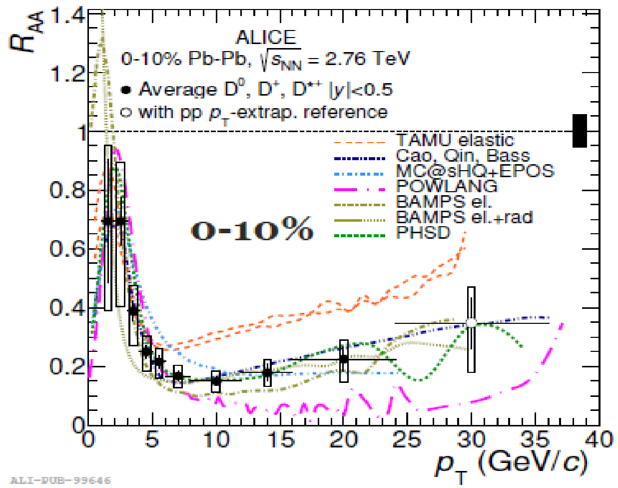

  2. Elliptic flow v_2:

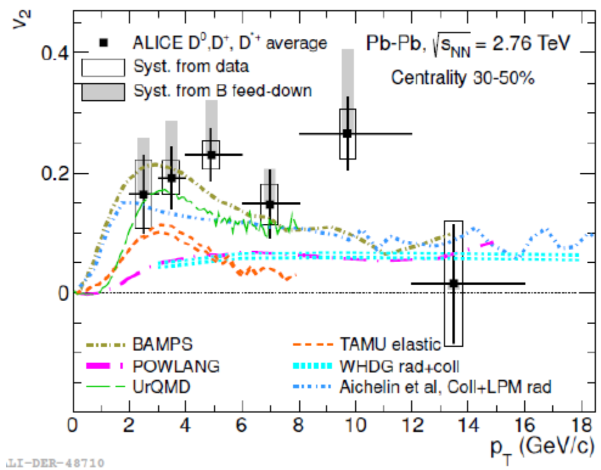

- **What is the origin for the "energy loss" of charm at large p_T?**

  Collisional energy loss (elastic scattering Q+q→Q+q)
  vs **radiative** (gluon bremsstrahlung Q+q→Q+q+g) ?

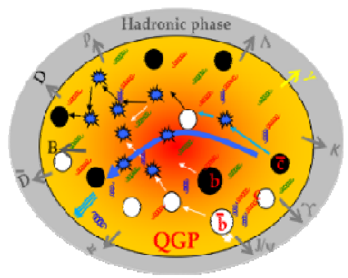

➔ **Challenge for theory:** simultaneous description of R_{AA} and v_2 !

Dynamics of heavy quarks in A+A

1. **Production of heavy (charm and bottom) quarks in initial binary collisions**

2. **Interactions in the QGP:**
   elastic scattering Q+q→Q+q → collisional energy loss
   gluon bremsstrahlung Q+q→Q+q+g → radiative energy loss

3. **Hadronization: c/cbar quarks →D(D*)-mesons: coalescence vs fragmentation**

4. **Hadronic interactions:**
   D+baryons; D+mesons

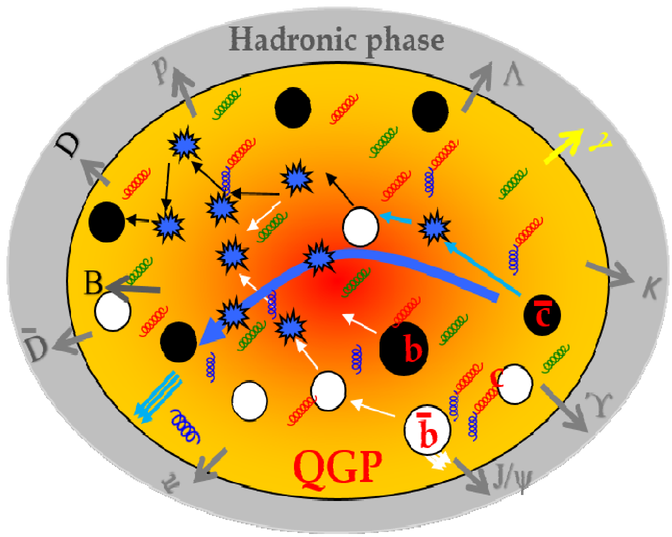

The goal: to model the dynamics of charm quarks/mesons in all phases on a microscopic basis

The tool: PHSD approach

Heavy quark/hadrons production in p+p collisions

1) Momentum distribution of heavy quarks: use ‚tuned' PYTHIA event generator to reproduce FONLL (fixed-order next-to-leading log) results (R. Vogt et al.)

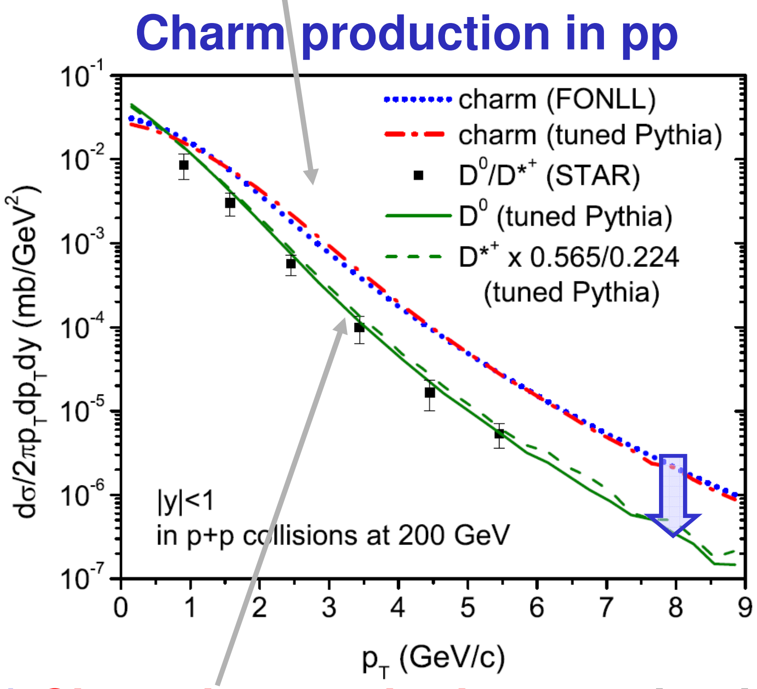

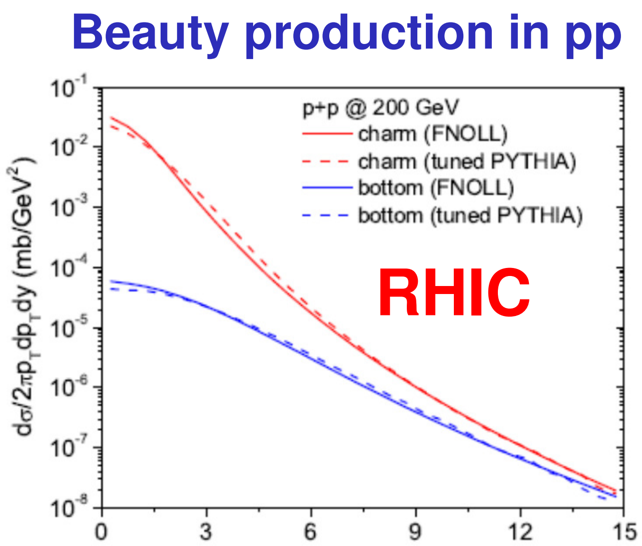

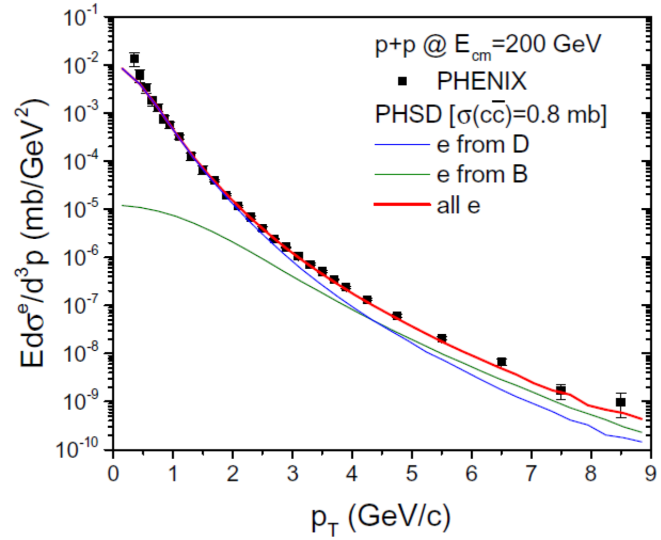

2) Charm/beauty hadron production in pp by heavy-quark fragmentation:

D^0 20 %
D^+ 17.4 %
D^{*0} 21.3 %
D^{*+} 22.4 %
Ds^+ 8 %
Λ_c 9.4 %

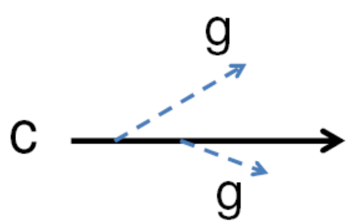

T. Song et al., PRC 92 (2015) 014910, arXiv:1503.03039

Heavy quark scattering in the QGP (DQPM)

- Elastic scattering with **off-shell massive partons Q+q(g)→Q+q(g)**

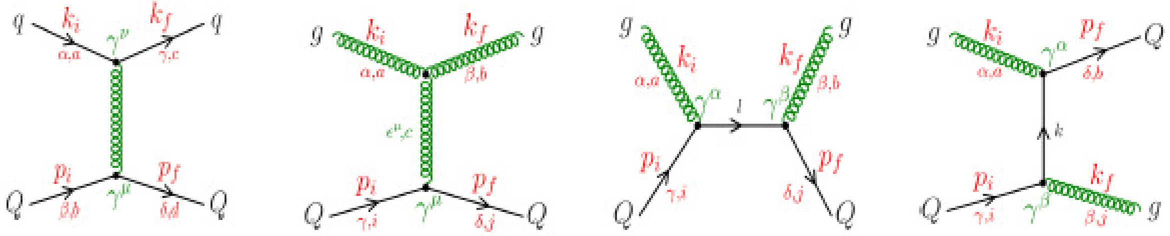

Non-perturbative QGP!

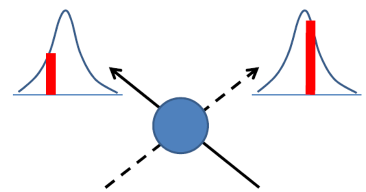

- **Elastic cross section uc→uc**

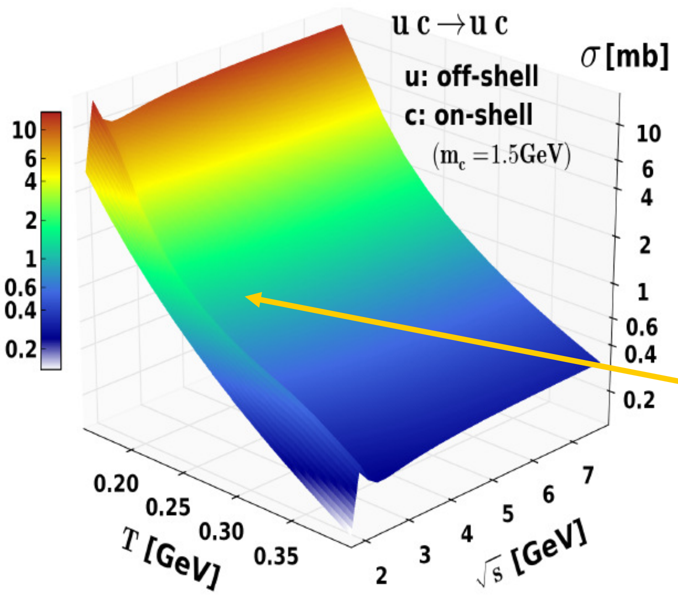

- **Distributions of Q+q, Q+g collisions vs $s^{1/2}$ in Au+Au, 10% central**

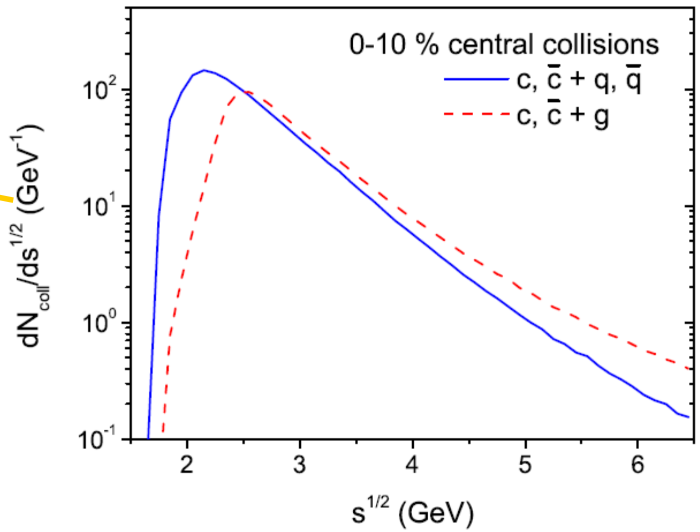

H. Berrehrah et al, PRC 89 (2014) 054901;
PRC 90 (2014) 051901; PRC90 (2014) 064906

Heavy quark scattering in the QGP

- **Differential elastic cross section** for uc→uc for $s^{1/2}$=3 and 4 GeV at 1.2T_C, 2T_C and 3T_C

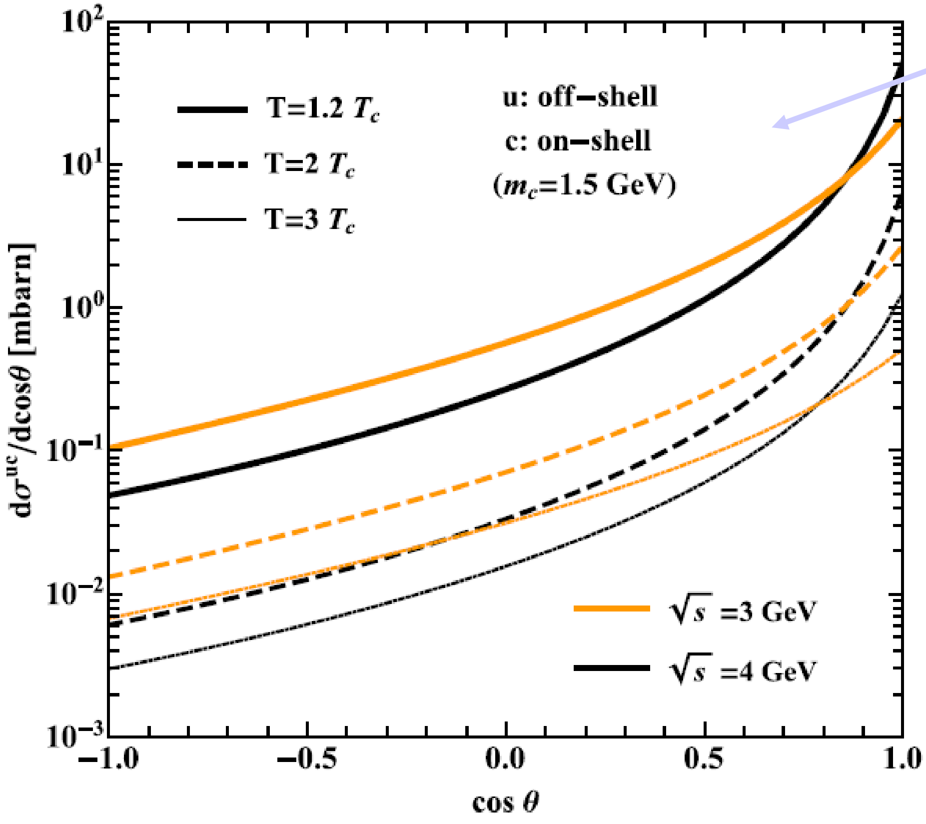

- **DQPM - anisotropic angular distribution**

Note: pQCD - strongly forward peaked
→ Differences between DQPM and pQCD :
less forward peaked angular distribution leads to more efficient momentum transfer

- **Central Au+Au, 200 A GeV:**
  N(cc) ~19 pairs,
  N(Q+q)~130, N(Q+g) ~85 collisions
  → each charm quark makes ~ 6 elastic collisions

→ Smaller number (compared to pQCD) of elastic scatterings with massive partons leads to a large energy loss

! Note: radiative energy loss is NOT included yet in PHSD,
it is expected to be small due to the large gluon mass in the DQPM

H. Berrehrah et al, PRC 89 (2014) 054901; PRC 90 (2014) 051901; PRC90 (2014) 064906

Hadronization of heavy quarks in A+A

❑ **PHSD: if the local energy density $\varepsilon \rightarrow \varepsilon_C$ ➔ hadronization of heavy quarks to hadrons**

T. Song et al., PRC 93 (2016) 034906

Dynamical hadronization scenario for heavy quarks :

coalescence with <r>=0.9 fm & **fragmentation**
$0.4 < \varepsilon < 0.75$ GeV/fm^3 $\varepsilon < 0.4$ GeV/fm^3

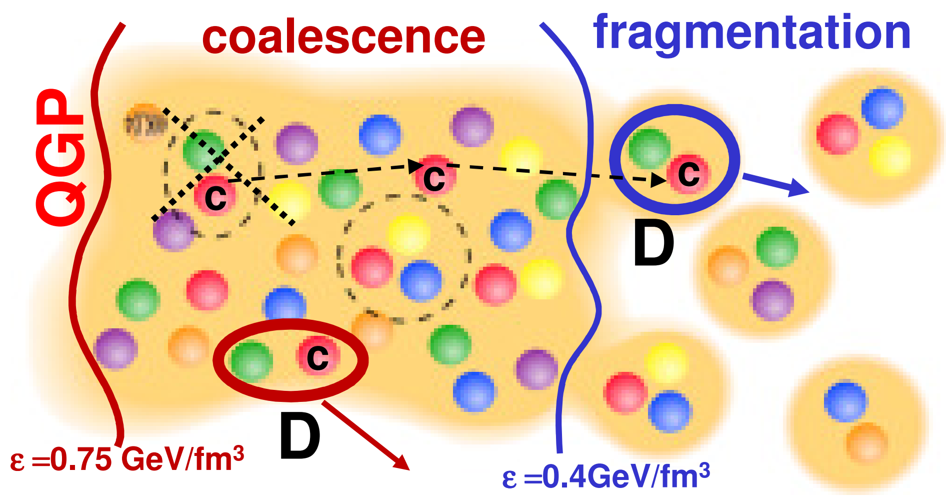

Coalescence probability in Au+Au at LHC

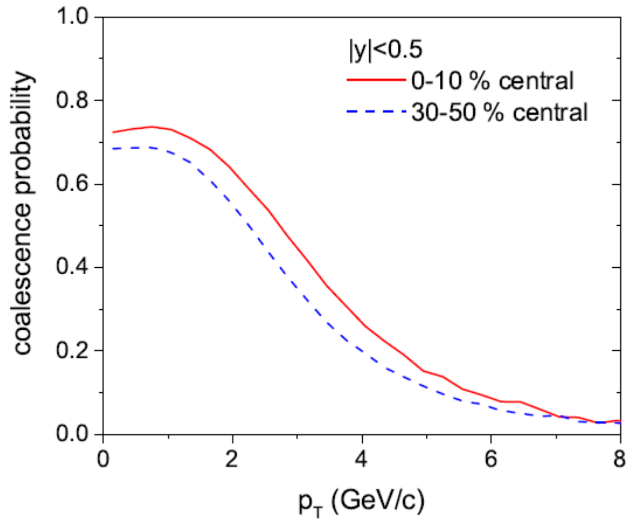

Coalescence probability for $c+\bar{q} \rightarrow D$

$$f(\boldsymbol{\rho}, \mathbf{k}_\rho) = \frac{8 g_M}{6^2} \exp\left[-\frac{\boldsymbol{\rho}^2}{\delta^2} - \mathbf{k}_\rho^2 \delta^2\right]$$

where $\boldsymbol{\rho} = \frac{1}{\sqrt{2}}(\mathbf{r}_1 - \mathbf{r}_2), \quad \mathbf{k}_\rho = \sqrt{2}\,\frac{m_2 \mathbf{k}_1 - m_1 \mathbf{k}_2}{m_1 + m_2}$

Width δ ← from root-mean-square radius of meson <r>:

$$\langle r^2 \rangle = \frac{3}{2} \frac{m_1^2 + m_2^2}{(m_1 + m_2)^2} \delta^2$$

Degeneracy factor : g_M = 1 for D, = 3 for $D^* = D^*_0(2400)^0$, $D^*_1(2420)^0$, $D^*_2(2460)^{0\pm}$

Modelling of D-meson scattering in the hadronic gas

1. D-meson scattering with mesons

Model: effective chiral Lagrangian approach with heavy-quark spin symmetry

L. M. Abreu, D. Cabrera, F. J. Llanes-Estrada, J. M. Torres-Rincon, Annals Phys. 326, 2737 (2011)

Interaction of D=(D^0,D^+,D^+_s) and D*=(D^{*0},D^{*+},D^{*+}_s) with octet (π,K,Kbar,η) :

$$\begin{aligned}\mathcal{L}_{LO} &= \langle \nabla^\mu D \nabla_\mu D^\dagger \rangle - m_D^2 \langle D D^\dagger \rangle - \langle \nabla^\mu D^{*\nu} \nabla_\mu D^{*\dagger}_\nu \rangle \\ &+ m_D^2 \langle D^{*\mu} D^{*\dagger}_\mu \rangle + ig \langle D^{*\mu} u_\mu D^\dagger - D u^\mu D^{*\dagger}_\mu \rangle \\ &+ \frac{g}{2m_D} \langle D^*_\mu u_\alpha \nabla_\beta D^{*\dagger}_\nu - \nabla_\beta D^*_\mu u_\alpha D^{*\dagger}_\nu \rangle \epsilon^{\mu\nu\alpha\beta}\end{aligned}$$

with

$$u_\mu = i\left(u^\dagger \partial_\mu u - u \partial_\mu u^\dagger\right)$$

$$U = u^2 = \exp\left(\frac{\sqrt{2} i \Phi}{f}\right) \qquad \Phi = \begin{pmatrix} \frac{1}{\sqrt{2}}\pi^0 + \frac{1}{\sqrt{6}}\eta & \pi^+ & K^+ \\ \pi^- & -\frac{1}{\sqrt{2}}\pi^0 + \frac{1}{\sqrt{6}}\eta & K^0 \\ K^- & \bar{K}^0 & -\frac{2}{\sqrt{6}}\eta \end{pmatrix}$$

2. D-meson scattering with baryons

Model: G-matrix approach: interactions of D=(D^0,D^+,D^+_s) and D*=(D^{*0},D^{*+},D^{*+}_s) with nucleon octet $J^P=1/2^+$ and Delta decuplet $J^P=3/2^+$

C. Garcia-Recio, J. Nieves, O. Romanets, L. L. Salcedo, L. Tolos, Phys. Rev. D 87, 074034 (2013)

Unitarized scattering amplitude ➔ from solution of coupled-channel Bethe-Salpeter equations: $T = T + VGT$

T. Song et al., PRC 92 (2015) 014910, arXiv:1503.03039

D-meson scattering in the hadron gas

1. D-meson scattering with mesons

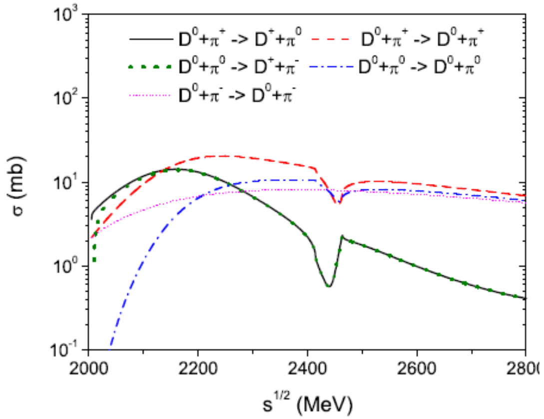

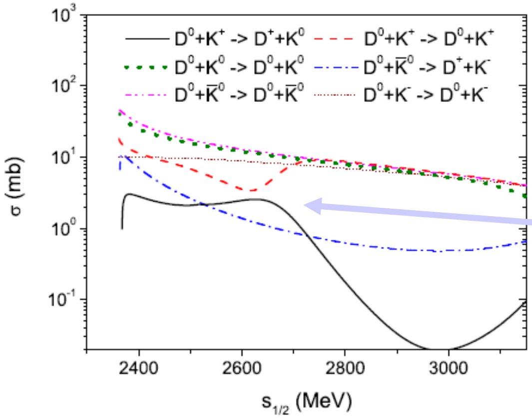

1a) cross sections with $m=\rho,\omega,\phi,K^*,\ldots$ taken as

$$\sigma(D, D^* + m) = 10mb$$

➔Strong **isospin dependence** and complicated structure (due to the resonance coupling) of D+m, D+B cross sections!

2. D-meson scattering with baryons

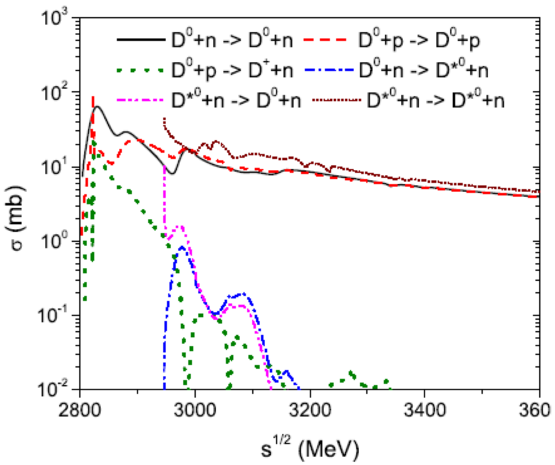

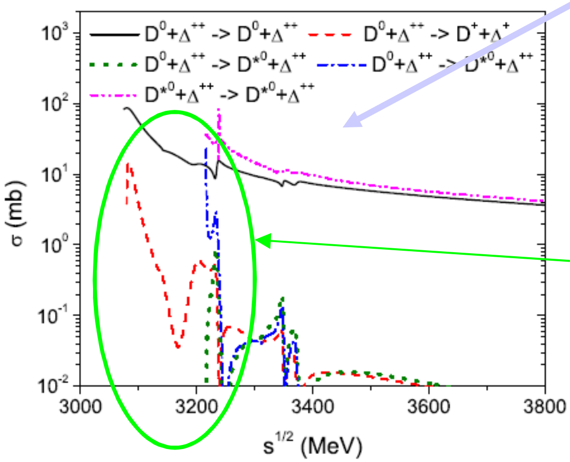

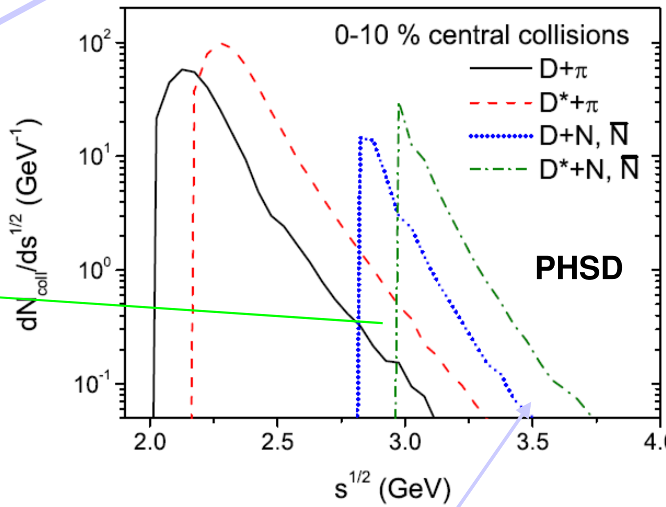

➔ **Hadronic interactions become ineffective for the energy loss of D,D* mesons at high transverse momentum (i.e. large $s^{1/2}$)**

R_{AA} at RHIC: hadronic rescattering

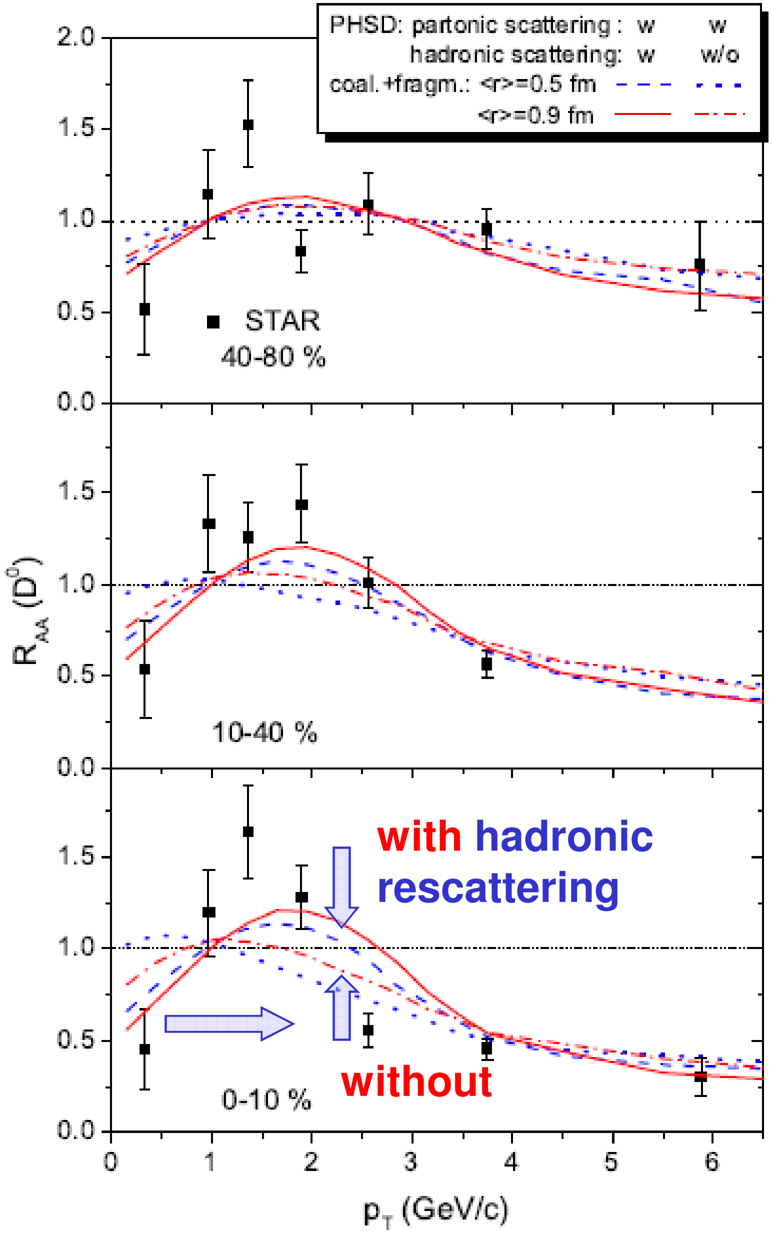

Influence of hadronic rescattering:

! Model study: (with partonic rescattering)
with / without hadronic rescattering

Central Au+Au at $s^{1/2}$ =200 GeV :
N(D,D*) ~30
N(D,D*+m) ~56 collisions
N(D,D*+B,Bbar) ~10 collisions
➔ each D,D* makes
~ 2 scatterings with hadrons

❑ **Hadronic rescattering moves R_{AA} peak to higher p_T !**

❑ **The hight and position of the R_{AA} peak at low p_T depends on the hadronization scenario: coalescence/fragmentation!**

T. Song et al., PRC (2015), arXiv:1503.03039
T. Song et al., PRC 92 (2015) 014910, arXiv:1503.03039

D-meson elliptic flow v_2 at RHIC

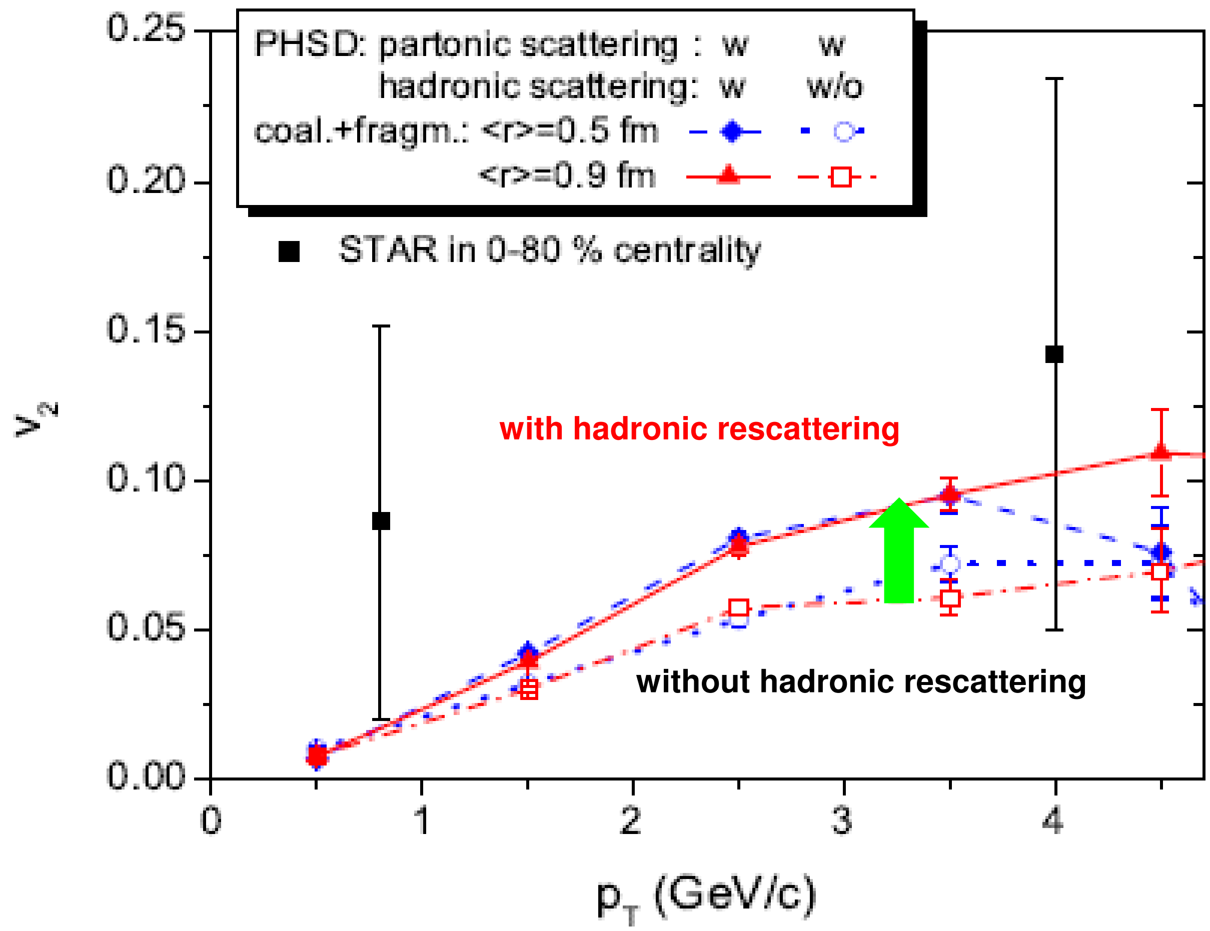

- ❑ Hadronic rescattering substantially increases v_2 at larger p_T
- ❑ v_2 is less sensitive to the hadronization scenarios than R_{AA}

T. Song et al., PRC 92 (2015) 014910, arXiv:1503.03039

Charm R_{AA} at LHC

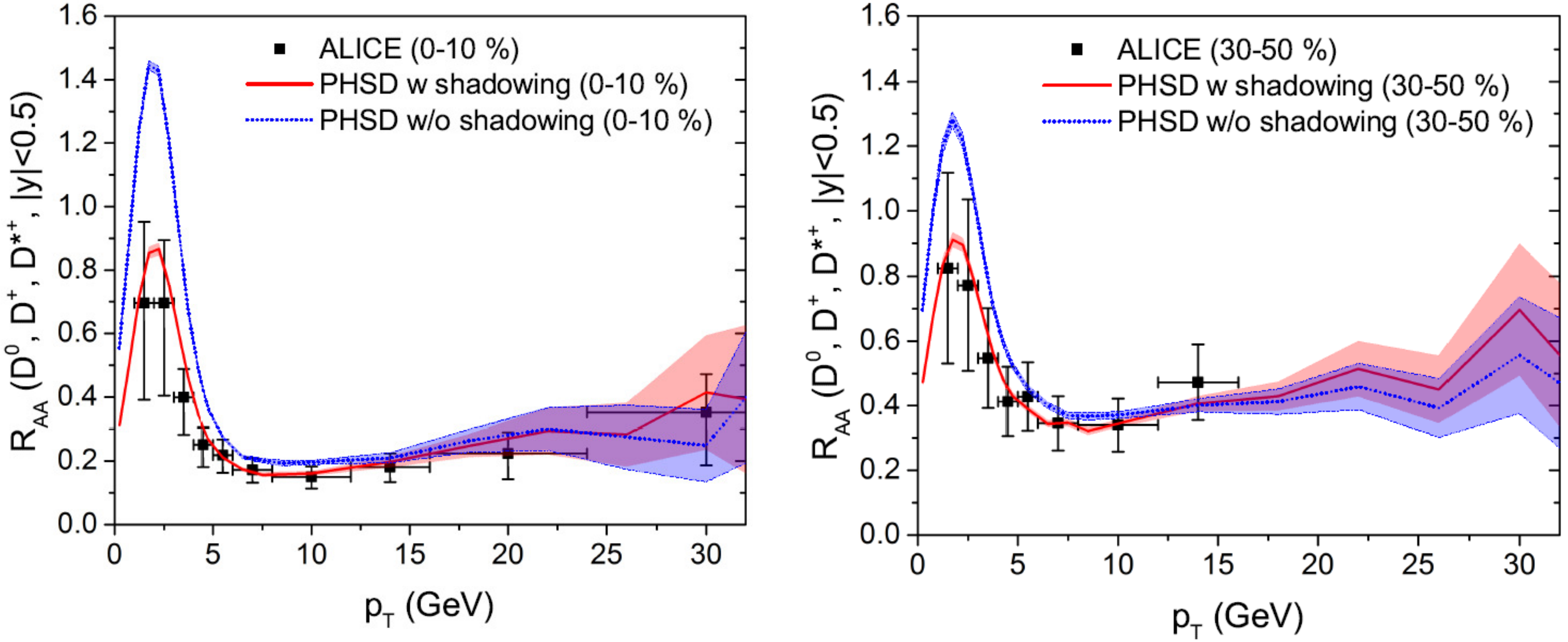

- in PHSD the energy loss of D-mesons at high p_T can be dominantly attributed to partonic scattering
- Shadowing effect suppresses the low p_T and slightly enhances the high p_T part of R_{AA}
- Hadronic rescattering moves R_{AA} peak to higher p_T

T. Song et al., PRC 93 (2016) 034906, arXiv:1512.0089

Charm v_2 at LHC

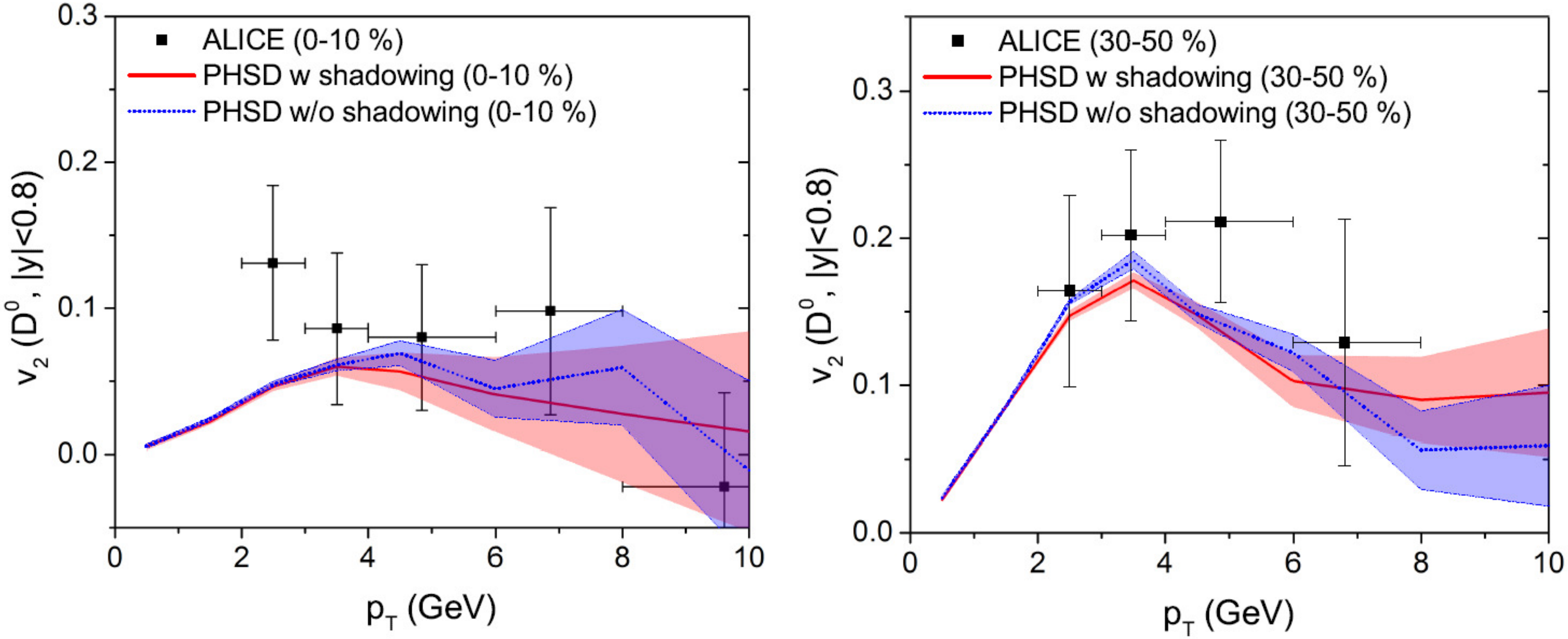

- Shadowing effect has small impact on v_2
- **Hadronic rescattering** increases v_2

T. Song et al., PRC 93 (2016) 034906, arXiv:1512.0089

R_{AA}^{e} and v_2^{e} from single electrons: beauty contribution

R_{AA} and v_2 vs p_T from single electrons in Au+Au @ 200 GeV

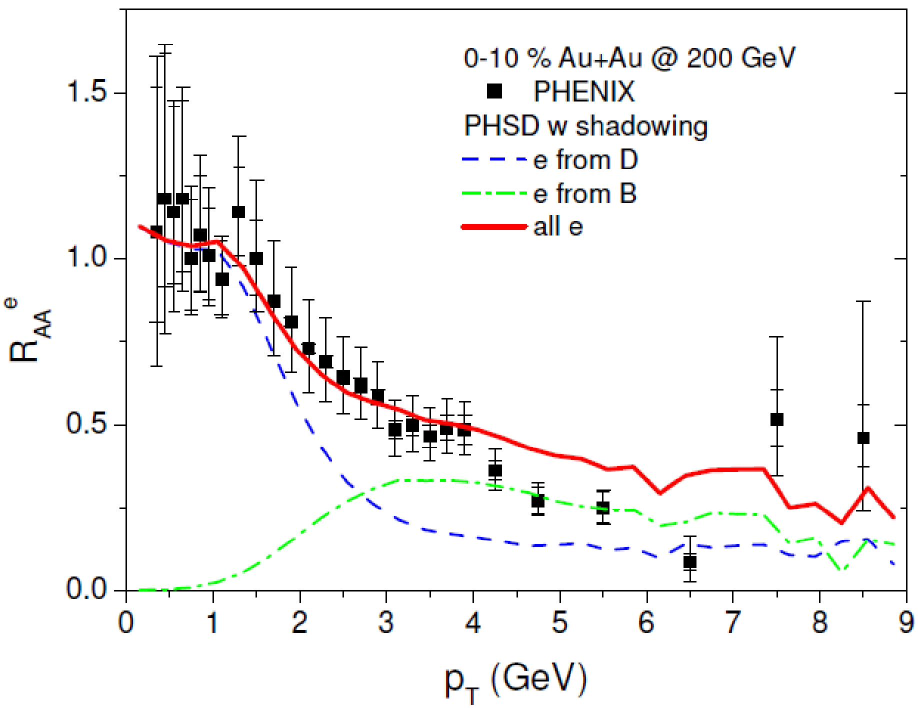

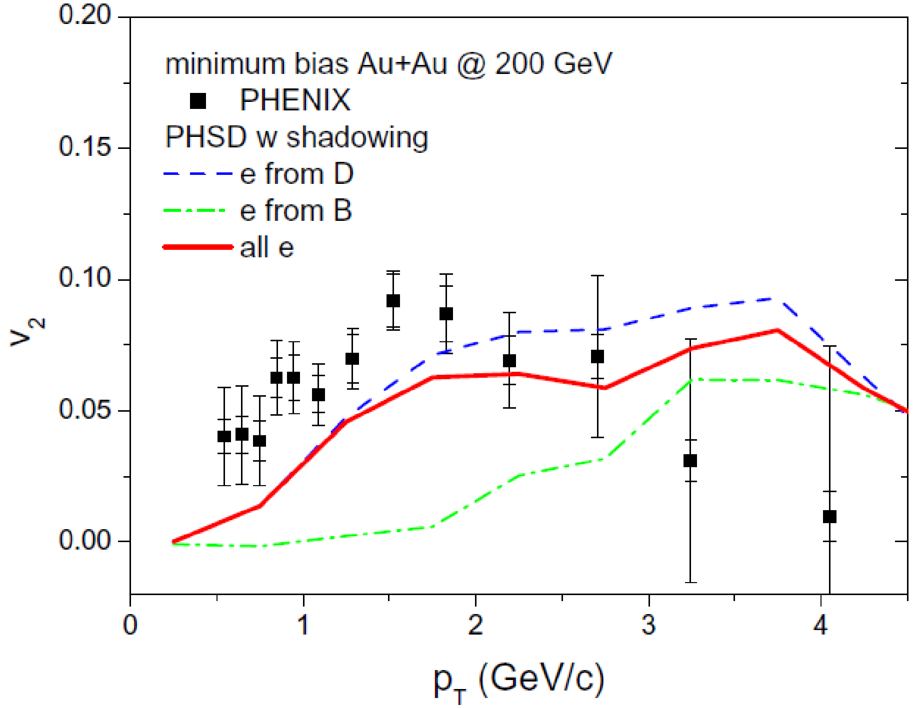

- Feed back from beauty contribution becoms dominant at p_T >3 GeV

T. Song et al., in progress

R_{AA}^e and v_2^e from single electrons from Au+Au at 62.4 GeV

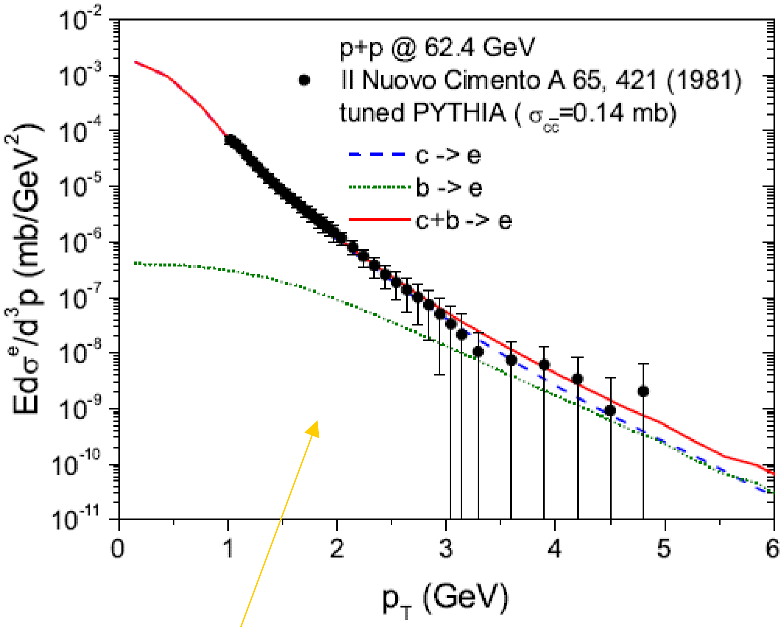

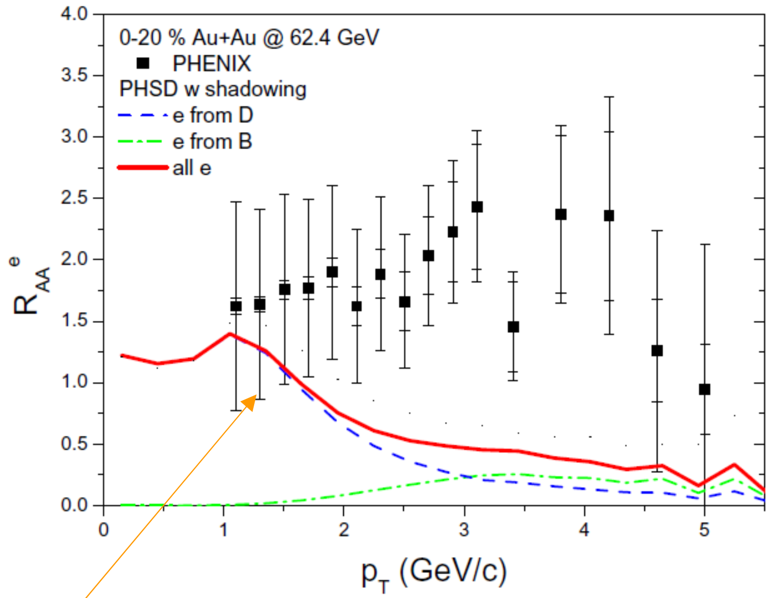

- PHSD: pp data on electron p_T spectra are well reproduced
- PHENIX data on R_{AA}^e from single electrons from Au+Au at 62.4 GeV are not reproduced
- v_2^e from single electrons from Au+Au at 62.4 GeV is in line with data

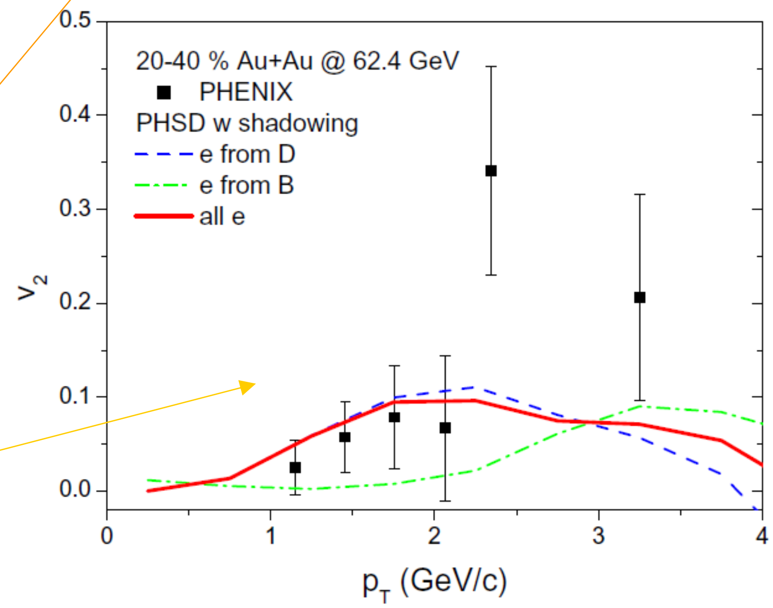

T. Song et al., in progress

R_{AA}^{e} from single electrons: 62.4 vs. 200 GeV

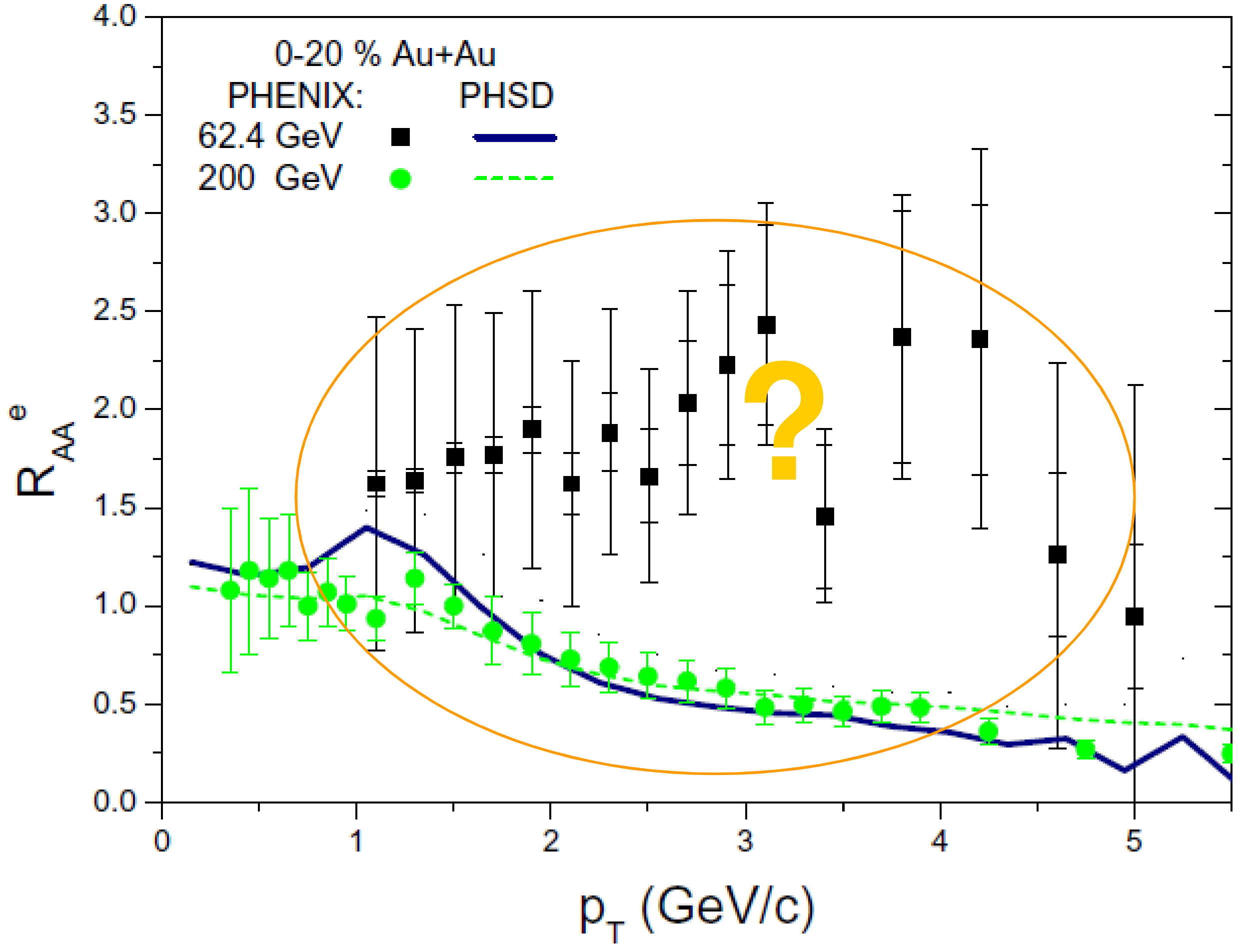

- **PHENIX:** R_{AA}^{e} from single electrons from **Au+Au at 62.4 GeV** are much **larger than at 200 GeV** !

Summary II

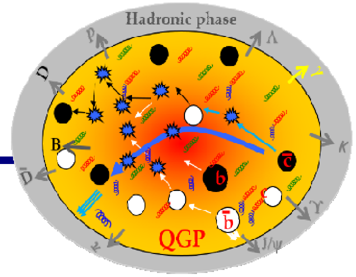

- **PHSD provides a microscopic description of non-equilibrium charm dynamics in the partonic and hadronic phases**

- **Partonic rescattering suppresses the high p_T part of R_{AA}, generates v_2**

- **Hadronic rescattering moves R_{AA} peak to higher p_T, increases v_2**

- **The structure of R_{AA} at low p_T is sensitive to the hadronization scenario, i.e. to the balance between coalescence and fragmentation**

- **Shadowing effects suppress R_{AA} at LHC**

- **The exp data for the R_{AA} and v_2 at RHIC and LHC are described in the PHSD:**
  by QGP collisional energy loss due to the elastic scattering of charm quarks with massive quarks and gluons in the QGP phase
  + by the dynamical hadronization scenario „coalescence & fragmentation“
  + by strong hadronic interactions due to the elastic scattering of D,D* mesons with mesons and baryons

- **Feed back from beauty contribution for $R_{AA}{}^e$ and $v_2{}^e$ from single electrons form Au+Au at 200 GeV becomes dominant at p_T >3 GeV**

Dileptons

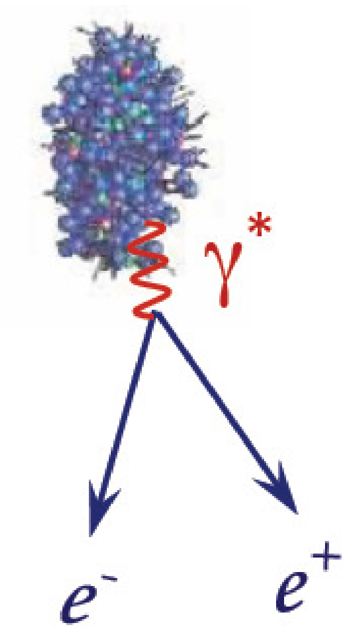

Thanks to Olena Linnyk

Dilepton sources

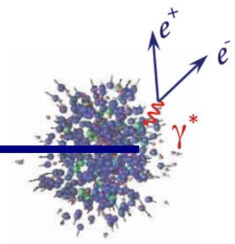

- **from the QGP via partonic (q,qbar, g) interactions:**

- **from hadronic sources:**

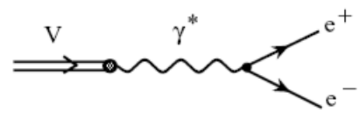

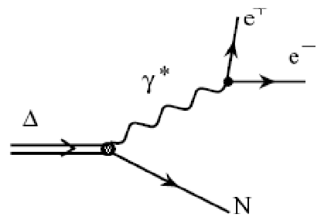

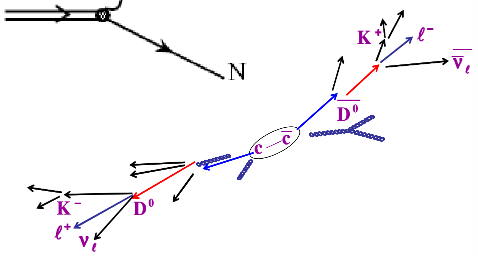

Plot from A. Drees

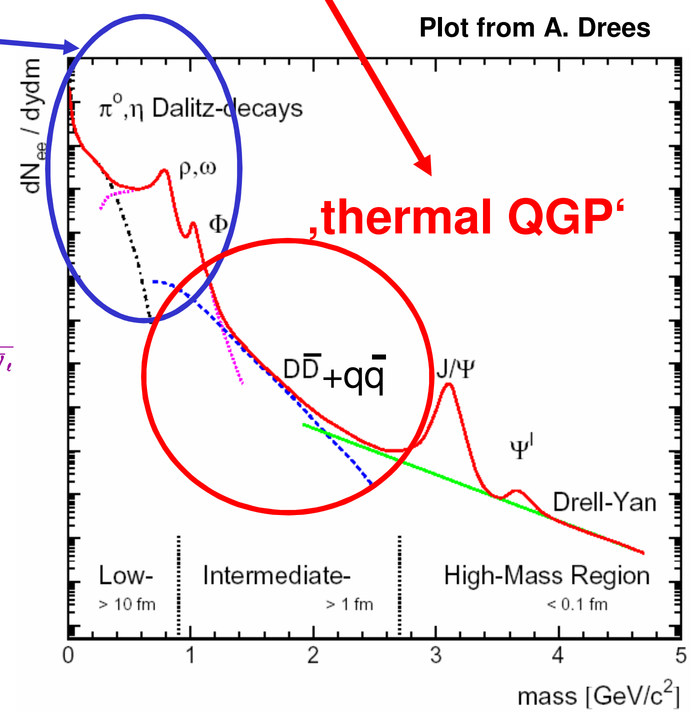

- **direct decay** of vector mesons (ρ,ω,φ,J/Ψ,Ψ')
- **Dalitz decay** of mesons and baryons (π^0,η, Δ,…)
- **correlated D+Dbar pairs**
- **radiation from multi-meson reactions** (π+π, π+ρ, π+ω, ρ+ρ , π+a_1) - ,4π'

! Advantage of dileptons:
additional „degree of freedom" (*M*) allows to disentangle various sources

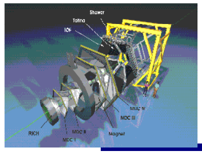

Dileptons at SIS energies - HADES

❑ **HADES: dilepton yield dN/dM scaled with the number of pions $N_{\pi 0}$**

❑ **Dominant hadronic sourses at $M>m_\pi$:**

- **η, Δ Dalitz decays**
- **NN bremsstrahlung**
- **direct ρ decay**

➢ **ρ meson = strongly interecting resonance**
strong collisional broadening of the ρ width

- **In-medium effects are more pronounced for heavy systems such as Ar+KCl then C+C**
- **The peak at M~0.78 GeV relates to ω/ρ mesons decaying in vacuum**

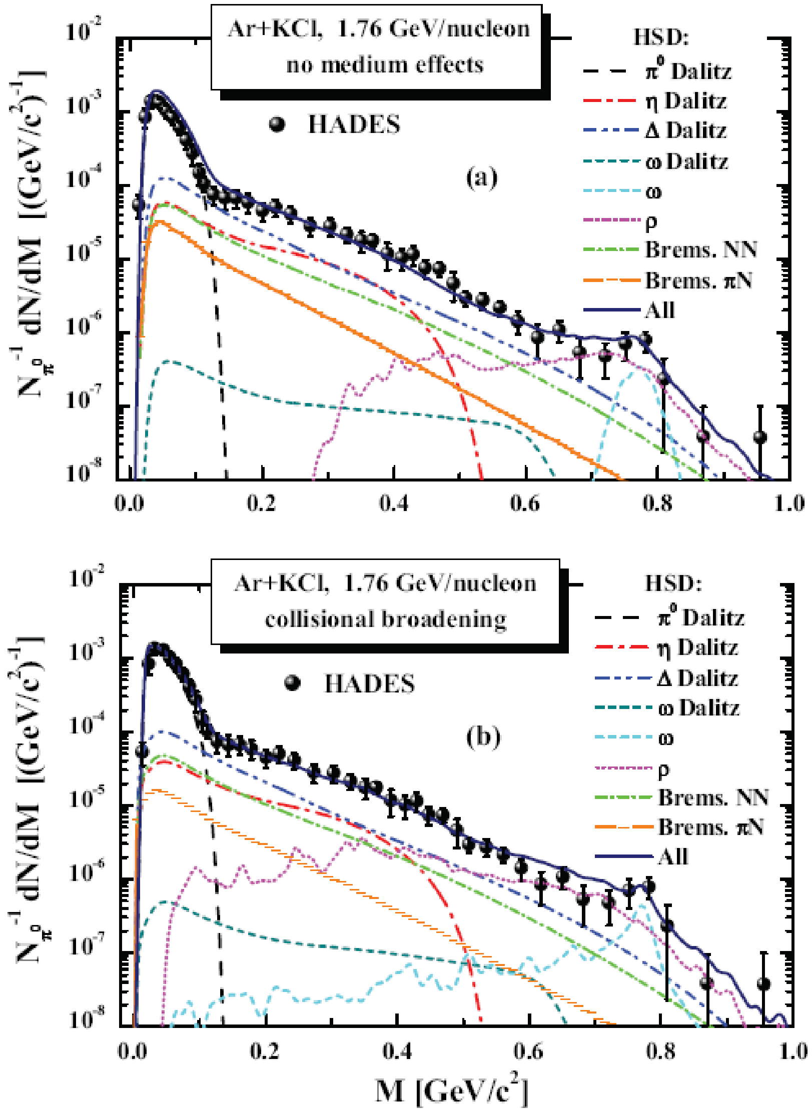

E.B., J. Aichelin, M. Thomere, S. Vogel, and M. Bleicher, PRC 87 (2013) 064907

Dileptons at SIS energies: A+A vs. N+N

- **ratio of AA/NN spectra** (scaled by $N_{\pi 0}$) after subtracted η contribution

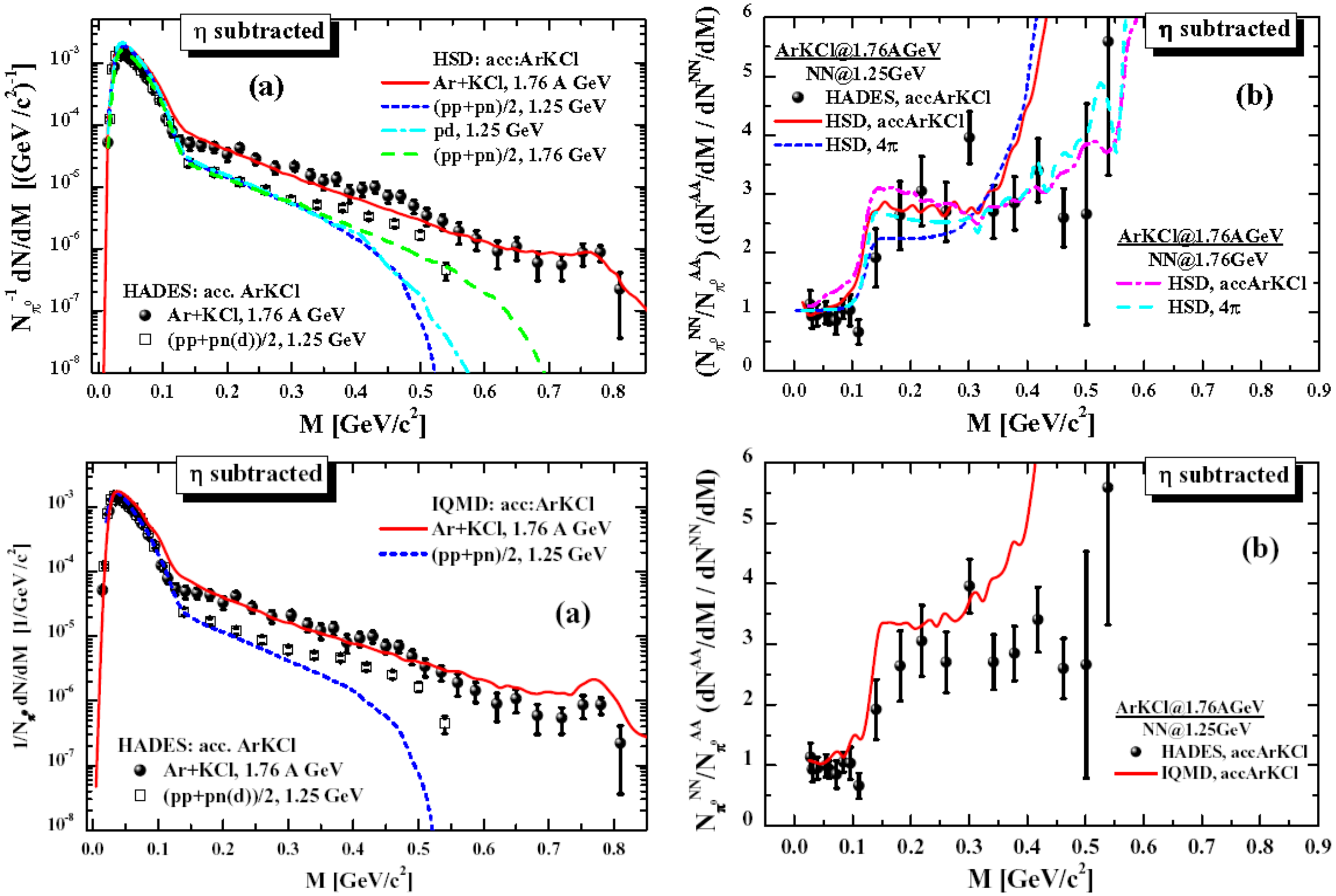

▪HSD

▪IQMD

➔ **Strong enhancement of dilepton yield in A+A vs. NN** is reproduced by HSD and IQMD for C+C at 1.0, 2.0 A Gev and Ar+KCl at 1.75 A GeV

E.B., J. Aichelin, M. Thomere, S. Vogel, and M. Bleicher, PRC 87 (2013) 064907

Dileptons at SIS (HADES): A+A vs NN

- Two contributions to the enhancement of dilepton yield in A+A vs. NN

1) the pN bremsstrahlung which scales with the number of collisions and not with the number of participants, i.e. pions;

2) the multiple Δ regeneration – dilepton emission from intermediate Δ's which are part of the reaction cycles Δ→πN; πN →Δ and NN→NΔ; NΔ→NN

- Enhancement of dilepton yield in A+A vs. NN increases with the system size!

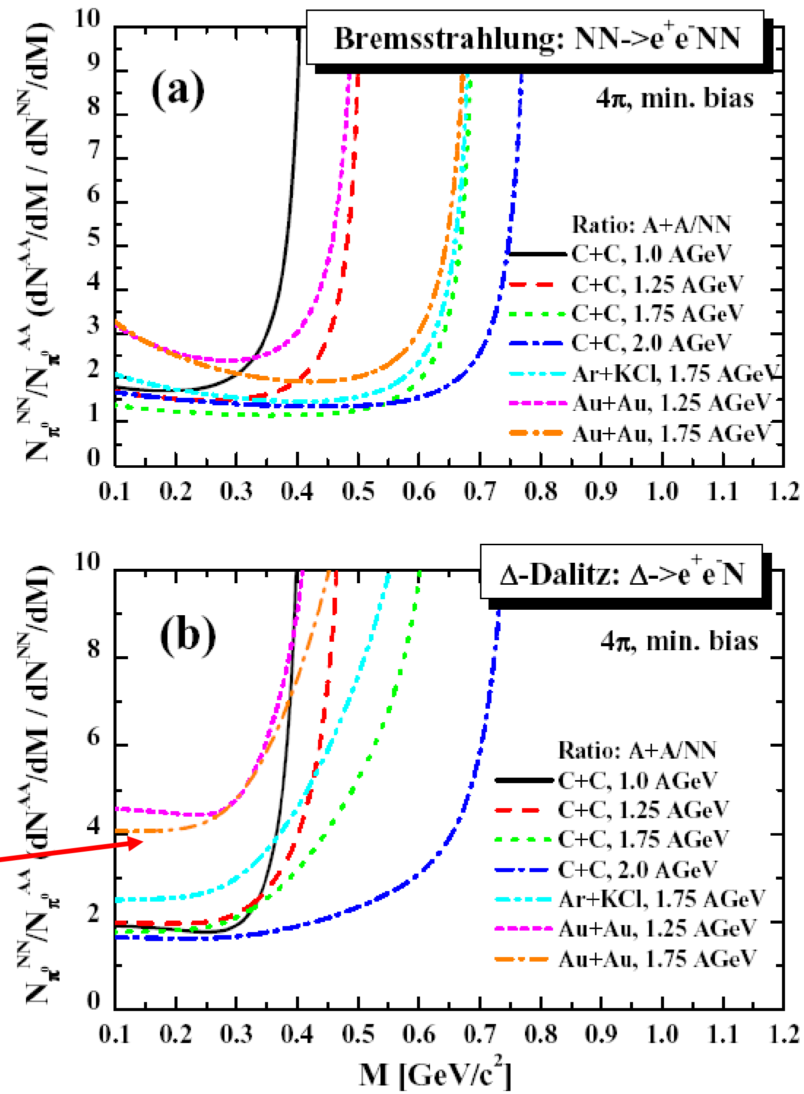

E.B., J. Aichelin, M. Thomere, S. Vogel, and M. Bleicher, PRC 87 (2013) 064907

Dileptons at SIS (HADES): Au+Au

HADES preliminary: Au+Au, 1.23 A GeV

T. Galatyuk, QM'2014

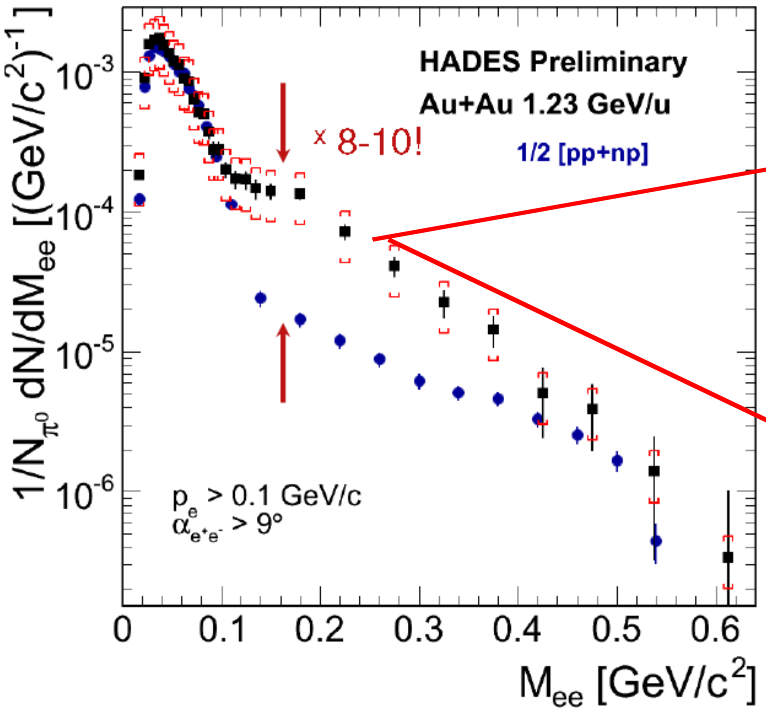

- **HSD predictions (2013)**

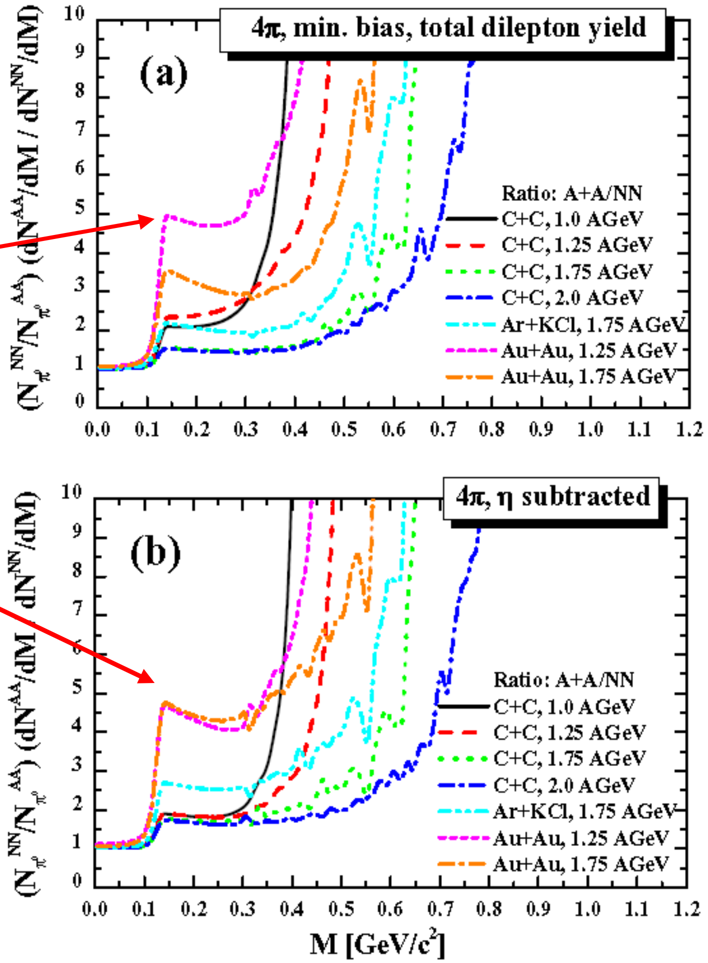

❑ **Strong in-medium enhancement of dilepton yield in Au+Au vs. NN**
➔ **related to Δ regeneration**

E.B., J. Aichelin, M. Thomere, S. Vogel, M. Bleicher, PRC 87 (2013) 064907

Lessons from SPS: NA60

❑ **Dilepton invariant mass spectra:**

NA60: Eur. Phys. J. C 59 (2009) 607

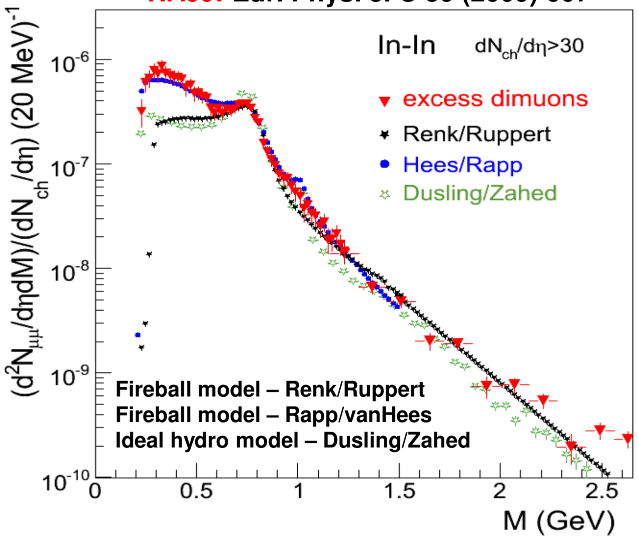

PHSD:
Linnyk et al, PRC 84 (2011) 054917

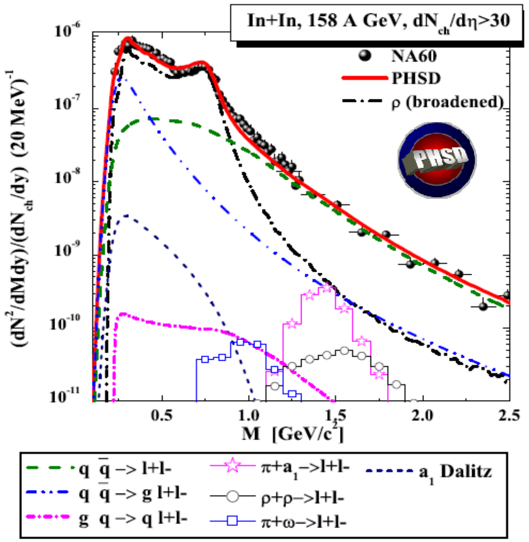

Hybrid-UrQMD:
Santini et al., PRC84 (2011) 014901

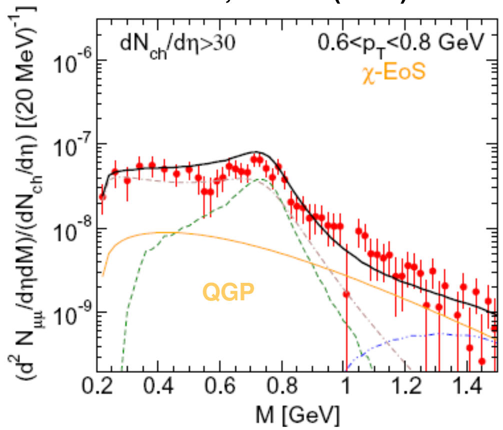

❑ **Inverse slope parameter T_{eff}:**

spectrum from QGP is softer than from hadronic phase since the QGP emission occurs dominantly before the collective radial flow has developed

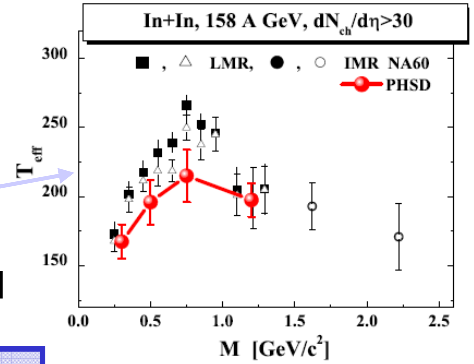

Message from SPS: (based on NA60 and CERES data)

1) **Low mass spectra - evidence for the in-medium broadening of ρ-mesons**
2) **Intermediate mass spectra above 1 GeV - dominated by partonic radiation**
3) **The rise and fall of T_{eff} – evidence for the thermal QGP radiation**
4) **Isotropic angular distribution – indication for a thermal origin of dimuons**

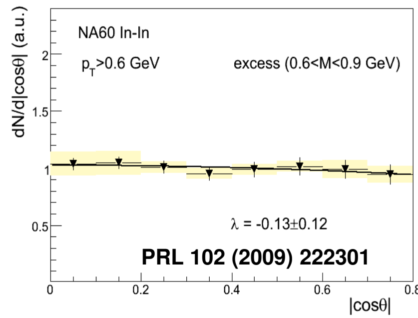

PRL 102 (2009) 222301

Dileptons at RHIC: STAR data vs model predictions

(STAR: arXiv:1407.6788)

Centrality dependence of dilepton yield

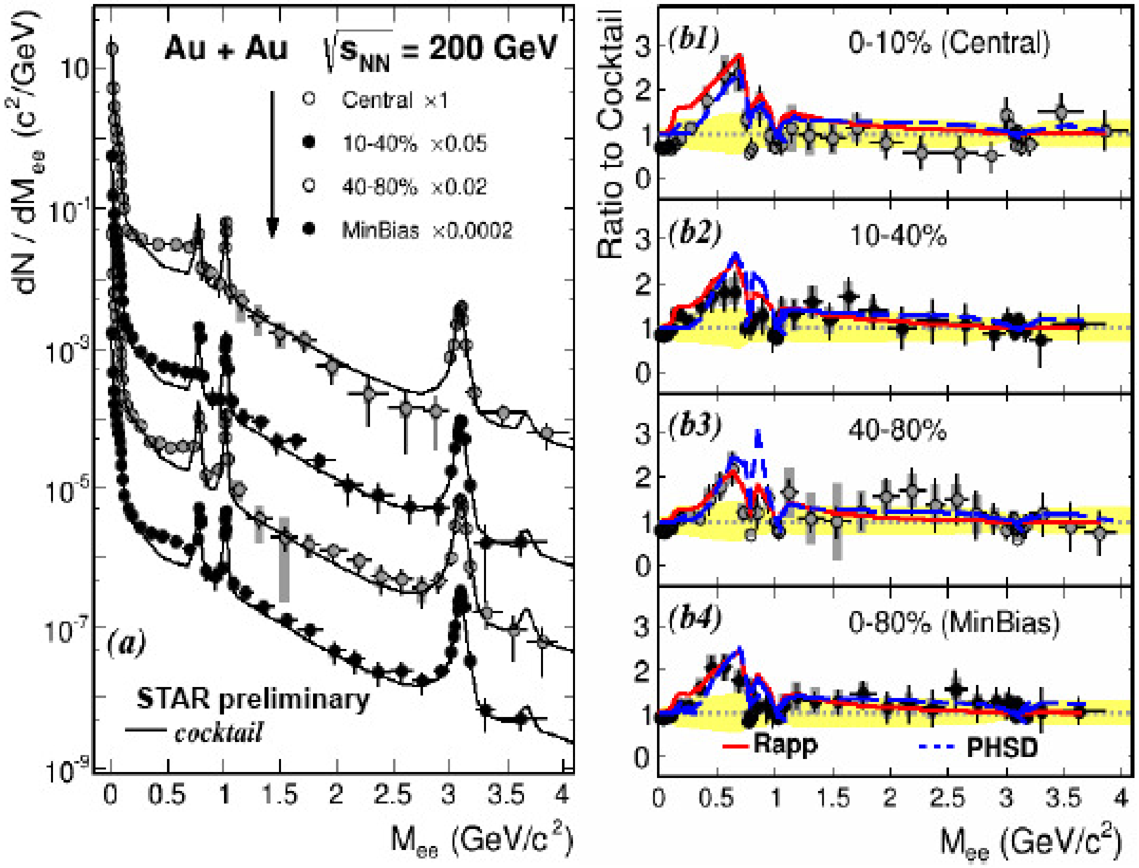

Excess in low mass region, min. bias

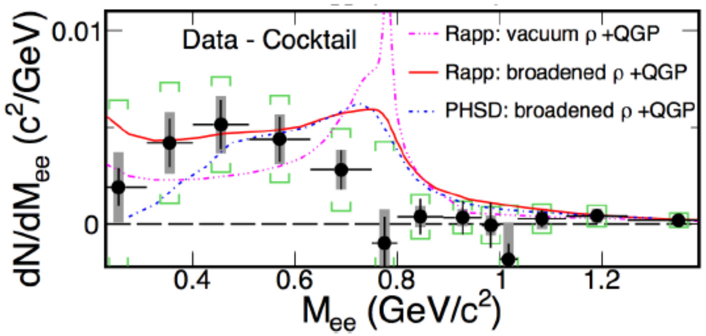

Models (predictions):

- **Fireball model – R. Rapp**
- **PHSD**

Low masses:

collisional broadening of ρ

Intermediate masses:

QGP dominant

Message: STAR data are described by models within a collisional broadening scenario for the vector meson spectral function + QGP

Dileptons from RHIC BES: STAR

(Talk by Nu Xu at QM'2014)

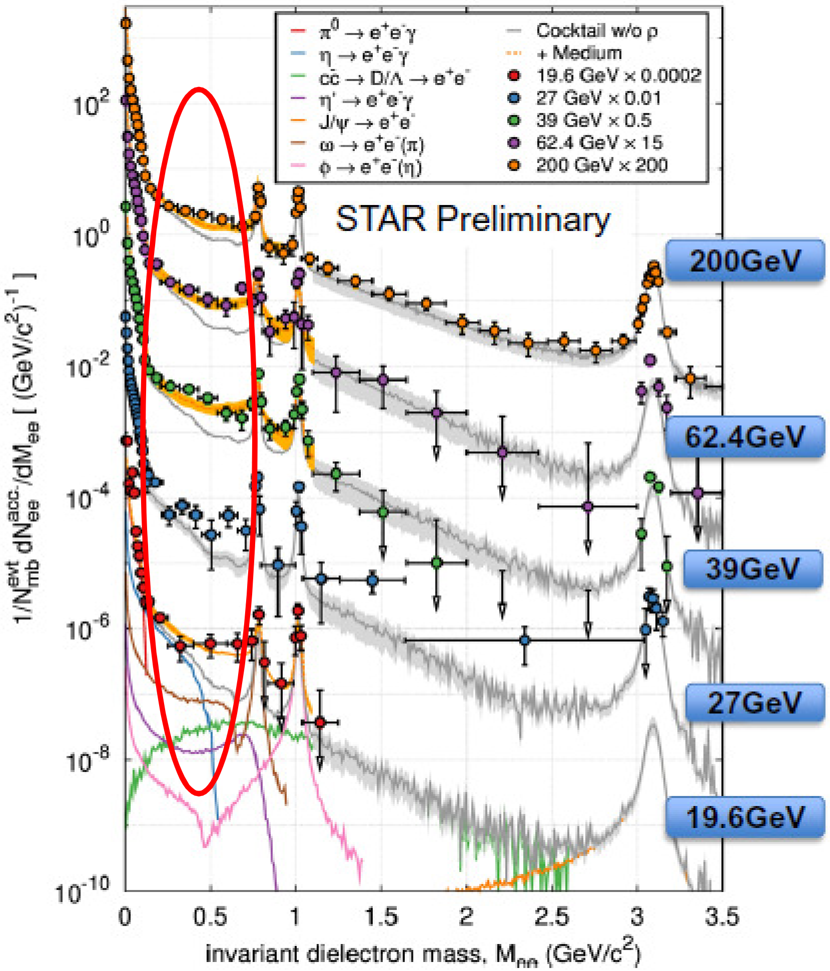

(Talk by Nu Xi at 23d CBM Meeting'14)

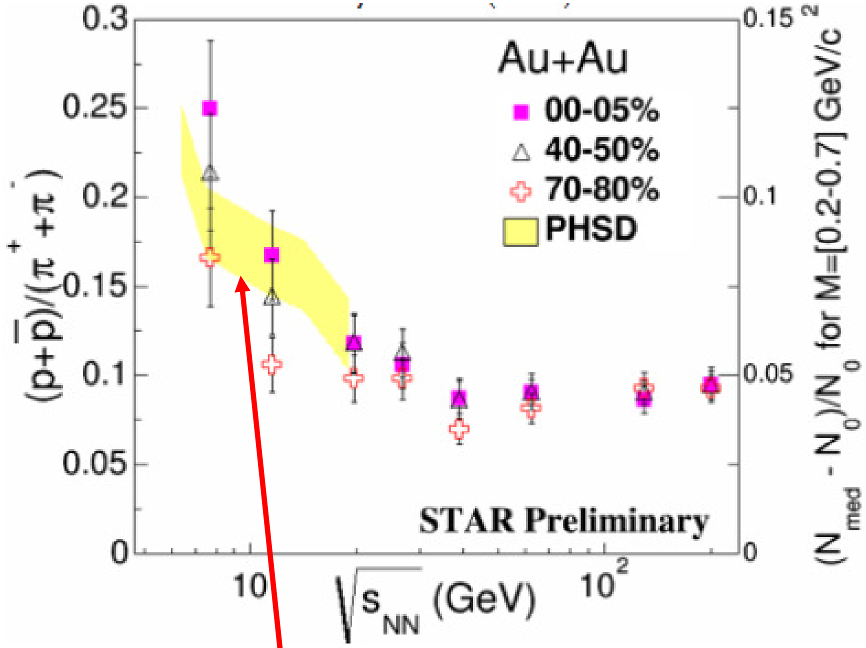

Message:

- **BES-STAR data show a constant low mass excess** (scaled with $N(\pi^0)$) within the measured energy range
- **PHSD model: excess increasing with decreasing energy** due to a longer ρ-propagation in the high baryon density phase

➔ **Good perspectives for future experiments – CBM(FAIR) / MPD(NICA)**

Dileptons at LHC

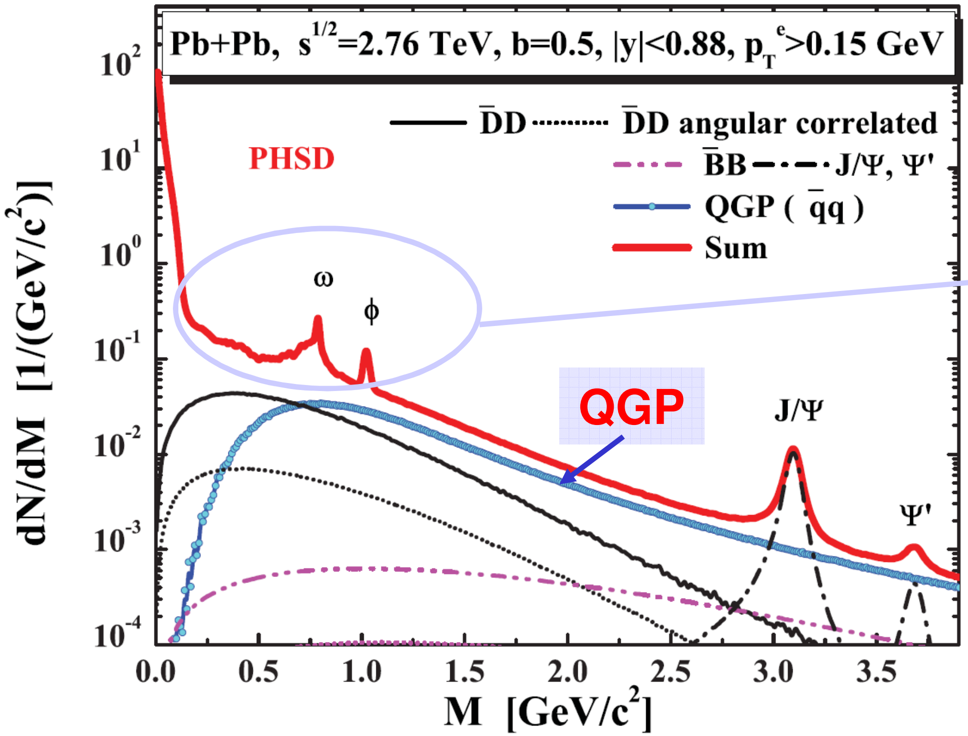

O. Linnyk, W. Cassing, J. Manninen, E.B., P.B. Gossiaux, J. Aichelin, T. Song, C.-M. Ko, Phys.Rev. C87 (2013) 014905; arXiv:1208.1279

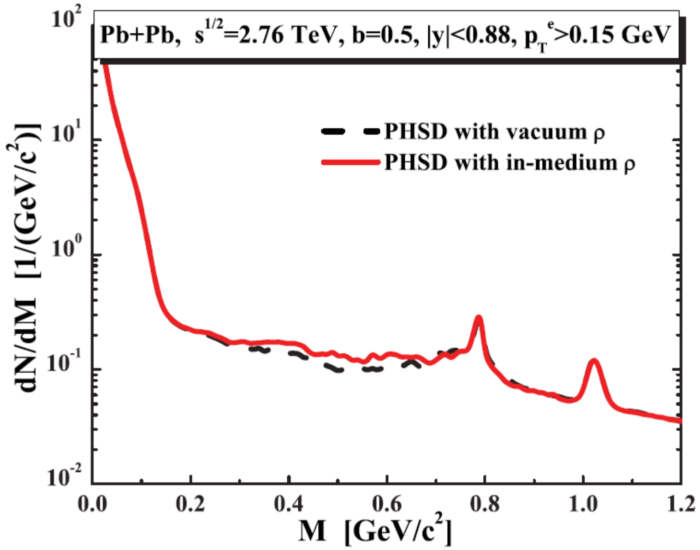

Message:

- low masses - hadronic sources: in-medium effects for ρ mesons are small
- intermediate masses: QGP + D/Dbar
  - charm 'background' is smaller than thermal QGP yield
  - QGP(qbar-q) dominates at M>1.2 GeV ➔ clean signal of QGP at LHC!

Summary III

Dilepton spectra - according to the PHSD predictions - show sizeable changes due to the different in-medium scenarios (as collisional broadening and dropping mass) which can be observed experimentally

- In-medium effects can be observed at all energies from SIS to LHC
- At SPS, RHIC and LHC the QGP (qbar-q) dominates at M>1.2 GeV

Review: O. Linnyk et al., Prog. Part. Nucl. Phys. 87 (2016) 50-115

Thanks to: PHSD group

FIAS & Frankfurt University
Taesoo Song
Pierre Moreau
Andrej Ilner
Hamza Berrehrah
Daniel Cabrera

Giessen University
Wolfgang Cassing
Olena Linnyk
Thorsten Steinert
Alessia Palmese
Eduard Seifert
Volodya Konchakovski

External Collaborations

SUBATECH, Nantes University:
Jörg Aichelin
Christoph Hartnack
Pol-Bernard Gossiaux
Vitalii Ozvenchuk

Texas A&M University:
Che-Ming Ko

JINR, Dubna:
Viacheslav Toneev
Vadim Voronyuk

Lyon University:
Rudy Marty

Barcelona University:
Laura Tolos
Angel Ramos

Thank you!

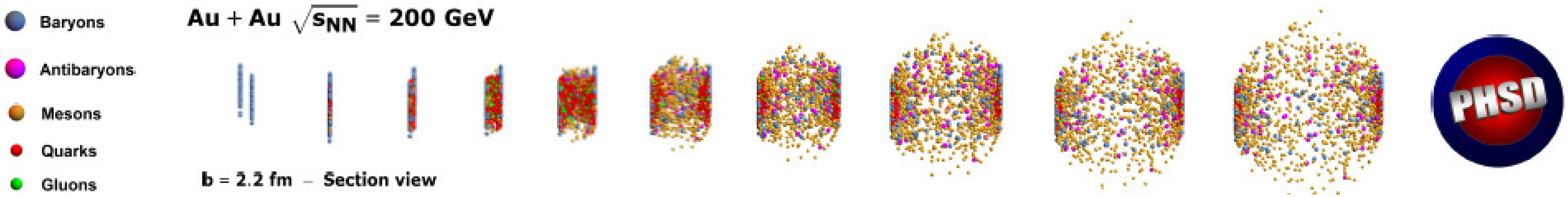
Baryons
Antibaryons
Mesons
Quarks
Gluons
Au + Au $\sqrt{s_{NN}}$ = 200 GeV
b = 2.2 fm – Section view
PHSD

Properties of the QGP in equilibrium using PHSD

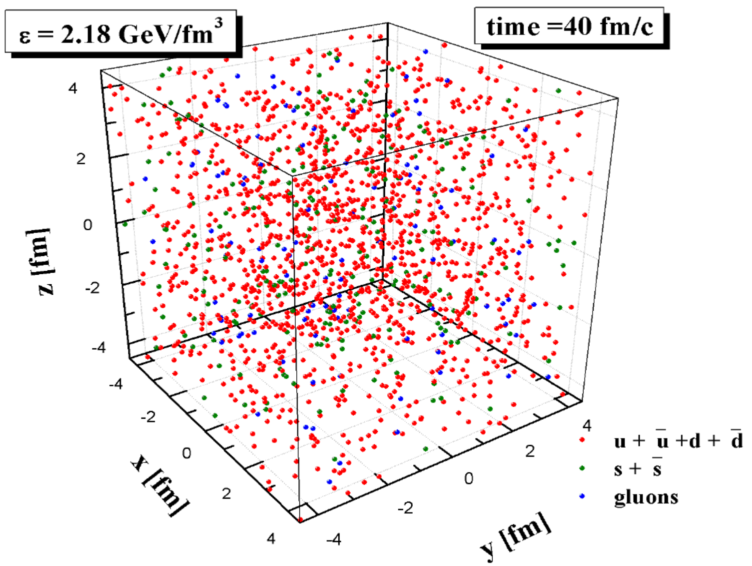

Properties of parton-hadron matter: shear viscosity

η/s using **Kubo formalism** and the **relaxation time approximation** (‚kinetic theory')

- **$T=T_C$: η/s shows a minimum (~0.1) close to the critical temperature**
- **$T>T_C$: QGP - pQCD limit at higher temperatures**
- **$T<T_C$: fast increase of the ratio h/s for hadronic matter ➔**
  - **lower interaction rate of hadronic system**
  - **smaller number of degrees of freedom (or entropy density) for hadronic matter compared to the QGP**

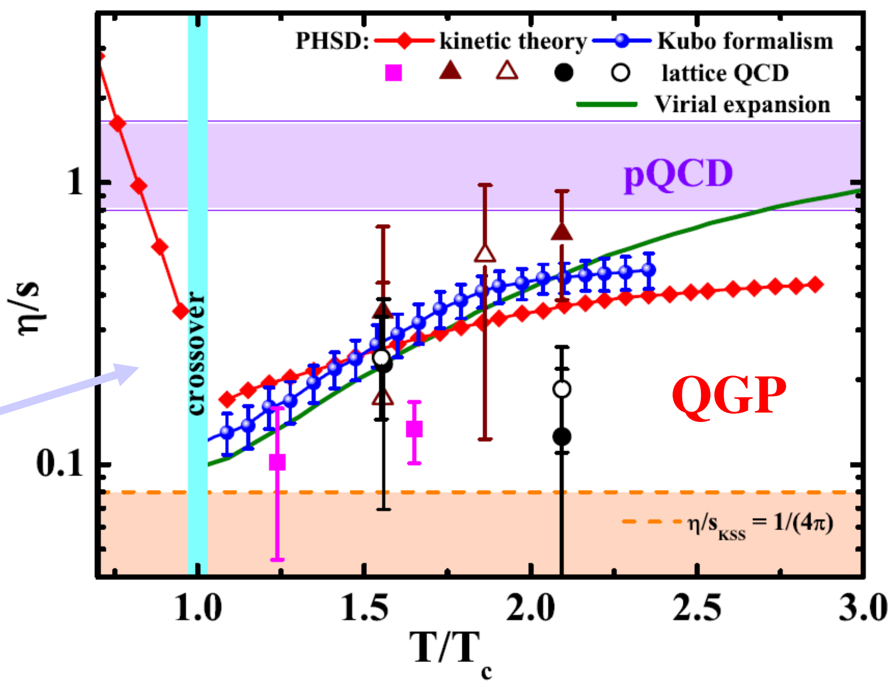

Virial expansion: S. Mattiello, W. Cassing, Eur. Phys. J. C 70, 243 (2010)

QGP in PHSD = strongly-interacting liquid

V. Ozvenchuk et al., PRC 87 (2013) 064903

QGP in equilibrium: Transport properties at finite (T, μ_q): η/s

Infinite hot/dense matter = PHSD in a box:

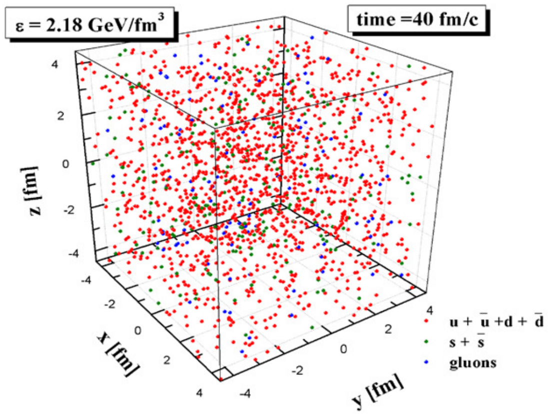

Shear viscosity η/s at finite T

V. Ozvenchuk et al., PRC 87 (2013) 064903

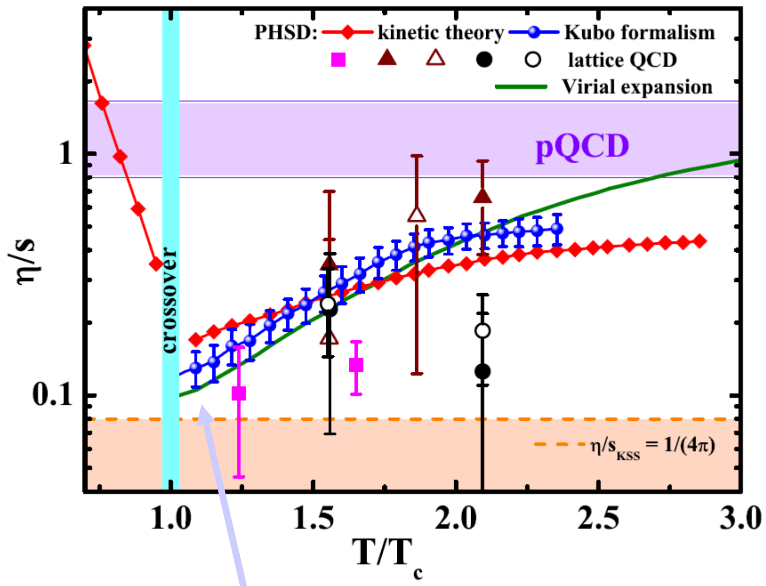

Shear viscosity η/s at finite (T, μ_q)

lQCD: $$\frac{T_c(\mu_q)}{T_c(\mu_q=0)} = \sqrt{1-\alpha\,\mu_q^2} \approx 1-\alpha/2\,\mu_q^2+\cdots$$

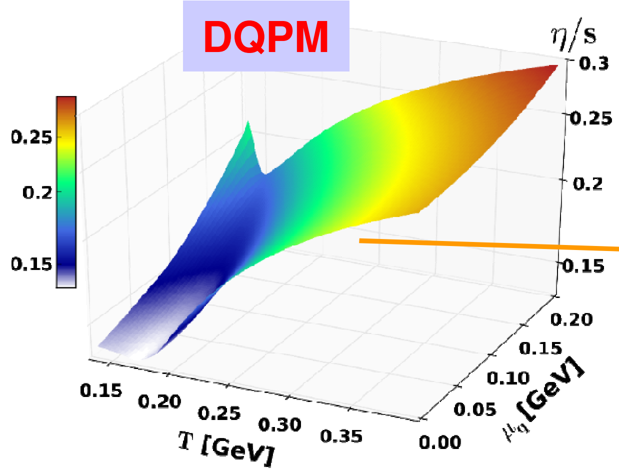

QGP in PHSD = strongly-interacting liquid

η/s: μ_q=0 ➔ finite μ_q: smooth increase as a function of (T, μ_q)

H. Berrehrah et al. arXiv:1412.1017

Properties of parton-hadron matter: electric conductivity

- The response of the strongly-interacting system in equilibrium to an external electric field eE_z defines the electric conductivity σ_0:

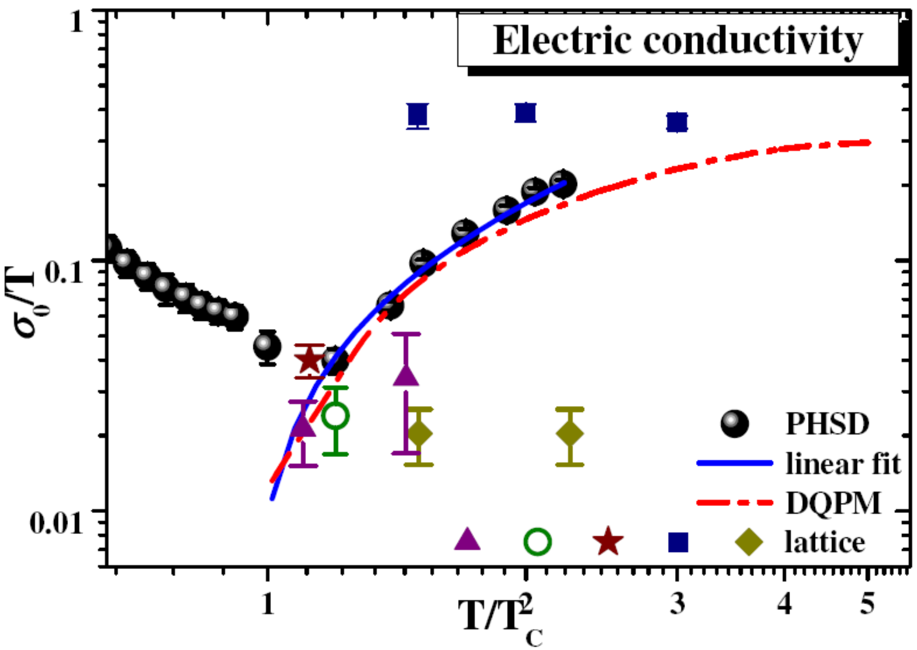

$$\frac{\sigma_0}{T} = \frac{j_{eq}}{E_z T},$$

$$j_z(t) = \frac{1}{V} \sum_j eq_j \frac{p_z^j(t)}{M_j(t)};$$

➔ the QCD matter even at T~ T_c is a much better electric conductor than Cu or Ag (at room temperature) by a factor of 500 !

- Photon (dilepton) rates at $q_0 \to 0$ are related to electric conductivity σ_0
➔ Probe of electric properties of the QGP

$$q_0 \left. \frac{dR}{d^4x\, d^3q} \right|_{q_0 \to 0} = \frac{T}{4\pi^3} \sigma_0$$

W. Cassing et al., PRL 110(2013)182301

Charm spatial diffusion coefficient D_s in the hot medium

- D_s for heavy quarks as a function of T for q = 0, μ_q=0

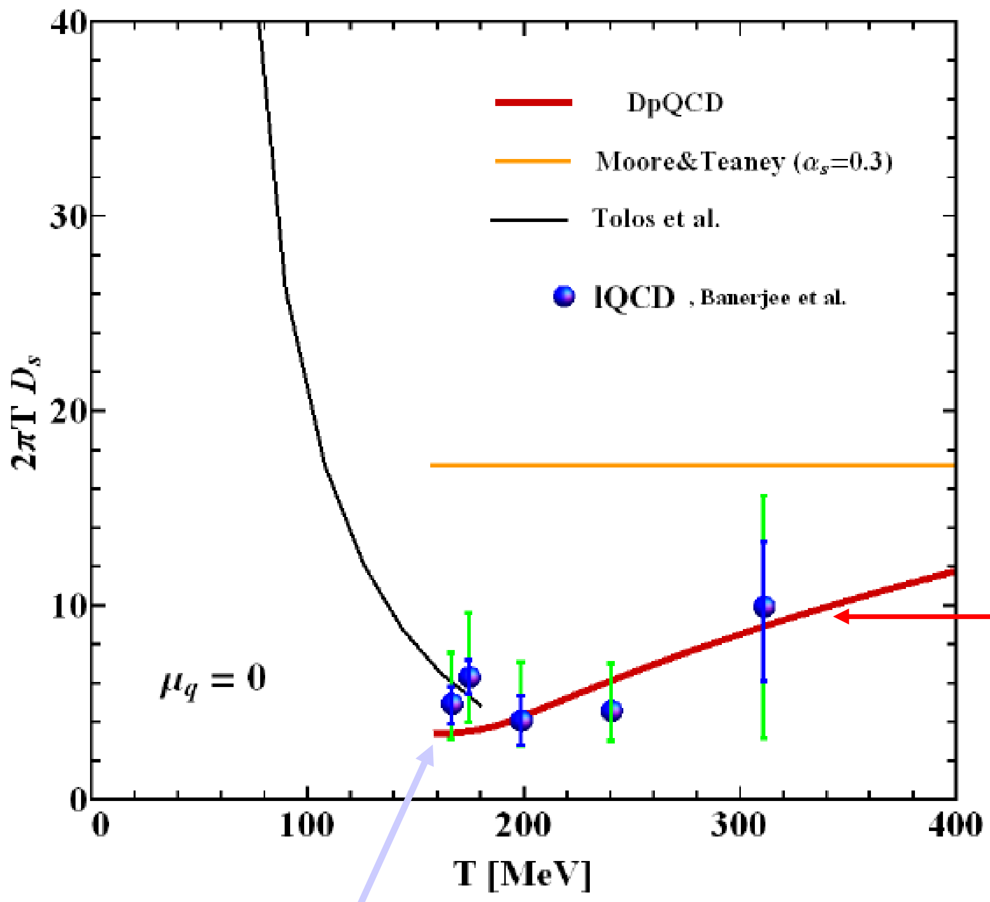

❑ T < T_c : hadronic D_s
L. Tolos , J. M. Torres-Rincon, Phys. Rev. D 88, 074019 (2013)

❑ T > T_c : QGP D_s

- pQCD - G. D. Moore, D. Teaney, Phys. Rev. C 71, 064904 (for a_s=0.3)
- DQPM - H. Berrehrah et al, arXiv:1406.5322 [hep-ph]
- lQCD - Banerjee et al., Phys. Rev. D 85, 014510 (2012).

➔ Continuous transition !

H. Berrehrah et al, PRC (2014), arXiv:1406.5322 [hep-ph]